

Turn on, tune in, turnover!

Target biology impacts *in vivo* potency, efficacy, and clearance

Johan Gabrielsson ^{1,3}, Stephan Hjorth ²

- 1) MedDoor AB, Engelbrektsgatan 5, 41127 Gothenburg, Sweden
- 2) Pharmacilitator AB, V. Bäckvägen 21B, SE-434 92, Vallda, Sweden
- 3) Address correspondence to: Professor.Gabrielsson@gmail.com

Keywords: Receptor pharmacology, target turnover, drug binding, clearance models, Michaelis-Menten equation, turnover model, PD scaling, drug delivery

Disclaimer: This review examines ‘open’- *versus* ‘closed’ system ligand-target-response models. The new ideas present the incorporation of free target and enzyme turnover as an additional independent component to ligand-target protein binding. This does not detract from the potential of the ‘open’ system, in contrast to the ‘closed’, to be influenced by other factors, such as metabolic, post target events (feedback, . . .) and external (placebo) that may equally well have an impact on the pharmacological effect.

Running title page

a) Target turnover impacts potency, efficacy and clearance

b) Corresponding author: Johan Gabrielsson

MedDoor AB, Engelbrektsgatan 5, 41127 Gothenburg, Sweden

Address correspondence to: Professor.Gabrielsson@gmail.com

c) Number of text pages (only main body of text): 70

Number of Tables: 9

Number of Figures: 15

Number of references: 276

Number of words in the Abstract: 250

Abbreviations

ACh	Acetylcholine;
AChE	Acetylcholine esterase;
ASA	Acetylsalicylic acid;
AUC	Area Under the plasma Concentration-time curve;
BAAM	Bromoacetyl-alprenolol menthane;
b.i.d.	<i>Bis in diem</i> , twice daily;
C	Total plasma concentration;
Cimet	Cimetidine;
Cmpd	Compound;
C_u	Unbound (free) plasma concentration;
Cl_(L)	Non-specific clearance of ligand;
Cl_(S)	Clearance of substrate;
COX-1	Cyclooxygenase-1;
E	Free enzyme concentration;
E₀	Free baseline enzyme concentration;
E_{max}/I_{max}	Efficacy parameter for <i>in vivo</i> maximum drug-induced effect (stimulatory effects/inhibitory effects) fitting the Hill-equation including baseline;
EC₅₀/IC₅₀	<i>In vivo</i> potency (stimulatory effects/inhibitory effects);
ECS	Electroconvulsive shock;
EEDQ	Ethoxycarbonyl-2-ethoxy-12-dihydroquinoline;
E_{ss}	Free enzyme concentration at equilibrium (steady-state);
ES_{ss}	Free enzyme-substrate complex concentration at equilibrium (steady-state);
E(t)	Free enzyme concentration as a function of time (disequilibrium);
GABAA	γ-Aminobutyric acid receptor type A;
GSECR	Gamma secretase;
Hist	Histamine;
Ibu	Ibuprofen;

<i>ISF</i>	Interstitial fluid rate;
<i>k_{cat}</i>	Fractional catabolic rate constant;
<i>k_{deg} (k_{out})</i>	Fractional turnover rate (also known as <i>k_{out}</i>);
<i>K_d</i>	Dissociation constant;
<i>k_{e(RL)}</i>	Ligand-target complex elimination rate constant;
<i>k_{irr}</i>	Second-order irreversible loss rate constant;
<i>k_{off}</i>	Dissociation rate constant of ligand-target complex;
<i>k_{on}</i>	Association rate constant of ligand-target complex;
<i>k_{syn}</i>	Turnover rate constant of target;
<i>L</i>	Ligand concentration;
<i>L-DOPA</i>	Levodopa;
<i>LFTR</i>	Ligand facilitated target removal;
<i>L_{ss}</i>	Ligand concentration at steady-state;
<i>K_m</i>	Michaelis-Menten constant;
<i>MABEL</i>	Minimal Anticipated Biological Effect Level;
<i>MAO-B</i>	Monoamine oxidase-B;
<i>MIC</i>	Minimum inhibitory concentration;
<i>MM</i>	Michaelis-Menten;
<i>mPBPk</i>	Minimal physiologically based pharmacokinetic model;
<i>Nap</i>	Naproxen;
<i>NiAc</i>	Nicotinic acid;
<i>NSAID</i>	Nonsteroidal anti-inflammatory drug;
<i>OVX</i>	Ovariectomized;
<i>PBZ</i>	Phenoxybenzamine;
<i>pEC₅₀</i>	Negative logarithm of <i>in vivo</i> potency;
<i>pK_d</i>	Negative logarithm of binding dissociation constant;
<i>PK-PD</i>	Pharmacokinetic-pharmacodynamic;

<i>PPI</i>	Protonpump inhibitor;
<i>Q_i</i>	Blood flow through the eliminating organ;
<i>R</i>	Target concentration;
<i>RL</i>	Ligand-target complex concentration;
<i>R_{ss}</i>	Target concentration at steady-state;
<i>RL_{max}</i>	Maximum ligand-target complex concentration;
<i>RL_{ss}</i>	Ligand-target complex concentration at steady-state;
<i>S_{ss}</i>	Substrate concentration at steady-state;
<i>TMDD</i>	Target mediated drug disposition;
<i>V</i>	Volume of distribution;
<i>V_{max}</i>	Maximum elimination (metabolic) rate;
<i>V_{max}(t)</i>	Maximum elimination (metabolic) rate during disequilibrium;
<i>V_{max}(0)</i>	Maximum elimination (metabolic) rate at baseline;
<i>6-OHDA</i>	6-hydroxydopamine;
<i>ρ</i>	Rho: transduction parameter for conversion of a ligand-receptor complex concentration to a pharmacological response, unique for each compound, target and response

e) Suggested section assignment: Drug Discovery and Translational Medicine

Abstract

Even though significant efforts have been spent in recent years to understand and define the determinants of *in vivo* potency and clearance, important pieces of information are still lacking. By introducing *target* turnover into the reasoning, we open up to further the understanding of central factors important to the optimization of translational dose-concentration-response predictions. We describe: *i)* new ('open' model) expressions of the *in vivo* potency and efficacy parameters which embody target turnover, binding and complex kinetics, also capturing full, partial, and inverse agonism, and antagonism, *ii)* a detailed examination of 'open' models to show what potency and efficacy parameters have in common and how they differ, and, *iii)* a comprehensive literature review showing that target turnover rate varies with age, species, tissue/subregion, treatment, disease state, hormonal and nutritional state, and day-night cycle. The new 'open' model expression which integrates system- and drug properties, shows that: fractional turnover rates rather than the absolute target or ligand-target complex expression determine necessary drug exposure via *in vivo* potency; absolute ligand-target expression determines the need of drug, based on the transduction Rho and *in vivo* efficacy parameters; the free enzyme concentration determines clearance and maximum metabolic rate; the fractional turnover rate determines time to equilibrium between substrate, free enzyme and complex; properties of substrate, target, and complex demonstrate non-saturable metabolic behavior at equilibrium; nonlinear processes previously referred to as capacity- and time-dependent kinetics may occasionally have been disequilibria; and, the 'open' model may pinpoint why some subjects differ in their demand of drug.

Significance statement

‘Understand the target turnover’ is a central tenet in many translational dose-concentration-response predictions. New ‘open’ model expressions of *in vivo* potency, efficacy parameter and clearance are derived and anchored onto a comprehensive literature review showing that target turnover rate varies with age, species, tissue/subregion, treatment, disease, hormonal and nutritional state, day-night cycle, and more. Target turnover concepts will therefore significantly impact fundamental aspects of pharmacodynamics and pharmacokinetics, thereby also the basics of drug discovery, development, and optimization of clinical dosing.

Table of contents

Running title page	2
Abbreviations	3
Abstract	6
Introduction.....	10
What is the problem?.....	10
What is then lacking?	11
How may we address the problem?.....	11
Pharmacologic systems and ligand-target interactions	12
<i>In vivo</i> ‘open’ systems; reversible vs. irreversible ligand-target interactions	12
Assessment of target turnover under different conditions	16
Age vs. target turnover (Table 1)	17
Species and tissues vs. turnover (Table 2)	19
Target pool turnover vs. functional recovery.....	21
Pharmacological effect and target turnover – dependency on baseline states	25
Chronic drug treatments and disease states vs. turnover (Table 4)	27
Up- and down-regulation of target – Impact of k_{syn} , k_{deg} and $k_{e(RL)}$	28
<i>In vivo</i> EC_{50} compared to <i>in vitro</i> K_d – dependency on k_{deg} , k_{off} and $k_{e(RL)}$	31
Examples of irreversible and reversible ligand-target interactions	33
Irreversible ligand-enzyme target systems	37
Reversible ligand-target interactions	39
<i>Key insights and translational potential of new in vivo potency expression</i>	42
<i>Inter-species scaling of in vitro and in vivo PD properties</i>	45
Background and pruning of data	45
Concepts of allometry	47
Literature case examples.....	48
Drug metabolism and the ‘open’ Michaelis-Menten system.....	53

Background to equations and models.....	53
Equilibrium states and clearance expression of (reversible) metabolic systems	55
Key insights and translational potential	59
Induction or inhibition of enzymatic and catalytic processes.....	60
Discussion	61
What is the challenge and why is it a problem?	61
Unifying and separating properties of ‘open’ systems	62
General conclusions and perspectives	63

Introduction

In vivo potency guides at which plasma exposure a drug is active, and clearance carries information about how efficiently the body removes the medicine. Combined they define the clinically efficacious dose range. Variability in drug potency and clearance is thus of key importance to ascertain proper dosing and assessment of risk, and need to be meticulously tested and documented in drug application filings. These topics have in recent years started to gain traction in basic research and drug discovery, yet the understanding of components essential to the definition of *in vivo* potency, efficacy parameter and clearance still remains incomplete.

What is the problem?

Traditionally, *in vivo* potency estimates are projected from *in vitro* target affinity, and clearance from enzymatic breakdown data. Drug disposition processes are likewise assayed *in vitro* and in preclinical species, and viewed as more or less fixed uptake and/or elimination elements, in line with conventional basic ‘mass action’ concepts. Importantly however, these measures are derived and modelled from ‘closed’ systems, typically at constant total protein expression levels – thus *in sharp contrast* to the inherent dynamics of a *living system*.

Proteins in the body are continuously produced and degraded, with turnover half-lives ranging from a few minutes to several days, months, or even longer *in vivo* (see, *e.g.*, (Boisvert et al., 2012). The turnover rates vary greatly among different organs and tissues, nutritional status, time of day, between sexes, across species, and also depending on age and life-span (for review, see, (Waterlow, 1984). Figure 1 schematically shows how *turnover* is addressed in this review.

Figure 1 approx here

Furthermore, the synthesis and degradation of drug and metabolic targets (k_{syn} and k_{deg} of receptor or enzyme protein) differ depending on the overall energy (heat) turnover in a particular species. In general, the smaller the species, the faster the loss of heat and therefore the higher energy turnover in order to maintain a 37 °C homeostasis (Adolph, 1949; Waterlow, 1984). Even more crucial from the individual patient perspective is that the disease and/or treatment context may significantly influence protein/target degradation k_{deg} (and synthesis k_{syn}) compared to normal healthy conditions. Examples include altered protein synthesis and degradation in fever or hyper-inflammatory states (*e.g.*, (Fearon et al., 1988; Waterlow, 1984) or after chronic drug treatment (*e.g.*, (Pich et al., 1987). Factors like the aforementioned may give rise to systematic deviations when predicting drug *in vivo*

potency and clearance from *in vitro* binding/metabolism data (Jansson-Lofmark et al., 2020).

Insufficient power of applied methods is also a challenge to inter-species *in vivo* extrapolations of pharmacological and metabolic data (Gabrielsson et al., 2018b). This is a contrast between reductionist approaches to define/assess mechanisms of drug action with ligands, cells or tissues (*in vitro* or *ex vivo*), and perhaps purified targets vs. *in vivo* studies in experimental animals or humans.

What is then lacking?

A more complete and mechanistic description of the determinants of potency, efficacy parameter and clearance properties is required to optimize predictions of *in vivo* pharmacologic effectiveness towards clinical use. Not least is there a crucial need for further insight into and quantification of the impact of turnover rates of corresponding target protein entities. Thus, taken together, a greater focus on *target biology* properties relative to drug features (such as binding affinity) is warranted.

How may we address the problem?

The time-dependent and varying turnover rates of target proteins across species are typically not captured by most contemporary *in vitro* assay systems or in preclinical profiling. Recently, we have therefore introduced new mathematical expressions of *in vivo* potency and efficacy parameter derived in part from target-mediated drug disposition (TMDD) reasoning (Gabrielsson and Peletier, 2017; Gabrielsson et al., 2018a), and shown how variations in target synthesis and loss might impact pharmacodynamic variability (Gabrielsson et al., 2018a). The present account builds further on these ideas, expanding the ‘open’ system concept and accompanying expressions to describe and take into consideration the dynamics of *in vivo* potency-, efficacy- as well as clearance-related parameters, with representative literature examples included to illustrate their impact. Among these, we discuss in particular drug target and metabolic enzyme turnover within the context of chronic treatment, aging, disease, and nutritional state influences. Figure 2 illustrates schematically the background and key differences between ‘closed’ and ‘open’ drug target and metabolic systems along with their corresponding parameters. By ‘open’ we mean that all major determinants of the pharmacological response and/or of clearance have input (synthesis, dosing, binding) and loss (elimination, dissociation, transport, clearance) terms.

Figure 2 approx here

Pharmacologic systems and ligand-target interactions

While *in vitro* ligand-target binding and functional preparations remain useful for the purpose of identifying fundamental *drug* properties, the impact of the *target* on drug responses in an integrated living organism can only be addressed by an ‘open’ *in vivo* system approach. Ranking of test compounds based on their *in vitro* binding affinities (K_d or *in vitro* potencies) and preclinical *in vivo* profiles, is standard practice in the drug discovery context. However, in the *in vivo* situation several factors (see, Introduction) pertaining to the synthesis and degradation rates (turnover) of corresponding *target proteins* may significantly influence the pharmacodynamic outcome of a drug.

To this end, *turnover models* and **target** turnover have been introduced to rejuvenate modelling and pharmacodynamic analysis, thereby expanding the quantitative assessment of response-time courses (Dayneka et al., 1993; Gabrielsson and Peletier, 2017; Nagashima et al., 1969). In the current account we further extend and develop this analysis with a comprehensive review of examples from the literature. Within this context we exemplify and discuss the importance of integrating *drug as well as target properties* in reversible and irreversible pharmacodynamic systems. This provides a background to the origin of the corresponding expressions and an illustration to how changes in target turnover may affect the *in vivo* drug-induced response outcome. It should be noted that specific target turnover (or half-life) may be different from the pharmacodynamic half-life (or *in vivo* biological half-life, biological half-life) as assessed from biomarker information (although related to target turnover) due to distributional- or transductional delays, or feedback being the rate-limiting step *in vivo*.

In vivo ‘open’ systems; reversible vs. irreversible ligand-target interactions

A reversible system can exhibit both bi-directional ligand-target binding interactions and removal of the ligand-target complex. In a living organism (*i.e.*, an *in vivo* ‘open’ system) situation, these three key components (free ligand L , free target receptor R , and target receptor-ligand complex RL) fluctuate over time. This is described by *Equation 1* where the dynamics of the free concentrations of L (drug) and of R (*i.e.*, free binding sites) depend on drug input In and first-order non-specific clearance $Cl_{(L)}$ of L , and on the zero-order turnover rate k_{syn} and first-order fractional turnover rate k_{deg} of free target R (see, **Figure 2**; second row, left), respectively. The changes in RL are governed by k_{on} and k_{off} for the L in question (the second-order association and first-order dissociation rate constant, respectively), and $k_{e(RL)}$ which is the first-order rate constant for irreversible loss via all relevant routes of complex removal (such as degradation, internalization, interstitial fluid turnover *etc.*).

$$\begin{cases} \frac{dL}{dt} = \frac{In}{V} - \frac{Cl(L)}{V} \cdot L - k_{on} \cdot L \cdot R + k_{off} \cdot RL \\ \frac{dR}{dt} = k_{syn} - k_{deg} \cdot R - k_{on} \cdot L \cdot R + k_{off} \cdot RL \\ \frac{dRL}{dt} = k_{on} \cdot L \cdot R - k_{off} \cdot RL - k_{e(RL)} \cdot RL \end{cases} \quad (Eqn. 1)$$

Thus, as evident from the above, the overall pharmacodynamic outcome in the *in vivo* context will depend on drug (ligand, *i.e.*, L) levels vs. input and elimination thereof (Cl) as well as affinity (*i.e.*, k_{off}/k_{on}) for its target R , but also on the actual levels, production (k_{syn}), and removal (k_{deg}) of R and of the target-ligand complex RL . From an *in vivo* biomarker- or clinical response perspective three key stages in the formation of a pharmacological effect may be discerned, *i)* the input and loss of the drug, which is only captured by the ‘open’ model (**Figure 2**, row 2); *ii)* the ligand-target binding process (k_{off}/k_{on}), captured by both the ‘closed’ *in vitro* - and ‘open’ *in vivo* models, target turnover- k_{deg} and complex kinetics $k_{e(RL)}$ captured exclusively by the ‘open’ *in vivo* model (**Figure 2**, rows 1 and 2); *iii)* transduction/conversion triggered by the target-ligand complex RL to a measurable *in vivo* (biomarker or clinical) response via a series of physiological- and mechanistic events (*e.g.*, amplification, feedback, synergy, buffering, parallel intertwined neuronal circuit processes), described by the Rho ρ parameter.¹

At equilibrium (*steady-state*), the relationships of free target R_{ss} (top line, *Eqn. 2*) and target-ligand complex RL_{ss} (second line) as functions of drug L_{ss} , and the *in vivo* potency expressions EC_{50} (third line) are described in *Eqn. 2* below (see, (Gabrielsson and Peletier, 2017) for a detailed derivation of the equilibrium relationships from the differential equation system in *Eqn. 1*). Note that the ‘open’ *in vivo* model derived from *Eqn. 1* will predict the same concentration EC_{50} for half-maximal drug-induced response of both free ligand L_{ss} and ligand-target complex RL_{ss} at steady state (*Eqn. 2*). RL_{ss} is indirectly predicted from free ligand L_{ss} via the nonlinear term in *Eqn. 2* (second line). However, an important observation is that the pharmacological response at steady-state, can be ‘driven’ by a nonlinear function of free ligand concentration L_{ss} , and the model parameters E_0 , E_{max} and EC_{50} (*Eqn.*

¹ Clinical efficacy is the maximum desired target-elicited effect, in the presence of a composite of integrated buffering, amplifying, and compensatory processes. Importantly, clinical efficacy is also limited to what is possible to attain regarding a specific functional response without jeopardizing patient health (safety, tox).

5, bottom line) which is numerically robust, conceptually pragmatic, and transparent from a translational point of view.

$$\left\{ \begin{array}{l} R_{ss} = \frac{k_{syn}}{k_{deg}} \cdot \frac{EC_{50}}{L_{ss} + EC_{50}} = R_0 \cdot \left(1 - \frac{L_{ss}}{L_{ss} + EC_{50}}\right) \\ RL_{ss} = \frac{k_{syn}}{k_{e(RL)}} \cdot \frac{L_{ss}}{L_{ss} + EC_{50}} = R_0 \cdot \frac{k_{deg}}{k_{e(RL)}} \cdot \frac{L_{ss}}{L_{ss} + EC_{50}} \\ EC_{50} = \frac{k_{deg}}{k_{e(RL)}} \cdot \frac{k_{off} + k_{e(RL)}}{k_{on}} = \frac{k_{deg}}{k_{e(RL)}} \cdot K_m \\ K_d = \frac{k_{off}}{k_{on}} \end{array} \right. \quad (Eqn. 2)$$

As seen from *Eqn. 2*, the ‘open’ system expressions now contain both free target turnover (k_{deg}) and complex kinetics ($k_{e(RL)}$) in addition to drug-target binding properties (k_{on} , k_{off}). Target turnover and complex kinetics are *in vivo* properties, therefore making *Eqn. 2* (third row) more versatile for translation across different species, particularly when species-specific terms for these parameters have been defined. The generic form of the ‘open’ *in vivo* potency expression EC_{50} in *Eqn. 2* allows predictions of efficacious concentrations of agonists, antagonists, inverse agonists and enzyme inhibition provided k_{on} , k_{off} , k_{deg} , and $k_{e(RL)}$ are known. The bottom row in *Eqn. 2* shows the expression of the ligand-target dissociation constant K_d . A graphical presentation of the *in vivo* potency EC_{50} expression in *Eqn. 2* is shown in Figure 3 (A-D).

Figure 3 approx here

As shown in the contour plots of *in vivo* potency EC_{50} (**Figure 3**) changes in k_{deg} and k_{off} (keeping $k_{e(RL)}$ set to 0.1 for comparisons around which k_{off} is varying) impact *in vivo* potency EC_{50} . Note the apparent plateau (‘ceiling’ effect) when $k_{off} < k_{e(RL)}$ (**Figure 3A**). In this situation, EC_{50} may be approximated by k_{deg}/k_{on} (irreversible system) and is still sensitive to changes in k_{deg} . For comparison, **Figure 3B** shows the influence of changes in k_{deg} and $k_{e(RL)}$ (with k_{off} set to 0.1) on *in vivo* potency EC_{50} . In contrast, when $k_{off} > k_{e(RL)}$, EC_{50} may be approximated with $(k_{deg}/k_{e(RL)}) \times (k_{off}/k_{on})$ (reversible system) and is still sensitive to changes in k_{deg} . **Figures 3C** and **3D** show the same simulations of *Eqn. 2*, but with EC_{50} presented on a log scale.

The exponential increase in *in vivo* potency EC_{50} stemming from concurrent higher values of k_{deg} and smaller values of $k_{e(RL)}$ (reversible system) is because of the multiplicative effect of changes in k_{deg} and

$k_{e(RL)}$. The graphical presentation of *in vivo* potency EC_{50} in Eqn. 2 thus i) distinguish between irreversible and reversible systems; ii) demonstrates individual contributions of k_{off} , $k_{e(RL)}$ and k_{deg} ; iii) illustrates determinants of necessary exposure; iv) gives the complex-to-free target ratio in k_{deg} -to- $k_{e(RL)}$; and, v) demonstrates that target turnover k_{deg} is always an important factor of EC_{50} and, hence, duration of pharmacological response. A typical example of the latter is proton-pump inhibitors where duration of action (suppression of acid secretion) is governed by the *de novo* synthesis ($t_{1/2kdeg}$) of proton pumps rather than by the (irreversible) drug-target interaction *per se*. Other examples include COX-1- and MAO-B inhibitors. Eqn. 2 is therefore applicable to both small- (Smith et al., 2018) and large (Gabrielsson et al., 2018a) molecule pharmacology.

As demonstrated above, *in vivo* potency thus contains information about route of target elimination, either via direct catabolism k_{deg} or internalization $k_{e(RL)}$ as a ligand-target complex. Increasing ligand concentrations pushes equilibrium further towards complex formation. The higher the ligand concentration, the more target is eliminated *via* the ligand-complex route ($k_{e(RL)}$). Hence, the higher the potency (*i.e.*, the lower its numerical value) the lower the necessary ligand (drug) concentration needed to drive target elimination *via* the complex route. At a ligand concentration equal to EC_{50} , when ligand impacts free target and complex equally (50%), the steady-state concentrations of free target R_{ss} and complex RL_{ss} are expressed as in Eqn. 3.

$$\left\{ \begin{array}{l} R_{ss} = \frac{k_{syn}}{k_{deg}} \cdot 0.5 \\ RL_{ss} = \frac{k_{syn}}{k_{e(RL)}} \cdot 0.5 \\ \frac{RL_{ss}}{R_{ss}} = \frac{k_{deg}}{k_{e(RL)}} \end{array} \right. \quad (Eqn. 3)$$

As evident from Eqn. 3 (bottom row), the steady-state concentration ratio of RL_{ss} -to- R_{ss} is governed by the $k_{deg}/k_{e(RL)}$ ratio. This therefore makes said parameters interesting also from a potency point of view (Eqn. 2). The intimate interdependence of pharmacology- and clearance-associated target dynamics factors is illustrated in **Figure 2**, and by the accompanying Eqns. 1-3 described above.

In certain situations, ligand binds to target, serves as a facilitator of target removal (see, (Chaparro-Riggers et al., 2012) and then returns to the free ligand pool. It is based on the 'Catch and Release Mechanism' in which the ligand is caught by the target and subsequently released when the ligand-target complex is cleared resulting in loss of target (Sarkar et al., 2002). The conceptual model for this process is referred to as *Ligand Facilitated Target Removal* (LFTR) which may be viewed as a form of "*ligand recycling*" (Peletier et al., 2021). A similar process is involved in the mechanism of

tocilizumab (Igawa et al., 2010), where a fraction of the ligand is returned to the free ligand pool and the remaining fraction is cleared via irreversible loss of complex. Other illustrative examples of LFTR include the selective estrogen receptor degrader (SERD) group of agents, *e.g.*, giredestrant (Liang et al., 2021), PCSK9 inhibitors (Hess et al., 2018), as well as an emerging number of drug classes aimed, *i.a.*, at cancer indications (Mullard, 2021).

Assessment of target turnover under different conditions

It is clear from the reasoning in the previous sections that states with alterations of the target turnover will affect the observed *in vivo* potency of a drug. In the current account we have chosen to focus on GPCR and enzyme targets, as these classes together dominate human targets for drugs in clinical use (see, (Rask-Andersen et al., 2011)).

While over time a number of novel methodological approaches to assess target turnover have emerged (*e.g.*, pulse-chase, proteomic analyses, protein synthesis inhibitors) it appears that these have mostly been applied in a ‘closed’ system context, and have different pros as well as cons (Morey et al., 2021). Regardless of assessment method it is also evident that the lifetimes of proteins vary widely between types and entities, depending on, *i.a.*, cellular environment and composition, subcellular fraction, function (*e.g.*, scaffolding, structural, synaptic), and abundance in different pathways, organelles, tissues, organs, or cells (*e.g.*, (Dorrbaum et al., 2018; Fornasiero et al., 2018; Price et al., 2010)). More recent methodological paths include developments in the organs-on-a-chip area (*e.g.*, (Sosa-Hernandez et al., 2018)), which may potentially further extend information gathering relevant to assess drug targets and PK features – however, still within a ‘closed’ system frame.

Notwithstanding the above, with few exceptions we find very little information derived from such methodologies pertaining to GPCR:s – targets to a therapeutically dominant class of drugs (*e.g.*, (Hauser et al., 2017; Sriram and Insel, 2018)). For comparison, there is a relative abundance of target half-life data for the latter type of agents using irreversible drug inactivation methods followed by monitoring of the time-course of receptor recovery *in vivo*. This ample literature source therefore to us represented a useful alternative approach to assess rates of target synthesis and degradation within the ‘open’ system setting². Agents used for the purpose include, *e.g.*, N-ethoxycarbonyl-2-ethoxy-1,2-dihydroquinoline (EEDQ; (Belleau *et al.*, 1968; Hamblin and Creese, 1983)), phenoxybenzamine (PBZ; (Nickerson and Goodman, 1947)), benextramine (Bodenstein *et al.*, 2005)),

² The target recovery half-lives presented in Tables 1, 2, and 4 are used as an *in vivo* proxy that may also encompass processes other than *de novo* target synthesis and degradation.

bromoacetyl-alprenolol menthane (BAAM; (Pitha *et al.*, 1982), and clocinnamox (Burke *et al.*, 1994), as well as a number of different irreversible enzyme and transporter inhibitors (*e.g.*, clorgyline, deprenyl, RTI-76).

The formation of permanent target complexes means that the normal recycling/trafficking process cannot impact k_{off} as drug dissociation from the target does not occur under these conditions (see further, (Norman *et al.*, 1987). Indeed, the protein synthesis inhibitor cycloheximide prevented the recovery of dopamine D2 receptors (D2R) after EEDQ treatment (Leff *et al.*, 1984), in line with the view that the contribution from recycled target receptors was negligible. The irreversible target inactivation approach therefore gives direct and useful information on the actual rate of recovery derived from *newly formed* GPCR molecules, a view supported by reports on corresponding increases at the mRNA transcription level (see, *e.g.*, (Raghupathi *et al.*, 1996b; Raghupathi *et al.*, 1996a). In addition, most literature studies use antagonist agents to label and monitor receptor sites to follow the rate of recovery. This avoids the potential confounding of shifts between low- and high-affinity states of one and the same target protein, as antagonists are considered to label the entire population indiscriminately. Indeed, there is data to suggest that recovery rates followed by means of agonist- vs. antagonist-labelled binding may not necessarily result in exactly the same figures (Nelson *et al.*, 1986; Ribas *et al.*, 1998).

Age vs. target turnover (Table 1)

It is well known that aging impacts drug dosing and responses (Andres *et al.*, 2019; Thurmann, 2020; Tumer *et al.*, 1992; Turnheim, 2003). The inevitable gradual decay of bodily function from adulthood to older age results in altered *pharmacokinetic* (PK; (Rowland and Tozer, 2011) but also *pharmacodynamic* (PD) characteristics. Age-related changes in drug uptake, distribution, metabolism, and elimination processes thus often necessitate adjustments relative to standard prescription dosages (Andres *et al.*, 2019). Several age-elicited physiological function modifications likewise contribute to this (*e.g.*, (Tumer *et al.*, 1992). However, less is known regarding shifts in target/transduction, circuit, and system homeostatic properties that may also influence the pharmacological treatment outcome in older as compared to younger adults (Levy, 1998).

Studies using irreversible target inactivation strategies in the rat and mouse suggest that turnover rates for receptor proteins normally become slower with age, across targets and tissues alike (possible exception: hippocampal 5-HT_{1A} sites; (Keck and Lakoski, 2000; Keck and Lakoski, 1996a), tentatively due to decreasing plasticity (*e.g.*, (Dorszewska, 2013; Mateos-Aparicio and Rodriguez-Moreno, 2019) in older compared to young subjects (**Table 1**). Thus, for example, following

annihilation of dopamine D2 receptors (D2R) the recovery rate is roughly 70% slower in senescent/aged as compared to young and mature rats (Kula *et al.*, 1992; Leff *et al.*, 1984; Norman *et al.*, 1987); likewise, recovery half-life of striatal D1 receptors (D1R) after EEDQ was ~65% slower in senescent than in mature rats (Battaglia *et al.*, 1988). In fact, the rat cerebral D1R and D2R appear to follow an almost identical log-linear correlation trajectory between age and turnover rate, with gradually slower rates from young to senescent animals (**Figure 4**). Similar observations have also been reported from rat studies of α - and β -adrenoceptor subtypes in heart, lung, and brain tissue regions (Pitha *et al.*, 1982; Zhou *et al.*, 1984), and of 5-HT₂ (Battaglia *et al.*, 1987) and mouse GABAA receptors (Miller *et al.*, 1991a) in different brain subregions. This is in accord with the key role of altered protein synthesis and degradation with age and senescence (*e.g.*, (Ryazanov and Nefsky, 2002), and may also be in line with a common, albeit not universal, increase in pharmacodynamic sensitivity seen in the elderly which agrees with a lowering of k_{deg} and therefore a subsequent increase in *in vivo* potency EC_{50} (*in vivo* EC_{50} numerically lower) (see, (Bowie and Slattum, 2007; Trifiro and Spina, 2011; Wanwimolruk and Levy, 1987). While changes in membrane receptor number and turnover thus represent an obvious underlying possibility here, modifications of intracellular transduction efficiency processes in old age may also contribute.

Consequently, it might be further predicted that depending on the afflicted organ (or subregion thereof) PD alteration-dependent drug dosing adjustments may be required towards optimization of therapeutic benefit in elderly patients. For example, the EC_{50} for the benzodiazepine GABAA enhancing agent midazolam to induce sedation/hypnosis was reported to be at least 50% lower in elderly compared to younger individuals despite similar PK parameters in both groups (Albrecht *et al.*, 1999; Jacobs *et al.*, 1995), thus warranting a dose reduction. Although there may of course be a number of different explanations, it is interesting to note in this context the nearly 3 times slower turnover of the benzodiazepine GABAA receptors in brain tissue of older compared to younger mice (**Table 1**; (Miller *et al.*, 1991a), a feature that if translatable may also contribute to the observations in man. Obviously, the chain of ligand-induced events for any biological response – from target and transduction processes, via circuit and tissue, to the whole-organism level – implicates multiple proteins. Thus, even if literature examples are sparse, it is highly likely that changes in protein turnover at one or more sites along the ligand-target-response chain may underlie a requirement for age-adjusted drug dosing (either jointly or in the absence of concurrent PK alterations). For agents engaging multiple targets in their mechanism of action the overall pharmacodynamic impact on function would also be expected to vary in relation to the affinities for the sites in question, but also to the corresponding relative target turnover rates – in turn, possibly leading to altered drug profile expressions in older compared to younger subjects. Within the context of drug research and

development it is therefore evident that consideration of age as a factor in the intended clinical treatment population may affect the projection from *in vitro* target data towards adequate (efficacious as well as safe) *in vivo* exposures for desired pharmacodynamic responses in humans. Since the fractional turnover rate k_{deg} of a target is a term in the *in vivo* potency EC_{50} expression of both reversible and irreversible systems it becomes evident how changes with size (body weight) in k_{deg} also impacts *in vivo* EC_{50} .

Regrettably very little turnover data are available in "non-adults". However, intuitively, it seems likely that such states would be decidedly much more variable and dynamic across stages (embryonic, fetal, infant, child/adolescent) overall, compared to adult and even aging conditions. Even if far more drugs are aimed at/used to treat adult (vs. "non-adult") diseases and disorders, further detailed insights into the particular target dynamic properties of the "non-adult" periods remain important tasks for future study also from a drug developmental and treatment perspective.

Table 1 approx here

Figure 4 approx here

Species and tissues vs. turnover (Table 2)

Any attempt to use target turnover information for drug response translation purposes inevitably needs to account for inter-species differences. While allometric predictions (for reviews of allometry principles, see: (Boxenbaum, 1982; Boxenbaum and Ronfeld, 1983) of *PK* variables are commonly based on the correlation of body mass to metabolic rate ("Kleiber's law", (Kleiber, 1947), it is less clear how translation of drug *PD* indices relates to species-dependent target turnover properties. In this regard, it is notable that Swovick et al. (Swovick et al., 2018) found a negative correlation of median fractional turnover rate k_{deg} values for the global proteome with maximal *lifespan* (i.e., faster protein degradation with shorter lifespan), but not with the adult body mass of 8 rodent species (~20g -> ~20kg). These authors also noticed that whereas there were clearcut species differences in the turnover across much of the proteome, turnover remained conserved for some proteins regardless of (rodent) species. Spector (Spector, 1974) further reported that there is a negative correlation between plasma protein turnover rates and animal longevity, including rodents, ruminants, and humans. The general applicability of these findings across target proteins and mammalian species remains to be established. Interestingly, and possibly concurring with the aforementioned (Spector, 1974; Swovick et al., 2018), the literature data for cerebral MAO-B protein

turnover half-life (days) for 5 different mammalian species (see, **Table 2**) seemed to correlate better vs. lifespan than vs. adult body (or brain; not shown) mass (**Figure 5**).

Table 2 and

Figure 5 approx here

Further, even though the very same target protein may be present in several different tissues throughout the body, turnover rates can vary significantly between locations, even within the same organ or tissue (see, **Table 2**). The half-life also varies among subcategories of receptor proteins responding to one and same transmitter (*e.g.*, 5-HT1B vs. 5-HT2A; **Table 2**). Although data from the same laboratory comparing rates between different organ tissues are scarce, the turnover of rat α 1-adrenoceptors was reported to be ~3-4 times slower in rat and rabbit brain than in submaxillary gland and spleen, respectively (Hamilton and Reid, 1985; McKernan and Campbell, 1982; Sladeczek and Bockaert, 1983). Similarly, the half-life of MAO-B in rat brain may be ~2-4 times slower than in liver, salivary glands, and small intestinal tissue (Goridis and Neff, 1971; Planz et al., 1972a; 1972b). It is relevant in this context that whereas cell types in the body differ in their dividing pace, the turnover of CNS neuronal cells is generally slow and sustained (Savage et al., 2007); although depending on function express a wide range of rates across the various cell constituents (*e.g.*, vesicular vs. receptor target proteins; (Dorrbaum et al., 2018). As a likely overarching principle, the functions of the specific target protein and dynamics of the associated complexes may determine the rate of turnover. Overall, data cited above are consistent with the observation that target half-lives in peripheral organs and tissues are often faster than in brain (see, *e.g.*, (Price et al., 2010), but also that turnover rates may vary among subregions and proteins within the brain and peripheral tissue (see further, **Table 2** for examples). Notably, Price et al. (Price et al., 2010) point out that turnover rates as determined *in vitro* vs. *in vivo* correlate poorly, possibly at least partly related to more rapid proliferation and less regulatory control in cultured cell lines compared to in a living organism. This further emphasizes the importance of knowledge of *in vivo* target turnover rates towards drug response predictions and translation efforts. Since the fractional turnover rate k_{deg} of a target is present in the *in vivo* potency EC_{50} expression of both reversible and irreversible systems it becomes evident from the compiled literature how species differences in k_{deg} also impact *in vivo* EC_{50} .

Most of the examples in **Table 2** involve pharmacological challenge. It is however worth noting the correspondence to data obtained using the Leu-incorporation methodology (*e.g.*, (Planz et al., 1972b), arguing that the pharmacological perturbation *per se* may leave the turnover process relatively untouched.

Target pool turnover vs. functional recovery

For biological responses to materialize, drugs or other ligands need to occupy molecular target proteins (*e.g.*, G-protein coupled receptors – GPCR, ion channels, enzymes, neurotransmitter transporters, polypeptides). However, there is a notable variation in the level of fractional occupancy (*i.e.*, proportion of targets occupied by a ligand) required for functional effect (see, *e.g.*, (Furchgott, 1966; Furchgott and Bursztyn, 1967; Grimwood and Hartig, 2009; Kenakin, 2016), and the level of receptor occupancy for a 50% response differs greatly for different agonists. What constitutes “adequate” occupancy thus differs between ligands and targets, but may also vary across tissues for one and the same target, and depending on the type of downstream effector response assessed – even within the same tissue (Hoyer and Boddeke, 1993).³

As most of the turnover data in **Tables 1, 2, and 4** represent studies of agents acting at GPCR:s, the discussion in the following section focuses on this therapeutically highly prevalent target class (*e.g.*, (Garland, 2013). The intrinsic activity or efficacy of a GPCR ligand describes its ability to trigger an intracellular transduction process *via* its target site – *i.e.*, defining stimulus ‘force’ – expressed relative to a defined full agonist (able to elicit 100% under the same experimental conditions (see, (Kenakin, 2013). For example, the neurotransmitter DA (by definition a full D2 receptor agonist) and the full D2 agonist NPA (N-n-propyl-norapomorphine) inhibit cAMP generation – one of the G-protein-mediated, immediate transduction pathways linked to said site – to a much greater extent than do partial D2 agonists like, *e.g.*, aripiprazole (Beaulieu and Gainetdinov, 2011; Jordan et al., 2007). This outcome may be envisaged in terms of ligand-induced changes in conformational states as a result of target binding, whereby agonists prompt (intracellular) second messenger amplification cascades and onwards signaling more effectively than do partial agonists, and antagonists fail to do so at all (intrinsic activity/efficacy = zero). However, for full (high-efficacy) agonists there is typically a non-linear relationship between drug-target occupancy and effect on functional output, as low receptor occupancy levels (2-30%) may suffice to trigger adequate – even near-maximal – functional responding (*e.g.*, (Grimwood and Hartig, 2009; Kenakin, 2016). In this situation a major proportion of available target sites therefore remain functional but temporarily idle/unoccupied, which reflects the high agonist sensitivity of the signaling pathway; aka ‘receptor reserve’ or ‘spare receptors’ (see, *e.g.*, (Kenakin, 2018; Neubig et al., 2003). For comparison, low(er)-efficacy agonists require high levels of target binding in order to elicit biological responses, and are often unable to reach maximal

³ In an “open” system context “occupancy” is defined as in **Table 3**.

functional responding even at target saturation in a defined assay system. Thus, the definition of efficacy for a drug along the agonist-antagonist spectrum is dynamic as it is expressly reliant on the size of the available receptor pool, and transduction function (Charlton, 2009). Consequently, efficacy may differ markedly, *i.a.*, between tissues (receptor amounts), responses measured, as well as upon alterations induced by disease states and chronic drug treatments thereof. As ligand efficacy is thus in part system-dependent, any given agent may behave as a full agonist for one tissue or particular readout while showing up as a partial agonist under other conditions (*e.g.*, (Kenakin, 2013). The interrelation between drug properties and number of receptor sites – and as a corollary, influences via target turnover thereupon (see, *Eqn. 4* below) – in any given situation is a thus central factor in determining response efficacy to an agent within a defined context.

From the above it follows that in order to reasonably gauge target turnover using functional *in vivo* output, an understanding of ligand efficacy in the system in question is vital (Grimwood and Hartig, 2009; Kenakin, 2017). To account for this element, the linear transduction factor ρ (*Rho*; being the signal or “stimulus” triggered in the cell by the ligand-target complex also known as the conversion of a chemical (complex concentration) or electrical (voltage) signal via amplification and/or feedback to a measurable *in vivo* pharmacological response (blood pressure, heart rate) is included to separate full and partial agonists from each other, and describe the efficacy parameter E_{max} (Choe and Lee, 2017). Hence, the *in vivo* efficacy parameter of a ligand, defined as the maximum drug-induced response by an individual ligand (E_{max} for stimulatory systems of agonists and antagonists, or I_{max} for inhibitory systems such as with inverse agonism), derived from *Eqns 1* and *2*, becomes

$$E_{max} = \rho \cdot \frac{k_{syn}}{k_{e(RL)}} = \rho \cdot [RL_{max}] \quad (Eqn. 4)$$

The *in vivo* efficacy parameter of ligand, E_{max} (or I_{max} if derived from inverse agonism), is the maximum obtainable response, composed by maximum complex concentration (RL_{max}) derived from $k_{syn}/k_{e(RL)}$ and the transduction factor ρ (strength of the ligand-target complex RL_{max} to elicit a pharmacological response; see above)⁴. Practically, E_{max} is the parameter obtained by fitting the Hill function (*Eqn. 5*, bottom line) to concentration-response- or response-time data where E_{max} is

⁴ The *in vivo* efficacy parameter E_{max} is observed in response-time data, maximum ligand-target complex concentration *in vivo* RL_{max} may be measurable in certain instances, which allows prediction of the transduction parameter *Rho*, ρ , from E_{max}/RL_{max} .

equivalent to the maximal drug-induced response as the ligand concentration approaches infinity (Choe and Lee, 2017; Gabrielsson and Weiner, 2016). *Eqn. 4* suggests that target synthesis k_{syn} and the degradation of ligand-target complex $k_{e(RL)}$ contribute to the overall capacity of the system (Gabrielsson and Peletier, 2017), rather than the ligand-target binding parameters *per se* (k_{on} , k_{off}). Elimination rate of complex $k_{e(RL)}$ is a shared parameter among *in vivo* potency and efficacy parameters, and hence connects these two pharmacological properties. A logistic expression of transduction ρ may in some cases be considered, provided supplementary information *in vivo* data is available and possible to access/extract.

The implications of the transduction (encompassing all steps involved in the conversion from a target-ligand complex concentration to a measurable pharmacological response *in vivo*) factor ρ are illustrated in a host of literature aimed at establishing the number of temporarily idle or ‘spare’ receptors (aka “receptor reserve”, see, ^{Error! Bookmark not defined.}), but also in some of the target inactivation-recovery studies cited in **Table 4**. In this regard, it was reported (Agneter et al., 1993; Pineda et al., 1997) that the recovery of $\alpha 2$ -adrenoceptor *function* was significantly faster than the regain of actual *target protein molecules*. This is in line with the view that high-efficacy agonists may produce a regain of function already by occupying relatively few receptors, *i.e.*, even low receptor-agonist ligand (*RL*) complex concentrations may elicit an adequate level of functional responding (Grimwood and Hartig, 2009). For comparison, return of target protein and functionality after inactivation of the DA transporter parallel each other (Rego et al., 1999). These latter observations agree with the high target binding required for functional responding in this target class (see above; (Grimwood and Hartig, 2009).

Table 4 approx here

A special case is when $k_{e(RL)}$ is equal to zero, which means that there is no irreversible loss of the complex as such via $k_{e(RL)}$. The ligand-target complex hence only functions as a storage pool, and can only be split into its principal parts *L* and *R* via dissociation – controlled by k_{off} . The free target concentration at steady-state R_{ss} returns to its baseline value R_0 since routes of production and loss of target are governed by k_{syn} and k_{deg} , respectively (Gabrielsson and Peletier, 2017; Gabrielsson et al., 2018a). This is a situation that may be observed as functional adaptation or ‘fading’ of the pharmacological response – “tolerance”. If suppression of the levels of free target (*e.g.*, antigen-antibody complexing) is the main goal, and proportional to pharmacologic effect, it will only be accomplished during a certain amount of time until target has returned to its baseline level and the

effect vanished. It is possible that the natural behavior of such a system might reflect a disequilibrium between ligand, target and complex rather than an example of functional adaptation.

Almquist *et al.* (Almquist et al., 2018) demonstrated the correspondence between *in vitro* (functional assays) and *in vivo* properties (EC_{50} by means of modelling) for a series of antilipolytic compounds (**Figure 6**).

Figure 6 approx here

An approximate estimate of the complex kinetics $k_{e(RL)}$ term is obtained by regressing the data in **Figure 6** of pEC_{50} (Y-axis) versus pK_d (X-axis), and inserting estimates of k_{deg} (denoted k_{out}) from Almquist *et al.* (Almquist et al., 2018). Unfortunately, plasma protein binding differences across compounds were not considered *in vivo*, which might potentially have improved the consistency between *in vitro* and *in vivo*, as was shown for a series of opioids (Kalvass et al., 2007) in mice. Similar *in vitro* and *in vivo* correlation data have also been collected for *in vitro* (K_i) and *in vivo* potency (EC_{50}) of benzodiazepines (Visser et al., 2003). These three examples illustrate good correlations between *in vitro* binding properties and *in vivo* potency EC_{50} for reversible systems – provided k_{off} is greater than $k_{e(RL)}$, and that k_{deg} -to- $k_{e(RL)}$ in Eqn. 2 of *in vivo* potency EC_{50} is a constant term across compounds.

Predictions of exposure levels for repeated dosing in animals *in vivo* are typically based on target *in vitro* IC_{50}/EC_{50} data, with the aim to attain a specific multiple of exposure above the *in vitro* potency. However, the required duration of exposure needed for a therapeutic pharmacological response can vary significantly, a point generally receiving very little attention. In fact, it is often implicit that predicted exposure coverage requires 24 hr/day for meaningful *in vivo* drug effects. Thus, based on the particular pharmacokinetic profile of a test compound a dosing rate (often involving multiple daily doses) may be set to ensure constant drug exposure at a pre-specified level of target engagement. However, if target half-life exceeds plasma half-life of drug with irreversible action (*e.g.*, proton-pump inhibitors), the duration of response will rather depend on *de novo* synthesis and half-life of the *target protein*. Conversely, if target half-life is shorter than plasma half-life of the drug, the duration of response will be determined primarily by the presence of drug at the target (*vide infra*).

The conventional notion of 24 hr/day exposure above a target concentration was recently challenged in the nicotinic acid (NiAc) treatment context (Kroon et al., 2017), emphasizing the importance of target biology integration with drug PK and PD features. Thus, these authors found that: “An *intermittent but not continuous NiAc dosing strategy, succeeded in retaining NiAc’s ability to lower*

plasma FFA and improve insulin sensitivity. Furthermore, a well-defined NiAc exposure, timed to feeding-periods, but not fasting-periods, profoundly improves the metabolic phenotype of this animal model". The discontinuous NiAc dosing approach hence minimized tolerance to the drug effect and lessened the impact with regard to counterbalancing feedback processes. Indeed, by incorporating biological properties such as turnover of the NiAc target and of insulin, Andersson *et al.* (Andersson *et al.*, 2019) succeeded in modelling and quantifying the inter-woven behavior of NiAc with FFA and insulin. The target turnover aspects described above is therefore also an example of a property to be considered within the multifaceted field of chronopharmacology (for a review, see (Dallmann *et al.*, 2014).

Pharmacological effect and target turnover – dependency on baseline states

In a typical closed *in vitro* system situation, the experimental set-up determines the (static) size of the target pool (*e.g.*, native tissue, or induced expression of a target in a select cell preparation), whether or not the readout is affinity only or a functional one (*e.g.*, receptor binding or the magnitude of a particular biosignal, respectively), and is also – needless to say – disconnected from fluctuations in drug/ligand exposure across time.

From a modelling point-of-view two principally different states may thus be envisaged: *i)* when the baseline target occupancy and effect *in vitro* is zero or negligible ('resting'), and *ii)* when the baseline activity is higher than the absolute zero, either as a consequence of endogenous ligand tone, or because target is constitutively active in the absence of ligand, or baseline variability due to unknown factors. Compared to *in vitro* controlled system assays (typically in non-native tissue or cells), the 'open', thermodynamically determined, *in vivo* situation confers many more options (variable receptor conformations, temperature changes, cell and tissue 'nutritional' fluctuations) for stimulating the receptor baseline behaviour. Thus, the situations described in *ii)* are more likely to be the case *in vivo*.

Figure 7 shows schematically the relationship between (A.) different maximum complex concentrations and the efficacy parameter E_{max} , and (B.) ligand concentration L and *in vivo* effect (solid blue line), free target concentration R (solid red line) and ligand-target complex (dashed red line), respectively. The pharmacological effect "Response" is a function of the baseline effect E_0 and the nonlinear E_{max} -function, where the efficacy parameter E_{max} and potency EC_{50} are model parameters (Eqn. 5).

Figure 7 approx here

$$\left\{ \begin{array}{l} EC_{50} = \frac{k_{deg}}{k_{e(RL)}} \cdot \frac{k_{off} + k_{e(RL)}}{k_{on}} \\ E_{max} = \rho \cdot RL_{max} = \rho \cdot \frac{k_{syn}}{k_{e(RL)}} \\ E_0 \propto \frac{k_{syn}}{k_{deg}} \text{ or constitutive activity} \\ Response = E_0 + \frac{E_{max} \cdot L}{EC_{50} + L} \end{array} \right. \quad (Eqn. 5)$$

We assume that the baseline effect E_0 is proportional to either an endogenous ligand-target interaction (at target baseline R_0) or to a putative constitutive activity level expressed by the target in the absence of ligand. In the former case, *i.e.*, endogenous ligand-target interaction, the endogenous species may be readily displaced by a more potent drug ligand L . The efficacy parameter E_{max} is the absolute difference between maximum drug (or ligand) induced effect *Response max* and the baseline effect E_0 .

The *in vivo* efficacy parameter E_{max} is mathematically expressed as the product of maximum ligand-complex RL_{max} ($k_{syn}/k_{e(RL)}$) and the transduction factor Rho (ρ) (Eqn. 5), and will be ligand and tissue specific. Here, ρ is presented as a linear scalar, but may in some instances be a nonlinear expression, provided independent experimental data support that. The use of a nonlinear ρ term multiplied by a nonlinear expression of L_{ss} is challenging from a numerical (overparameterization of embedded expressions), conceptual (which parameter contributes to what) and translational (how are products/ratios of parameters scaled across species) point of view.

Rho (ρ) is an additional parameter taking stimulus into account, which corresponds to transduction of RL_{ss} complex concentration into a pharmacological response (relative ability of a ligand-target complex to trigger downstream transduction events) – *i.e.*, a parameter defining stimulus strength of the ligand; a full agonist has a $\rho \gg 0$ which is greater than that of a partial agonist $\rho > 0$ or an antagonist where $\rho = 0$ (*i.e.*, $E_{max} = 0$). Analogously, when the ligand-target complex activity is less than the natural constitutive tone of the ‘naked’ target in the absence of a ligand (in the case of inverse agonism) there is an attenuation of the constitutive signal Eqn. 6 (**Figure 7, A.**) thus becomes

$$\left\{ \begin{array}{l} IC_{50} = \frac{k_{deg}}{k_{e(RL)}} \cdot \frac{k_{off} + k_{e(RL)}}{k_{on}} \\ I_{max} = \rho \cdot RL_{max} = \rho \cdot \frac{k_{syn}}{k_{e(RL)}} < 0 \\ Response = E_0 - \frac{I_{max} \cdot L}{IC_{50} + L} \end{array} \right. \quad (Eqn. 6)$$

to describe a maximum drug-induced response *lower* than the baseline activity E_0 (**Figure 7, A.**). The Rho parameter ρ is a conglomerate of multiple individual transduction processes (*e.g.*, target signaling cascades, cellular and tissue environments, physiological amplification and dampening processes, feedback *etc.*; *e.g.*, (Cooper, 2000) across different organs, which may well be species/strain-, sex-, and disease dependent. Rho (comprising all target-associated elements affecting the neuronal signal studied, conversion from a chemical or electrical signal to a pharmacologically measurable response) will for an inverse agonist ligand, change to a negative term in *Eqn. 6* (I_{max}) that is analogous to E_{max} in *Eqn. 5*. Inverse agonists are therefore said to have negative intrinsic efficacy (the ability to decrease the activity of a constitutively active receptor). Such agents may display different degrees of negative intrinsic efficacy, resulting in strong and weak (partial) inverse agonists, analogously to ‘classical’ agonist stimulatory intrinsic efficacy for full- (strong) and partial (weaker) agonists (Berg and Clarke, 2018; Costa and Herz, 1989).

Whereas *in vitro* assays may quite easily be set up to discriminate pure antagonist from inverse agonist properties of drugs at various targets, it is decidedly more difficult to differentiate in the *in vivo* situation (Berg and Clarke, 2018). Currently we are aware of only one drug that purports to derive its therapeutic efficacy from inverse agonism. The US FDA has recently approved pimavanserin as a 5-HT_{2A} receptor inverse agonist to treat psychosis associated with Parkinson’s disease (Cummings et al., 2014). Whether this is indeed the true molecular mechanism of pimavanserin remains to be further investigated, as according to a recent review constitutive activity at 5-HT_{2A} receptor sites may be rare *in vivo* (De Deurwaerdere et al., 2020).

Chronic drug treatments and disease states vs. turnover (Table 4)

Typically, the treatment of many physiological perturbations and disease states requires repeat drug administration over shorter or longer time periods. Although studies are not uncommon reporting net changes in the target density following different periods of chronic dosing, there is relatively little data on the impact of repeated drug treatment – and withdrawal thereof – on the *dynamics of target turnover* rates k_{syn} and k_{deg} that underlie the changes in receptor numbers.

Table 4 approx here

However, studies on D2R recovery following acute or more chronic depletion of endogenous DA, either by (6-OHDA-induced) denervation or repeated reserpine treatment, did find an acceleration of D2R reappearance (Leff et al., 1984; Neve et al., 1985), as might be expected for a compensatory process. Chronic monoamine depletion accompanying reserpine treatment likewise accelerated the return of cortical α 2-adrenoceptors (Ribas et al., 2001). These reserpine-induced accelerations of turnover were reported to primarily reflect an increase in k_{syn} rather than a decrease in k_{deg} , and to result in an increased density of (high-affinity state) receptors. For comparison, chronic administration of the NA-selective reuptake blocking antidepressant desipramine shortened the half-life of α 2-adrenoceptors in rat brain tissue, mainly via increased k_{deg} , although alterations in k_{syn} were also noted (Barturen and Garcia-Sevilla, 1992). Similarly, repeat administration of the bipolar disorder medication lithium resulted in a significant reduction of α 2-adrenoceptor half-life in the rat cortex (Carbonell et al., 2004), as did chronic MAO A inhibition by means of clorgyline (Ribas et al., 1993). Repeat ECS or citalopram treatment approximately doubled rat striatal D2R half-life, while limbic D2R turnover remained essentially unchanged (Nowak and Zak, 1991a). Repeat ECS treatment also enhanced striatal D1R turnover (Nowak and Zak, 1989) but did not modify the cortical α 1-adrenoceptor half-life (Nowak and Zak, 1991b) in the rat. Estrogen is known to modulate central D2R, and chronic estradiol in female ovariectomized rats lead to a slowing of striatal D2R recovery (Levesque and Di Paolo, 1991). Interestingly, Kuhar and collaborators (Joyce et al., 2006; Kuhar, 2009; Kuhar and Joyce, 2001; 2003) have also discussed in a series of papers the hypothesis that altered target turnover is an important contributor to the slow onset of the therapeutic as well as dependence-inducing actions of CNS-acting agents. Since the fractional turnover rate k_{deg} of a target is present in the *in vivo* potency EC_{50} expression of both reversible and irreversible systems it becomes evident from the compiled literature how chronic drug treatment and disease states changes k_{deg} also impacts *in vivo* EC_{50} .

Up- and down-regulation of target – Impact of k_{syn} , k_{deg} and $k_{e(RL)}$

As discussed above, repeat drug administration may result in pharmacological target up- or down-regulation. However, although an up- or down-regulation of target synthesis rate (turnover rate; k_{syn}) will impact the baseline level of target (R_0) and therefore change the efficacy parameter E_{max} of ligand L at steady-state, it will not affect the potency, EC_{50} (Table 5 and Eqns. 2 and 3). The explanation for this, is that efficacy will be determined by the *total concentration* of receptors but also by the transduction parameter ρ (Eqn. 4), which refers to the ligand-target complex stimulus strength, if different from endogenous agonists or baseline activity (R_0).

Different to ‘closed’ system predictions (Black and Leff, 1983; Stephenson, 1956), the present deliberations demonstrate that *in vivo* potency is not affected by the target expression level (R_0) *per se*. Instead, it is contingent on a conglomerate of fractional turnover rates of target and complex; hence, potency (Eqn. 2) is a function of binding and degradation rates (k_{deg} , $k_{e(RL)}$, k_{off} and k_{on}). For comparison, efficacy is composed by ligand-target complex expression level ($k_{syn}/k_{e(RL)}$) and the transduction parameter (ρ). Thus, ligand-target binding properties (k_{off} and k_{on}) *per se* will not influence the efficacy parameter (E_{max}) in the ‘open’ model. The relative impact of individual changes in the turnover parameters k_{syn} , k_{deg} and $k_{e(RL)}$, respectively, are shown in **Table 5** and **Figure 8** (see, Eqn. 2).

Table 5 approx here

A corollary of these expressions and reasoning is that an increase in the fractional turnover rate of ligand-target complex ($k_{e(RL)}$) alone, results in an increased ligand potency (the numerical EC_{50} value decreases) and decreased efficacy (decrease in the efficacy parameter E_{max}). In other words, the compound is able to operate at lower concentrations but displays less efficacy, provided transduction (ρ) remains the same.

Figure 8 approx here

In addition to drug-induced processes, cancerous and miscellaneous inflammatory states have also been reported to change (mainly increase) the rate of protein turnover (review, see, *e.g.*, (Biolo et al., 2003). Alterations in synthesis as well as breakdown have been described, the magnitude, distribution, and allocation of which also depends on the severity of the condition (Biolo et al., 2003; Fearon et al., 1988; Powell-Tuck et al., 1984). Myasthenia gravis, an autoimmune condition, appears associated primarily with enhanced breakdown ($k_{deg} \uparrow$) of the muscular ACh receptor protein (Appel et al., 1977; Sher and Clementi, 1984). For comparison, mice with the Ax^1 (ataxia) mutation display impaired GABAA receptor turnover, possibly associated with deficient protease activity, *i.e.*, reduced degradation ($k_{deg} \downarrow$) of the receptors (Lappe-Siefke et al., 2009). Other examples of likely alterations in target k_{syn} and/or k_{deg} as a consequence of the disease and medications thereof include Parkinson’s disease (increased levels of DA receptors, tolerance to L-DOPA treatment; *e.g.*, (Antonini et al., 1997), delayed onset of antidepressant drug action in major depressive states (downregulation of 5-HT, NA autoreceptors; *e.g.*, (Commons and Linnros, 2019),

neuroleptic-induced motor and psychotic supersensitivity conditions (tardive dyskinesia, DA supersensitivity psychosis; *e.g.*, (Stahl, 2017; Thompson et al., 2020), and reversal of such alterations upon withdrawal from drug treatment.

Based on these and several other examples (see, (Biolo et al., 2003) it appears reasonable to speculate that not only disease states like the aforementioned, but also numerous other less grave situations would be associated with alterations in the turnover of the whole or specific parts of the proteome; conditions including, *e.g.*, hormonal and nutritional state, day-night cycle, various forms of stress (surgical, trauma, environmental, etc.), to mention a few (*e.g.*, (Adam and Oswald, 1983; Biolo et al., 2003; Richardson and Rose, 1971).

Summary of target turnover-modifying influences

Taken together, it is evident that the rate of target turnover is subject to modification by several factors and conditions. Distinct variations are found across organs and tissues, as well as between species and stage of the life cycle. It is evident therefore that any of these may impact the translation of *in vitro* to *in vivo* pharmacodynamic outcome (*viz.* ‘closed’ vs. ‘open’ systems) and, in turn, predictions of drug responses from experimental animal work to clinical efficacy in man. Thus, to recapitulate, some key elements that may significantly influence target half-life are

- Age
- Species (and strain/ethnicity)
- Organ/tissue and region (/subregion)
- Chronic treatment/withdrawal and disease states

Hence, *in vivo* potency and efficacy should not be expected to be constant across species, age, tissues, or upon chronic drug treatment. Further, it appears reasonable to hypothesize that sex differences in target turnover may also play a role in observed male vs. female-related disparities in pharmacodynamic drug responding, although so far, such data remain scarce. In fact, barring studies addressing medications intended for female-specific conditions, most of the preclinical as well as clinical literature in general is still dominated by investigations carried out in the male sex. The topic of target turnover is no exception in this regard; this is indeed a limitation, and one that certainly deserves more attention. Apart from scattered reports (of conceivable clinical implication?; *e.g.*, (Abou Sawan et al., 2021; Farrell et al., 2021), sex differences in target turnover remain to be further documented and defined. Additionally, recent developments suggest that factors such as target genetic variants/SNPs, RNA stability, epigenetic effects, transcriptional and post- transcriptional

regulation, targets existing in protein complexes and/or in cellular sub-compartments, may also influence target expression, turnover, and net resultant output (Corradin et al., 2016; Esteller, 2008; Pereira et al., 2010). While not specifically addressed in the present review, it is clear that response differences may also result from diverse sub-cellular (micro- or nano-domains) locations of the targets, and involve various post-translational modifications, possible dimeric/heteromeric co-existence, partner proteins/lipids, etc.

Needless to say, the more defined and detailed knowledge about target turnover in a particular disease condition, the more precise prediction from *in vitro* and *in vivo* animal models to *in vivo* clinical target response. The relative importance and implications of the aforementioned factors thus need to be considered not only within the context of the actual intended therapeutic target but also taking into account characteristics of state and trait within the intended clinical treatment population.

Obviously, observed changes in target turnover may relate to alterations in target synthesis (k_{syn}) and/or breakdown (k_{deg}) as well as in the elimination of the target-ligand complex ($k_{e(RL)}$). In the following section these aspects will be further gauged and scrutinized, including associated examples of possible clinical relevance and impact.

In vivo EC_{50} compared to *in vitro* K_d – dependency on k_{deg} , k_{off} and $k_{e(RL)}$

A common misconception in drug discovery contexts is that unbound therapeutic concentrations (C_u) have to be a *fixed multiple* greater than *in vitro* potency (K_d or *in vitro* IC_{50}) in order to demonstrate a satisfactory pharmacological response *in vivo* (Jansson-Lofmark et al., 2020). They reported that over 70% of 167 drugs across various chemical and pharmacological classes have an efficacious C_u -to-*in vitro* potency ratio (Eqn. 7) of less than unity. In fact, 30 and 50 % of the compounds studied were found to have an *in vivo*-to-*in vitro* ratio of less than 0.1 and 0.3, respectively.

Occasionally, the *in vivo* potency of a drug exceeds the prediction from *in vitro* binding K_d (i.e., displaying an *in vivo* EC_{50} value numerically *lower* than its K_d), and *vice versa*. As shown in Eqn. 7 this depends primarily on the absolute size of k_{off} and $k_{e(RL)}$.

Case I: If $k_{e(RL)}$ is greater than k_{off} , the system behaves irreversibly and *in vivo* potency EC_{50} may be approximated by k_{deg}/k_{on} alone (see **Figure 9**). K_d is still k_{off}/k_{on} , and therefore the relative magnitude of the EC_{50} -to- K_d (*in vivo*-to-*in vitro*) ratio is governed by k_{deg}/k_{off} (Eqn. 7)

Figure 9 approx here

$$\left\{ \begin{array}{l} \text{Ratio} = \frac{EC_{50}}{K_d} = \frac{k_{deg}}{k_{e(RL)}} \cdot \frac{k_{off} + k_{e(RL)}}{k_{on}} \cdot \frac{1}{\frac{k_{off}}{k_{on}}} = \frac{k_{deg}}{k_{e(RL)}} \cdot \frac{k_{off} + k_{e(RL)}}{k_{on}} \cdot \frac{k_{on}}{k_{off}} \\ \frac{EC_{50}}{K_d} = \frac{k_{deg}}{k_{e(RL)}} \cdot \frac{k_{off} + k_{e(RL)}}{k_{off}} \\ \frac{EC_{50}}{K_d} = \frac{k_{deg}}{k_{off}} \text{ when } k_{off} \ll k_{e(RL)} \\ \frac{EC_{50}}{K_d} = \frac{k_{deg}}{k_{e(RL)}} \text{ when } k_{off} \gg k_{e(RL)} \end{array} \right. \quad (\text{Eqn. 7})$$

where k_{deg} represents turnover of the target and k_{off} the dissociation rate constant of ligand-target binding. This implies an essentially irreversible system, in which fractional turnover rate of target becomes more important for the level of the *in vivo* EC_{50} than does the ligand-to-target affinity parameters *per se*. Examples of this situation are discussed further below with proton pump inhibitors.

Case II: When $k_{e(RL)}$ is smaller than k_{off} , the system behaves reversibly and *in vivo* EC_{50} is approximated by $(k_{deg}/k_{e(RL)}) \times K_d$ (see, **Figure 9**). Hence, the relative magnitude of the EC_{50} -to- K_d ratio is then governed by $k_{deg}/k_{e(RL)}$ where k_{deg} represents turnover of target and $k_{e(RL)}$ loss of the (non-dissociated) target-ligand complex. If k_{deg} is smaller than $k_{e(RL)}$ the *in vivo* EC_{50} will be numerically lower (potency higher) than anticipated from the *in vitro* binding K_d . Therefore, conversely to Case I, complex loss $k_{e(RL)}$ plays a relatively greater role for the magnitude of *in vivo*-to-*in vitro* potency ratio than does k_{off} . Hence, it is evident that the magnitude of the target turnover k_{deg} influences the relation between *in vitro* and *in vivo* potency in both cases, and should not be ignored.

While the above clearly applies to most single therapeutic drug entities, how do you deal with the situation when a drug has (an) active metabolite(s)? A potential approach is to predict the active moiety of the parent and metabolite(s) at steady-state. For example, the M₃-muscarinic receptor antagonist tolterodine and its 5-OH-methyl metabolite have similar *in vitro* binding affinity (K_i 2.7 and 2.9 nM, respectively) at muscarinic receptors (Brynne et al., 1997; Nilvebrant et al., 1997). Brynne et al. (Brynne et al., 1999) therefore used the sum of the unbound concentrations of drug and

metabolite at steady-state as the active moiety. The corresponding efficacious unbound plasma concentration of active moiety-to- K_i ratio will then be less than 0.1. Again, this is yet another example consistent with the finding (Jansson-Lofmark et al., 2020) that a multiple of *in vitro* potency *greater than* unity is not a compulsory requirement for an acceptable clinical effect.

The *in vivo*-to-*in vitro* ratio is influenced by k_{deg} and will be less than unity if the turnover of target k_{deg} is slower than either complex kinetics $k_{e(RL)}$ or dissociation rate of complex into ligand and target k_{off} for reversible and irreversible systems, respectively. Recall though, that irrespective of the efficacious concentration C_u where a drug operates, the turnover of target will impact the 'Ratio', as EC_{50} is an element comprising *both drug and target properties* (see, Eqn. 7). Uncritical use of a 'Ratio' approach for ranking of drug candidates should thus be avoided unless a reasonable scientific foundation is at hand.

Examples of irreversible and reversible ligand-target interactions

Most therapeutically used drugs interact with their corresponding target(s) in a reversible, non-covalent, manner, but the pharmaceutical arsenal also contains several irreversibly acting agents of significant clinical importance. Below, we discuss examples of reversible as well as irreversible ligand-target interactions in relation to target turnover parameter impact, and consequences thereof.

We define an irreversible system as one where removal of the ligand-target complex as such ($k_{e(RL)}$) dominates over first-order dissociation of ligand-target complex (k_{off}). Irreversible ligand-target interactions are indeed utilized pharmacologically, *i.e.*, among acetylcholine-esterase-, COX-1, H^+/K^+ -ATPase- and MAO-B inhibitors (Arnett et al., 1987; Colovic et al., 2013; Freedman et al., 2005; Gedda et al., 1995; Kang et al., 2007; Mbonye et al., 2006; Vane and Botting, 2003; Wallmark et al., 1985). In these cases, the ligand off-rate (k_{off}) from complex is negligible in comparison to elimination of the ligand-target complex as such ($k_{e(RL)}$). The duration of the pharmacological effect will therefore depend on target *de novo* synthesis and its half-life. An example of this is the duration of effect of the gastric proton pump inhibition following a single dose of omeprazole. The pharmacokinetic half-life of omeprazole is about 1 hour in humans whereas the half-life of the proton pump falls in the range of 15-20 hours, thus making once a day dosing a practical approach (Wallmark et al., 1985). When the half-life of the target protein is shorter, plasma half-life and presence of drug become more important for the dosing interval and duration of response.

Using the derived generic expression of *in vivo* potency (EC_{50}) valid under a wide range of circumstances, the below illustrates the performance of an *irreversible* system. Here the removal of

ligand-target complex $k_{e(RL)}$ dominates over regeneration k_{off} of free ligand L and target R from the complex pool RL (see, Eqn. 8 and **Figure 8**). The route of elimination of the ligand-target complex RL will therefore indirectly be important to the elimination of *both* ligand and target *per se*.

Figure 8 approx here

Recall that for the *irreversible* system shown in **Figures 2** and **9**, the expression of *in vivo* potency from Eqn. 2 can be simplified to the ratio of k_{deg} -to- k_{on} (Eqn. 8).

$$\left\{ \begin{array}{l} EC_{50} = \frac{k_{deg}}{k_{e(RL)}} \cdot \frac{k_{off} + k_{e(RL)}}{k_{on}} \\ EC_{50} = \frac{k_{deg}}{k_{e(RL)}} \cdot \frac{k_{off} \ll k_{e(RL)}}{k_{on}} = \frac{k_{deg}}{k_{e(RL)}} \cdot \frac{k_{e(RL)}}{k_{on}} \\ EC_{50} \propto \frac{k_{deg}}{k_{on}} \end{array} \right. \quad (Eqn. 8)$$

The notion of drug-target residence time, defined as $1/k_{off}$ (Copeland, 2016; Copeland et al., 2006), deserves some comment in this context. Within this frame, and a ‘closed’ system setting, target off-rate may be an important factor determining drug potency K_d and *in vivo* effect duration (Bosma et al., 2017; Copeland, 2016; Dahl and Akerud, 2013; Hothersall et al., 2016; Lu and Tonge, 2010); but has also been questioned (Folmer, 2018). The concept of ligand-receptor ‘rebinding’, still based on a ‘closed’ system *in vitro* approach, has also been introduced as a potential contributory mechanism with implications for duration of drug action *in vivo* (Vauquelin, 2010; Vauquelin and Charlton, 2010), and it has further been argued that target saturation is an important component to extended duration of a pharmacological effect (de Witte et al., 2018). However, in an ‘open’ system, the loss of (non-dissociated) drug-target complex is an additional route of removal, and the drug-target residence time expression becomes $1/(k_{off} + k_{e(RL)})$. Therefore, despite a very small k_{off} – suggestive of a long drug-target residence time and an extended duration of response according to the ‘closed’ system nomenclature – rapid replenishment of target (k_{deg} fast) or removal of the ligand-target complex ($\sim 1/k_{e(RL)}$) can appreciably shorten the apparent residence time and hence duration of the drug-target effect (see also, (Corzo, 2006). On the other hand, even when the size of k_{off} and $k_{e(RL)}$ confers a short residence time, the response duration may still be substantial due to a slow regeneration of free target levels in an ‘open’ *in vivo* system (e.g., proton pump inhibitors; PPI). In the latter case, it is the target half-life that governs duration of response rather than the degree of saturation of the target system, as suggested by de Witte *et al.* (de Witte et al., 2018) using ‘closed’ model arguments.

An instructive example is a comparison of the new PPI IY-81149 and omeprazole (Kwon et al., 2001). The *in vitro* IC_{50} of H^+K^+ -ATPase activity of IY-81149 and omeprazole were 6 μ M and 100 μ M, respectively, demonstrating a substantial difference in the *in vitro* binding affinities to the target. Based only on relative *in vitro* binding, IY-81149 would have been expected to be about 15 times more potent than omeprazole *in vivo*. However, the potency difference was more or less abolished when the effects were studied in a dog model *in vivo* (e.g., histamine-stimulated gastric secretion in the Heidenhain pouch; (Kwon et al., 2001). No clinical differences were seen between compounds (Wang et al., 2019). This outcome is consistent with *Eqns. 2 and 8* and an irreversible system, where $k_{e(RL)} \gg k_{off}$ is required for irreversibility and hence *in vivo* potency is governed by target turnover k_{deg} ; thus, basically independent of further changes in k_{off} . It is evident that the notion about drug-target residence time according to ‘closed’ system nomenclature does not hold since k_{deg} – rather than k_{off} – will be the major determinant of pharmacological *in vivo* potency of an irreversible system (*Eqn. 8* and **Figure 9**).

If target half-life is longer than drug plasma half-life, the duration of response will be governed by *de novo* synthesis of target and the target protein half-life. This reasoning is applicable to irreversible target interactions (e.g., H^+K^+ -ATPase, COX-1, MAO-B; **Table 6**). Conversely, if the reverse is true – i.e., target half-life shorter than drug plasma half-life – the drug has to be present at adequate inhibitory concentrations throughout the desired duration of the pharmacological effect, since target loss (through $k_{e(RL)}$) is quickly replenished by newly synthesized target molecules.

Table 6 approx here

An interesting example is the COX-1 enzyme (prostaglandin-endoperoxide synthase, PTGS), involved in the generation of prostaglandins throughout body organs and tissues. Drugs that are inhibitors of this enzyme (aka non-steroidal anti-inflammatory drugs; NSAID), may be acting either reversibly (ibuprofen, naproxen) or irreversibly (acetylsalicylic acid; ASA). In the case of the archetypal NSAID, ASA, the COX-1 enzyme interaction is irreversible, and the duration of the biological effect thus entirely dependent on the turnover of the enzyme *per se* and/or the turnover of the COX-1-containing tissue. Despite a short plasma half-life of ASA (15-20 min), the return of platelet function to baseline thus occurs only after 72-96 hours, as a result of irreversible COX-1 interaction (Hong et al., 2008) and the slow regeneration rate of blood platelets. For comparison, ibuprofen and naproxen are both reversible and therefore much more short-acting COX-1 inhibitors (see, **Table 6**). The pharmacodynamic action of these agents is thus less dependent on fractional target turnover and more on ligand-target dissociation or ligand clearance *per se*. A slow off-rate (k_{off}) has been suggested to play a key role in the *in vivo* profiles of, i.a., LABA and LAMA (e.g., tiotropium; (Disse et

al., 1999) drugs for COPD treatment. However, although likely contributory, receptor kinetics may not be the full explanation for the clinical action duration and profiles of such agents (Sykes and Charlton, 2012; Sykes et al., 2012).

As discussed above, efforts to optimize compound affinity (*in vitro* binding potency) will be essentially futile if target a/o tissue turnover k_{deg} is faster than the dissociation rate k_{off} . In such a case the duration of response will be determined by the k_{deg} process. The 'open' model system allows estimation of potency of both reversible- and irreversible ligand-target interactions. The 'open' model additionally has the potential to explain the pharmacodynamic drug-interaction potential between two or more compounds.

For example, Hong *et al.* (Hong et al., 2008) studied the inhibition of platelet aggregation in a single-blinded, randomized, three-way crossover study. Single doses of aspirin (acetylsalicylic acid, ASA; 325 mg) and ibuprofen (400 mg) vs. concomitant administration of ASA and ibuprofen were studied in patients with musculoskeletal disorders and a high cardiovascular risk, with a 2-week washout between the study occasions. A substantial inhibition (77%) of platelet aggregation was seen within 2 hours and return to baseline values within 72-96 hours after ASA dosing. In contrast, treatment with ibuprofen alone *or together with ASA* resulted in *only a transient inhibition* of platelet aggregation, and a return of responding to baseline levels within 6-8 hours. The mechanism-based model of Hong et al (2008) contains a common single parameter comprising fractional turnover rate of target as well as complex, denoted k_{out} . The model includes irreversible loss of free enzyme by ASA and reversible binding by ibuprofen. The estimated half-life of enzyme activity was 33 hours, which markedly differs from the first-order dissociation rate half-life of ibuprofen from the target complex (5.6 h).

Superficially, it may seem paradoxical that there is an attenuated response (suppression of platelet aggregation) when ASA and ibuprofen were administered simultaneously as compared to when ASA is given alone. However, this may be attributed to the available target enzyme being occupied by ibuprofen binding (temporal protection as a reversible drug-target complex with slow irreversible loss of the ibuprofen-target complex *per se*) thereby shielding against (irreversible) simultaneous ASA interaction. This illustrates a pharmacodynamic drug-drug interaction which requires a strict dosing order of ASA (first) and ibuprofen or naproxen (later) taking into account both target recovery time (dependent on k_{deg}) and pharmacokinetic properties (plasma half-life) of ligand.

The combined interaction at equilibrium between ibuprofen and ASA is given by Eqn. 9 (Peletier and Gabrielsson, 2018).

$$R_{ss,ASA+ibu} = R_0 \cdot \left(\frac{1}{1 + \frac{k_{irr}}{k_{out}} \cdot C_{ASA} + \frac{1}{EC_{50}} \cdot C_{ibu}} \right) \quad (Eqn. 9)$$

and the second-order irreversible loss k_{irr} of ASA (denoted K in (Hong *et al.*, 2008).

What will be the outcome then if naproxen instead of ibuprofen is used together with ASA in the above patient category? Naproxen displays a more extensive irreversibility ($k_{out} > k_{off}$) than ibuprofen and also a much longer half-life in plasma (12-17 hrs), in addition to its higher potency (0.3 μ M) compared to ibuprofen (12 μ M; (Gierse *et al.*, 1999).

Using *Eqn. 9* for the interaction between ASA and ibuprofen using data from Hong ($k_{irr} = 0.152$ (mg \cdot L⁻¹)⁻¹ \cdot h⁻¹, $k_{deg} = 0.0209$ h⁻¹, Mw(ASA) = 180) yields

$$R_{ss,ASA+ibu} = R_0 \cdot \left(\frac{1}{1 + \frac{k_{irr}}{k_{deg}} \cdot C_{ASA} + \frac{1}{EC_{50,ibu}} \cdot C_{ibu}} \right) = R_0 \cdot \left(\frac{1}{1 + 40.4 \cdot C_{ASA} + 0.083 \cdot C_{ibu}} \right) \quad (Eqn. 10)$$

where $EC_{50,ibu}$ equals 12 μ M (Gierse *et al.*, 1999). The interaction model of ASA and naproxen is given as

$$R_{ss,ASA+nap} = R_0 \cdot \left(\frac{1}{1 + \frac{k_{irr}}{k_{deg}} \cdot C_{ASA} + \frac{1}{EC_{50,nap}} \cdot C_{nap}} \right) = R_0 \cdot \left(\frac{1}{1 + 40.4 \cdot C_{ASA} + 3.3 \cdot C_{nap}} \right) \quad (Eqn. 11)$$

where $EC_{50,nap}$ is 0.3 μ M (Gierse *et al.*, 1999) and all other parameters the same as for ASA in the ibuprofen model. It is evident from *Eqns. 10* and *11* that ASA has the greatest inhibitory impact upon platelet aggregation per mole of drug (40.4), followed by naproxen (3.3) and ibuprofen (0.083). The equilibrium model predicts that at fixed free plasma concentrations the irreversible effect of ASA will be 486 (=40.4/0.083) and 12.2 (=40.4/3.3) times more effective than the reversible effects of ibuprofen and naproxen, respectively.

A similar model of second-order target removal, with the same rate of removal for the target and ligand-target complex ($k_{deg} = k_{e(RL)}$), was used for assessment of H⁺/K⁺-ATPase turnover (half-life 15-20 h) in the dog after drug intervention of the proton pump inhibitor omeprazole (Äbelö *et al.*, 2002).

Irreversible ligand-enzyme target systems

Important but less common are situations with irreversible loss of the substrate-enzyme complex as such, and irreversible binding of substrate to the enzyme in question so that no enzyme is

regenerated from substrate-enzyme complex after binding. This permanent obliteration of the enzyme therefore affects the associated biological response until sufficient quantities of the enzyme protein have been produced again to restore functionality. The use of acetylcholinesterase (AChE) inhibitors such as poisonous nerve gases and similar agents with intended harmful effects are illustrative, including, *i.a.*, the recent incident with the organophosphorous chemical Novichok with potentially life-threatening consequences like convulsions, asphyxiation, and cardiac arrest (Greathouse et al., 2021; Steindl et al., 2021).

However, there are also multiple instances of irreversible enzyme inhibitors with important therapeutic uses. In addition to the COX-1 and PPI drug classes discussed above (see, (Singh et al., 2021), and associated text portions), penicillin is perhaps one of the most immediate examples that springs to mind. Penicillins act by covalently modifying the bacterial enzyme transpeptidase, thereby preventing the synthesis of bacterial cell walls and hence become bactericidal (Yocum et al., 1980). The dosing of such agents is however typically primarily based on *in vitro* estimates of minimum inhibitory concentrations (MIC) for bacterial growth, and a set ratio of (free) *in vivo* plasma exposures across time (*e.g.*, *AUC*) vs. the MIC level (Mouton et al., 2018). Regarding antibiotic therapies focus is still to use simple exposure metrics (*AUC*, C_{max} etc.) as a replacement of a more meaningful PD metric related to the mechanism(s) of action. It would be interesting to know whether a dosing approach taking into account the turnover of the actual enzyme target (*i.e.*, transpeptidase) would improve and refine the specificity and PK-PD modeling, to the benefit of treatment protocols – and downstream limiting antibiotic resistance development (see, *e.g.*, (Khan, 2016). A related example, this time with human cells, is cancer treatment where irreversible enzyme inhibitors (*e.g.*, 5-fluorouracil) may block certain growth-critical enzymes in cancer cells and thus act oncolytic. While drug tissue distribution and penetrance obviously are important factors for efficiency against different tumor varieties, perhaps studies of target turnover rates might also contribute to further optimize personalized PK-PD based cytostatic medication regimens? Irreversible GABA transaminase (GABA-T) inhibitors are used in the treatment of epilepsy (Ben-Menachem, 2011), and covalent unselective MAO inhibitors like phenelzine and tranylcypromine are still available as (license) options for affective disorder (Birkenhager et al., 2004). Similarly, to the aforementioned antimicrobial and antiviral cases, it remains an open question if taking target turnover into account in an extended PK-PD algorithm may help further optimizing treatment schedules in these latter conditions.

In the global pharmacotherapeutic armamentarium, irreversible target ligands are relatively scarce, but appear to have received a renewed interest over the last decade – perhaps at least partly related to oncology indications (Bauer, 2015). The overarching issue with covalently bound agents has been

the widespread view that they all carry increased safety and (on- as well as off-target) toxicity risks (see, (Bauer, 2015). Nonetheless, several irreversibly-acting ligands have provided therapeutically important advances in the treatment of a variety of human afflictions. Such agents include, *e.g.*, ASA, penicillin, rivastigmine, rasagiline, and a host of recent anti-cancer agent varieties. Furthermore, situations involving prolonged drug residence time (k_{off}) may be described as a pseudo-irreversible ligand-target interaction – thus, a variation of a strictly irreversible process where k_{off} and $k_{e(RL)}$ operate in the same time domain.

As discussed by Bauer (Bauer, 2015), some of the pros with irreversible or pseudo-irreversible agents include less frequent dosing (convenience to the patient), the potential for lower doses (due to high and prolonged efficiency against competing endogenous ligands), and less off-target issues. Naturally, these advantages need to be balanced against the theoretical risk for idiosyncratic toxicity, as well as the toxicity inherent in the reactive ligand chemistry *per se*. However, the irreversible drug approach should not be *a priori* discarded without a thorough benefit/risk analysis, particularly if the drug ligand design may produce tissue/target-directed selectivity. However, Bauer (Bauer, 2015) unfortunately also concluded – based on ‘closed’ system reasoning – that the k_{inact}/K_i metric for compound ranking is preferred over *in vivo* IC_{50} . As shown by Eqn. 8, a better metric would be k_{deg}/k_{on} for an irreversible system. Moreover, within the present context it is worth noting that dependent on the desired clinical outcome vs. indication, conditions involving targets with rapid turnover or requiring *only* short-lived or partial target response modification may be less accessible for irreversible ligand treatment (Bauer, 2015). This said, when both of these target aspects (rapid turnover, partial response) co-exist, an irreversible ligand may still be an option to trigger a useful clinical response.

Reversible ligand-target interactions

In the development of therapies to treat more or less severe excess gastric acid-induced afflictions (*e.g.*, ulcer, reflux), the historical approach relied on drugs that interact with ‘upstream’ targets influencing the acid secretion, such as, *i.a.*, antihistaminergic and anticholinergic agents. These medications may now be largely obsolete for the indications mentioned, as they have been replaced by compounds like omeprazole, lansoprazole and the like, the metabolites of which directly and irreversibly interact with the ‘downstream’ H^+/K^+ -ATPase-dependent pump in the gastric parietal cells, thereby inhibiting the final step of acid production (Wallmark et al., 1985).

To contrast with the irreversible proton pump inhibition resulting from omeprazole discussed above, it may be illustrative to consider and compare to the fate of a reversible ‘upstream’ treatment for the

same indication. Thus, an example of reversible drug (cimetidine) interaction with an endogenous ligand (histamine) is the therapeutic effect of cimetidine mediated by the histamine H2 receptor modulating acid secretion in the stomach. Since the target protein is the same for both cimetidine and histamine, the differences in *in vivo* potency values are primarily due to ligand-target binding affinities of these two reversible agonists, and not target turnover per se. The interaction model of two ligands acting on one target at equilibrium is given by Eqn. 12 for the 'open' *in vivo* system (Peletier and Gabrielsson, 2018)

$$R_{ss,Cimet+Hist} = R_0 \cdot \left(1 - \frac{C_{Cimet}}{C_{Cimet} + \theta \cdot C_{Hist} + EC_{50,Cimet}} - \frac{C_{Hist}}{C_{Hist} + \frac{1}{\theta} \cdot C_{Cimet} + EC_{50,Hist}} \right) \quad (Eqn.12)$$

where θ equals the ratio $EC_{50,Cimet}/EC_{50,Hist}$. Therapeutic plasma concentrations ($C_u = 0.8 \mu\text{M}$ at steady-state corresponding to a daily dose of 1 g) of cimetidine, taking human plasma protein binding into account ($f_u = 0.2$), corresponds to its *in vitro* binding affinity ($K_d = 0.79 \mu\text{M}$). Therefore, substantially lower *local* concentrations of cimetidine ($0.80 \mu\text{M}$ as compared to histamine $165 \mu\text{M}$) will suffice for 50 % acid reduction of free target. Since the partial agonist cimetidine exhibits very low efficacy, it will behave like an antagonist in presence of histamine. See also Lin (Lin, 1991) for review.

A reversible process removes free target (R) temporarily by pushing the ligand-target-complex equilibrium towards complex formation (see, **Figure 2**). This process is typically saturable and therefore requires substantial exposures beyond the potency to be efficient. Accordingly, the response duration will depend on target turnover and the ligand half-life. To achieve less frequent dosing, a long half-life – as for naproxen (12h) compared to ibuprofen (2h) – is thus favourable. The longer half-life of naproxen also allows time for more of the complex to be (irreversibly) removed as such. When free drug (ligand) levels then decline, equilibrium starts shifting back from complex towards free target and ligand. Thereby, as a consequence of diminished complex concentration the response begins to decline. High exposures (multiples of the potency) are therefore typically needed in order to fully execute suppression of free target and build-up of complex in order to maintain a reversible drug action over longer periods of time. For example, the reversible inhibitory action by cimetidine upon gastric acid-secretion modulating H1 receptors, requires high daily doses (~1 g of drug).

The reversible GSECR inhibitor (**Table 6**) has a plasma half-life of 2 hours in mice. Due to shorter target half-life (20 min) of GSECR in mouse brain tissue, the experimental compound needs to be constantly present at substantial exposure for adequate inhibitory effect. Assuming a similar relation

between drug and target half-life also in man results in a relatively large projected human daily dose (Gabrielsson and Weiner, 2016). Similarly, to the GSECR inhibitor, exposure is the rate-limiting factor also for the ACh-esterase (AChE) inhibitor donepezil, but in this case only low clinical doses (5 to 10 mg/d) are required (Doody et al., 2008). This may seem paradoxical, but is explained by *i)* the high bioavailability and low clearance of the latter (Lee et al., 2015) compared to the experimental GSECR inhibitor compound which has a very short half-life, and *ii)* the long target half-life of AChE vs. the very short of GSECR (**Table 6**). That is, even if the GSECR inhibitor compound half-life is ~6 times longer compared to its target (**Table 6**), a drug half-life of 2 h is simply not sufficient to provide for low and convenient dosing within a *reversible* mode of target interaction where instead a continuous exposure would be required. In fact, even if the GSECR drug had been acting irreversibly with the same half-life, it would have been challenging to produce a very much prolonged action given the rapid regeneration of its target. An interesting parallel is the pseudo-irreversible (slow k_{off}) AChE inhibitor rivastigmine, which due to its mode of target interaction coupled with the slow target turnover can be dosed in very low dosage (1.5-6 mg, *b.i.d.*) for clinical effect, despite a modest bioavailability (~40%) and very short drug half-life (~1h; (Jann, 2000)). The above examples again demonstrate the importance of integrating target- as well as drug-related (PK *and* PD) properties for optimization towards attaining clinically effective dosing regimens.

An *irreversible* process removes free target *R* permanently and newly synthesized target has to replenish the loss. This means that duration of response will depend upon – and potentially benefit from – a long *target* half-life, which determines time of return of target levels towards baseline. Therefore, a short *ligand* half-life does not exclude a long duration of response. An irreversible process, such as for PPI:s, may also show a faster onset of action as the removal of target is immediate. The irreversible PPI omeprazole requires low daily doses of 20–40 mg for effective and rapid reduction in acid secretion

A special case of reversible or irreversible action is when the pharmacological response discloses synergistic mechanisms. Synergism may be seen with combinations of drugs or during mono-therapy with agents carrying multiple mechanisms of action. An illustrative example of synergistic action in the same drug molecule on lipid metabolism, is shown for the anti-lipolytic compound tesaglitazar (Oakes et al., 2005). The simultaneous reversible inhibition of fatty acid production (50% reduction of k_{syn}) and stimulation of plasma fatty acid loss (5.8-fold increase in k_{deg}) resulted in a dramatic synergistic (multiplicative) effect in Zucker rats after three weeks of treatment at a single dose level. The authors concluded that thiazolidinediones ameliorate hypertriglyceridemia by lowered hepatic triglyceride (TG) production and augmented TG clearance. This highlights how a mechanism-based

pharmacodynamic ('open') model demonstrates its superiority over 'closed' systems in analyzing and communicating complex pharmacodynamic processes. Similar results have been obtained also for other thiazolidinedione derivatives (Oakes et al., 2001). The assessment of drug interactions relevant to pharmacodynamic turnover models have been provided elsewhere (Earp et al., 2004; Gabrielsson and Weiner, 2000; Peletier and Gabrielsson, 2012).

To summarize, drug efficacy primarily impacts the onset and intensity, whereas potency impacts onset and effect duration, particularly for irreversible reactions.

The examples discussed above further emphasize the advantages of 'open' vs. 'closed' system approaches. As shown by these cases, inclusion of target (a/o tissue) dynamics together with knowledge of ligand-target interaction characteristics and ligand pharmacokinetics further increases the precision in predictions of *in vivo* concentrations to elicit defined drug responses. It is therefore worth highlighting the need to assess each and every new drug candidate on a uniquely case-by-case basis, taking into account turnover of its intended target, the type and characteristics of ligand-target interaction, as well as clearance of the ligand itself. Only by doing so, improvements in the precision of projections to clinical properties and usage may be achieved.

Key insights and translational potential of new in vivo potency expression

If the major component in a pharmacological response was only derived from ligand-target binding, this alone would still not explain why two different subjects may require different doses at steady-state, provided their bioavailability and clearance are the same. However, differences in the target turnover may help to explain differences in the actual requirement of drug. New expressions of *in vivo* potency (Eqn. 2) and efficacy (Eqn. 5) show that these are inextricably linked via target turnover.

The data of Betts *et al.* (Betts et al., 2010) demonstrates the translational power of the 'open' model explanatory potential in *in vivo* pharmacology. **Table 7** shows the *in vitro* dissociation constant K_d for humanized prototype anti-Dickkopf-1 IgG2 antibody against osteoporosis, and the corresponding *in vivo* potency EC_{50} values predicted from these data by means of Eqn. 2.

Table 7 approx here

These data illustrate the discrepancy across different species with respect to target binding affinity (>30 fold) and *in vivo* potency (10-fold). Clearly, using the target affinity data of rat or monkey as

guidance of human doses in this case will gravely misdirect predictions of dose. Even though the EC_{50} -to- K_d ratios of rat and monkey are similar (= 64 and 66), the markedly slower target k_{off} in man is accompanied by a 10-fold higher *in vivo* potency and an EC_{50} -to- K_d ratio of 188. These observations unequivocally stress the important role of including target turnover in defining efficacious concentrations, and thereby the required dose. *In vitro* binding affinities clearly underestimate necessary drug exposure and human dose predictions and may therefore result in (costly) late phase project failure. In this regard, while *in vitro* target binding affinity (defined by the physico-chemical parameters k_{off} and k_{on}) may be similar across species they may also differ significantly, shown in **Table 7** (e.g., k_{off} varies 100-fold but k_{on} only 6-fold), and thus give rise to major ‘downstream’ effects on translational efforts during drug development.

Target-mediated drug disposition (TMDD) captures the capacity-limited binding and/or loss of drug via its ‘target’ (receptor, enzyme, transporter etc.), such that this interaction impacts the disposition of the drug. This phenomenon is commonly observed for antibody kinetics with high ligand specificity, where ligand and target often appear at equimolar concentrations. So far, it has received rather little attention for small molecules, but might become important also in clinical studies of such entities (An, 2017; 2020; Smith et al., 2018; van Waterschoot et al., 2018). All in all, understanding the biology of the target – including expression level and target turnover properties – is therefore necessary in drug discovery programs for enhanced benefit/risk precision prior to delivering drug candidates to humans.

Chronic diseases imply repeated dosing and steady-state, and several therapeutic biologics agents have been developed aiming at selective and efficient treatments for, e.g., inflammatory states. In a commendable aim to address unresolved issues in drug efficiency against different autoimmune diseases, a minimized physiologically based pharmacokinetic model (mPBPK) was recently used to assess the role of tissue fluid turnover rate on the magnitude and duration of soluble target suppression by therapeutic antibodies (Li et al., 2018). In this work, simulations were used incorporating fractional turnover rate of interstitial fluid (ISF) to explain and classify the therapeutic outcome in Crohn’s disease vs. arthritis-associated joint synovium across a series of antibody compounds. It was concluded that, *i.a.*, ISF turnover rates strongly influenced the speed of drug-target complex removal, particularly in situations with slow ligand-target binding kinetics (k_{off}). Although the paper did not discuss target turnover *per se*, we were curious as to whether application of our derivations of the ligand-target and ligand-complex equilibrium relationships coupled to the mechanistic expression of *in vivo* potency (Eqn. 2) could further enhance the transparency of the

findings. This notwithstanding, the duration of a pharmacological response may still be rate-limited by target half-life.

As discussed above, *in vivo* potency of Eqn. 2 (see also, **Figure 3**) of *in vivo* potency summarizes the interrelations of target- and drug-associated properties, covering the entire spectrum from reversible (governed by k_{off} and binding) to irreversible interactions (governed by $k_{e(RL)}$ representing *all routes* of first-order ligand-target complex loss), and demonstrates the importance of target turnover (k_{deg}) in both situations. Thus, Eqn. 2 demonstrates that for irreversible systems *in vivo* potency will be governed by k_{deg}/k_{on} (primarily determined by target turnover and association rate; fast k_{on} is favoured) whereas the $(k_{deg}/k_{e(RL)}) \times (k_{off}/k_{on})$ relation governs reversible interactions (*i.e.*, primarily determined by target turnover, complex loss and binding properties; high affinity binding will be favoured). Applying Eqn. 2 on the data by (Li et al., 2018), but with $k_{e(RL)}$ replacing the ISF turnover-based expression, we find that this may be an alternative, and transparent option to help prioritizing compounds in development of therapeutic antibodies for various diseases (see, **Figure 10** below). Note that target loss k_{deg} is still an important factor to consider in both cases.

Figure 10 approx here

The use of ‘Minimal Anticipated Biological Effect Level’ (MABEL) approach is recommended for high-risk medicinal products for first-time-in-human dose predictions (EMA, 2018). The MABEL is the anticipated dose level leading to a minimal biological effect level in humans. The calculation of the MABEL dose should consider target binding and receptor occupancy studies *in vitro* in target cells from human and the relevant animal species and exposures at pharmacological doses in the relevant animal species. However, the MABEL-approach of human dose predictions of bi-specific antibodies may not be directly applicable using binding affinity K_d (Saber et al., 2019). A tumor cell (target as such) has typically a slower turnover k_{deg} (longer half-life) than the bispecific ligand-target complex $k_{e(RL)}$. Tumor shrinkage will therefore increase via the complex since $k_{e(RL)}$ is faster than k_{deg} of the tumor cell *per se*. Since k_{deg} -to- $k_{e(RL)}$ ratio in Eqn. 2 is less than unity, the *in vivo* potency EC_{50} will be higher (numerically less) than predicted from K_d (MABEL-approach). Therefore, the conclusions by Saber *et al.* (Saber et al., 2019) indirectly support application of the ‘open’ model expression of *in vivo* potency (Eqn. 2) for first-time-in-human (FTH) dose predictions of bispecifics, rather than commonly used receptor occupancy K_d .

Recently, van Waterschoot *et al.* (van Waterschoot et al., 2018) highlighted the poor knowledge of the actual target concentration commonly encountered in small-molecule discovery projects. The consequences of this lack of target information can range from unreliable compound potency to

highly variable pharmacokinetics. Smith *et al.* (Smith et al., 2018) conclude that TMDD phenomena are more common for small molecules than currently appreciated and should be factored into discovery projects. *Eqn. 2* show that *target* properties are equally important to ligand binding characteristics (Gabrielsson and Peletier, 2017; Gabrielsson et al., 2018a; b; Gabrielsson and Hjorth, 2018). A high correlation between *in vivo* potency EC_{50} and *in vitro* K_d relationship is not to be expected unless $k_{deg}/k_{e(RL)}$ in *Eqn. 2* is a constant term across compounds (see also **Figure 6**). It is not surprising that this correlation fails for *irreversible* systems, since *in vivo* potency EC_{50} is proportional to k_{deg}/k_{on} and therefore less affected by ligand-target binding changes (**Table 3**).

Inter-species scaling of in vitro and in vivo PD properties

Background and pruning of data

Inter-species scaling of pharmacodynamic PD properties aims at quantitative prediction of parameters responsible for onset, intensity and duration of a pharmacological response in different species. Following mechanism-based modelling of biomarker data, results need to be verified by extended approaches to assess factors influencing target function. To our knowledge, few studies specifically anchor their kinetic-dynamic modelling efforts to encompass properties derived from target behaviour *per se* (e.g., turnover). This makes modelling results less reliable, particularly for inter-species scaling of pharmacodynamic PD properties. Hence, not only the origin and quality of *in vitro* and/or *in vivo* data but also the methods for PD scaling have to be scrutinized.

The pharmacological response is typically expressed by means of the Hill-function including a baseline parameter (*Eqn. 5*, bottom) E_0 (see, (Choe and Lee, 2017; Danhof et al., 2007; Gabrielsson and Weiner, 2016; Mager et al., 2009). The baseline E_0 may be a single parameter (constant) or function (of, e.g., time or an endogenous ligand concentration). E_0 may be due to biological variation such as diurnal oscillation, endogenous ligands, stress, disease or potentially constitutive activity. E_0 is often a conglomerate of processes that, in summary, are displayed as a baseline response. Typical biomarker responses are blood pressure, heart rate, depression scores, body weight, body temperature etc, that all originates from a baseline time course prior to drug administration. Two additional parameters, the *in vivo* potency EC_{50} and the efficacy parameter E_{max} are defined as in *Eqns. 2-5*. One regresses the Hill function simultaneously to (two or more) response-time profiles letting the plasma ligand concentration-time course 'drive' the response, and then simulate (with the final parameter estimates) the steady-state ligand concentration-response relationship. The efficacy parameter E_{max} (Choe and Lee, 2017) is the absolute distance between the maximum response and the baseline in a concentration-response plot. If RL_{max} is measured it can be input as a constant and Rho, ρ , as a model parameter to be estimated. If some of the target- and binding properties k_{deg}, k_{off}

and k_{on} are known for a particular species (or humans), the $k_{e(RL)}$ parameter can be estimated in the *in vivo* potency expression.

Prior to use for comparisons across species, any confounding covariates such as plasma protein binding, active or interactive metabolites or endogenous agonists to a PK or PD parameter must be accounted for. As a first step, data *pruning* should be performed to make sure that systemic exposure, aka *unbound* plasma concentration, is used across species (Benet and Hoener, 2002; Rolan, 1994; Smith et al., 2010). Chronic indications and treatment imply PD and PK equilibrium between plasma and target tissue. Under these conditions, the steady-state unbound plasma-to-unbound tissue/biophase concentration ratio will form a constant ratio. This ratio may be less than, greater than or equal to unity but remains constant nevertheless; therefore, the unbound plasma concentration serves as a relevant proxy reference for assessment of *in vivo* potency. Time-variant influences – *e.g.*, as a consequence of (patho-)physiological drift factors – on the biophase may include perfusion rate fluctuations, energy and protein turnover (Fearon et al., 1988; Pich et al., 1987), capillary permeability, transporters (Peletier and Gabrielsson, 2018), drug metabolism (Zanger and Schwab, 2013) and disease progression (Holford and Nutt, 2008), have to be incorporated into the prediction as complementary steps. The interplay between unbound plasma- and tissue concentration is schematically illustrated for simple diffusion, active transport, clearance *etc.* in **Fig. 11**.

Figure 11 approx here

Because the unbound plasma concentration is less influenced by species-dependent plasma protein binding differences, conversion from total to unbound plasma concentrations should be performed for each species. As discussed above, the unbound plasma concentration is a proxy for the thermodynamically active exposure at the target biophase and hence indirectly ‘*drive*’ pharmacological response at equilibrium. Unbound plasma concentrations represent both practical experimental measures (easily measured in all mammalian species including humans) and may be used for translational purposes. Together with unbound clearance the free drug concentrations determines the oral dose necessary for therapeutic effect, and will be of importance for assessment of safety data as well (Miida et al., 2008). In conditions with adequate knowledge of (peripherally located) targets and corresponding dysfunctional tissue – including ability to sample actual tissue levels of the ligand – assessment of potency has to consider plasma-to-target tissue concentration differences (Kalvass et al., 2007). This situation has recently been addressed conceptually (Peletier and Gabrielsson, 2018).

Use of the equilibrium unbound drug concentration C_u in plasma coupled to a robust and meaningful PD biomarker is a good strategy for cross-compound comparisons and for developing kinetic-dynamic relationships, irrespective of reversible- or irreversible mechanisms of action. An excellent review of drug concentration asymmetry in tissues *versus* plasma addresses this topic for small molecule-related modalities (Zhang et al., 2019). Additional information on how endogenous ligands (Kroon et al., 2017), active or interactive metabolites (Obach, 2013), and target expression in animals and humans (Simon et al., 2013) are applied, may be helpful in cross-species pruning of data (Levy, 1998).

Concepts of allometry

Let us briefly review how inter-species scaling is done and then give a few recent examples related to mechanistic interpretation of modelling output with related problems and pitfalls. We start by focussing on the most commonly used approach, namely allometry. Allometry, in its broadest sense, describes how the characteristics of for example mammals change with size. Adolph (Adolph, 1949), Boxenbaum (Boxenbaum, 1982), Kleiber (Kleiber, 1947), and Schmidt-Nielsen (Schmidt-Nielsen, 1984) provide seminal background reviews. Allometric relationships are given as power functions

$$Y_{animal} = a \cdot BW_{animal}^b \quad (Eqn. 13)$$

where Y is the physiological- (*e.g.*, blood flow), pharmacokinetic- (*e.g.*, clearance) or pharmacodynamic (rate constants in the *in vivo* potency or efficacy expressions) variable, BW the body weight of the particular animal (or human), and a and b are allometric parameters. When scaling properties from animals (*e.g.*, primate) to man, the allometric relationship between the two species becomes

$$Y_{human} = Y_{primate} \cdot \left(\frac{BW_{human}}{BW_{primate}} \right)^b \quad (Eqn. 14)$$

where the scaling factor is the body weight ratio human-to-primate raised to the allometric exponent b . Y_{dog} has to be the absolute parameter based on the total body weight and *not normalized per kg*. In the 'open' model (Eqns. 1, 2 and 5) we have the three important properties (k_{deg} , k_{off} , $k_{e(RL)}$) expressing *in vivo* potency which guide the operating concentration range in many situations. As first-order rate constants a practical approach is to use simple allometry (Equations 13 and 14) or use independent (literature) data for inter-species predictions (Gabrielsson and Weiner, 2016; Gosset et al., 2017). The fractional rate constant k_{deg} of target can be scaled according to

$$k_{deg,human} = k_{deg,animal} \cdot \left(\frac{BW_{human}}{BW_{animal}} \right)^{-b} \quad (Eqn. 15)$$

where BW and b (-1/4 power law with typical range 0.1-0.3 for first order rate constants; (Gabrielsson and Weiner, 2016) denote body weight and the allometric exponent, respectively. Scaling the apparent synthesis rate $k_{syn,human}$ (with units amount/(volume · time)) of target is done by multiplying the target expression level in humans $R_{0,human}$ by the scaled fractional rate constant of target k_{deg} .

$$k_{syn,human} = R_{0,human} \cdot k_{deg,human} \quad (Eqn. 16)$$

If clearance of target $Cl_{trg,human}$ and target expression level $R_{0,human}$ are known, the corrected synthesis rate $k_{syn,human}$ (with units amount/time) of target becomes

$$k_{syn,human} = R_{0,human} \cdot Cl_{trg,human} \quad (Eqn. 17)$$

Since parameters like, organ blood flows, clearances and synthesis rates requires energy often follow the $\frac{3}{4}$ power law, the corrected synthesis rate $k_{syn,human}$ will also scale in a similar way. Hence, target synthesis rate (amount/time) k_{syn} may be scaled from animal data according to

$$k_{syn,human} = k_{syn,animal} \cdot \left(\frac{BW_{human}}{BW_{animal}} \right)^b \quad (Eqn. 18)$$

where the allometric exponent falls in the range of 0.6-0.9 ($\frac{3}{4}$ power law see (Adolph, 1949; Schmidt-Nielsen, 1984) and similar, for how clearance is predicted. For practical case studies and inter-species scaling concepts see text book by Gabrielsson and Weiner (Gabrielsson and Weiner, 2016).

Physiological time (e.g., half-lives) may be scaled by means of Eqn. 19

$$time_{human} = time_{animal} \cdot \left(\frac{BW_{human}}{BW_{animal}} \right)^b \quad (Eqn. 19)$$

where the allometric exponent falls in the range of 0.2-0.3.

Literature case examples

The following list of inter-species scaling case examples is not intended to be exhaustive, but nevertheless demonstrates some problems and solutions commonly encountered in the literature.

Frequently, studies lack accounting for plasma protein binding differences across compounds and

species, resolving the contribution of active or interactive metabolites, incorporation of endogenous ligands, considerations of the link between the biomarker applied and the target function, and consolidating modelling results with independent literature data.

A recent report studied TNF_α turnover after LPS challenge, listing half-lives of the inflammatory marker TNF_α in mice, rats, and humans without reference to a specific target behaviour (Larsson et al., 2021). The approach was a meta-analysis of several preclinical studies in rats comparing the anti-inflammatory activity of new compounds with roflumilast. Proper assessment of unbound plasma concentrations, active metabolites and a clear link to target function was however lacking.

Gosset *et al* (Gosset et al., 2017) presented interesting data on fractional turnover rates k_{deg} (denoted k_{out}) as a function of size (body weight) of the core body temperature in mice, rats and dogs upon intervention with PF-05105679, a moderately potent TRPM8 ion-channel blocker evaluated for the treatment of cold pain sensitivity. In this case, however, results were not validated by independent turnover data of the intended TRPM8 target, and the model also failed to account for feedback – a central mechanism in body temperature control.

In a retrospective analysis, Ito et al (Ito et al., 1997) found a high correlation ($r^2 = 0.961$ and slope 1.038) between the unbound plasma concentration C_u and dissociation constant K_d of 19 benzodiazepines BZ when aiming at 40-60 % occupancy at the GABA-BZ site *in vivo*. Visser *et al*. (Visser et al., 2003) compiled similar data between the EEG effects of nine prototypical GABA_A receptor modulators (six benzodiazepines, one imidazopyridine, one cyclopyrrolone, and one β -carboline) and their *in vivo* ‘closed’ model receptor affinity. Again, no quantitative information was given about the target receptor beyond drug-receptor affinities in spite of available quantitative literature data (Borden et al., 1984; Lyons et al., 2000) that might otherwise have been used for consolidating the validity of modelling results.

In a seminal paper by Kalvass *et al*. (Kalvass et al., 2007) results of seven opioids were presented, with a high *in vitro* K_i to *in vivo* EC_{50} correlation ($r^2 = 0.995$) when data were corrected for plasma protein binding differences across compounds and species. This suggests that the unbound plasma concentration C_u is a better predictor of PD response than total plasma concentrations. The authors discussed why *in vivo* EC_{50} values correlated better with receptor binding K_i values than with EC_{50} values obtained from *in vitro* ^{35}S GTP γ S experiments. It should be noted that K_i measures affinity only, whereas *in vitro* ^{35}S GTP γ S EC_{50} (*i.e.*, functional) values may be contaminated by other parameters in a non-steady-state cell system.

Acute dosing estimates of total *in vivo* potencies uncorrected for plasma protein binding of dual G-protein-coupled receptor 81/109A (GPR81/GPR109A) agonists were compared to their *in vitro* binding data (Almquist et al., 2018). The analysis made no efforts to dissect *in vitro/in vivo* differences beyond general covariates such as anaesthetics. It is not clear whether experiments with compound intervention also measured and modelled active metabolites and the endogenous ligand nicotinic acid (NiAc). Simultaneous fitting of all experiments, particularly based on unbound test compound concentrations, and allowing individual efficacy parameters (I_{max}), would have allowed a more mechanistic approach.

A turnover model capturing inactive and active proton pump pools was applied to acid secretion data in cannulated Heidenhain pouch dogs (Abelo et al., 2000). It allowed estimation of fractional turnover rate used for prediction of gastric acid secretion inhibition upon repeated human dosing. Rate constants were scaled allometrically but not related to independent experiments of target, nor was the binding dissociation rate of complex compared with fractional turnover rate. The application of such reasoning might have been of importance for optimizing the ligand synthesis program.

In two seminal reviews including inter-species scaling of pharmacodynamic data the authors referred to binding properties based upon the ‘closed’ system approach keeping total amount of target fixed to the baseline level (Danhof et al., 2007; Mager et al., 2009). Both reviews concluded that pharmacodynamic parameters such as potency and efficacy tend to be species independent. However, it is more likely that *in vivo* potency will demonstrate the opposite if system properties such as target turnover k_{deg} varies across different species (Betts et al., 2010; Gosset et al., 2017). Surprisingly, Danhof *et al.* (Danhof et al., 2007) state that “*For drugs acting at extracellular targets, ... binding to plasma proteins and other blood constituents can restrict distribution to the biophase*”, contrary to the well-known fact that plasma protein binding does *not* restrict a compound from distributing to a target site. Unbound exposure of small molecules after oral dosing is governed by dosing rate and unbound clearance (Benet and Hoener, 2002).

Inter-species scaling of the efficacy parameter E_{max} is still a challenge since transduction, denoted ρ , may vary depending on age, sex, tissue, species *etc.* Transduction contains not only conversion of a chemical or electrical signal in the cell to physiological action, but also the cascade of events leading to downstream gene-modified amplification and/or feedback control. For example, gene expression patterns in the ischemic penumbra differed strikingly between mice and rats at both 2 h and 6 h after permanent middle cerebral artery occlusion MCAO (Wu et al., 2021). The faster cessation of penumbral oxidative stress in preclinical animal models (Nilsson et al., 1990) as compared to humans (Benveniste et al., 1984; Bullock et al., 1995a; Bullock et al., 1995b), may be an

important factor that differentiates clearcut therapeutic effects in small animals, but lack thereof in humans. Adjustments for differences in physiological time (species longevity differences; (Dutta and Sengupta, 2016; Mestas and Hughes, 2004) may be a starting point when designing future human stroke studies. Positive outcomes of 3-5 days dosing duration in for example the gerbil stroke model MCAO (100 g body weight), may correspond to 3-4 weeks (21 days using *Eqn. 19*) treatment in humans. To our knowledge no stroke trials have specifically addressed physiological time differences between animals and man. A physiological time difference of oxidative stress was unfortunately neglected also in clinical stroke trials of the radical scavenger NXY-059 which had demonstrated good neuroprotection in several animal models (Marshall et al., 2003). Obviously, multifaceted biomarkers (such as size of the penumbra in this case) are consequences of a host of target interactions and distributional phenomena, thus not specifically mirroring a *single target* turnover but rather a cascade of events. Therefore, beyond scaling determinants of ligand-target complex expression $[RL]$, such as target synthesis rate k_{syn} and complex removal $k_{e(RL)}$, few attempts have been made to scale the transduction parameter Rho , ρ .

Kroon et al (Kroon et al., 2017) formulated a dosing strategy based on PD findings of the highly intricate NiAc and plasma free fatty acid FFA interaction, that “*An intermittent but not continuous NiAc dosing strategy, succeeded in retaining NiAc’s ability to lower plasma FFA and improve insulin sensitivity. Furthermore, a well-defined NiAc exposure, timed to feeding-periods, but not fasting-periods, profoundly improves the metabolic phenotype of this animal model*”. This was concluded from refining the design of *in vivo* experiments (Kroon et al., 2017) and mechanistic PKPD modeling (Andersson et al., 2019), which allowed best timing of dosing, and shaping of NiAc exposure to improve therapeutic value. Their approach captures better what is necessary for understanding the onset, intensity and duration of a therapeutic effect.

It appears unlikely that certain therapeutic areas such as behavioural (CNS) effects can be reliably predicted from *in vitro* data *per se*. The symphony of interactions that impact turnover of the target systems involved (DA, 5-HT, Glu, and more) may have entirely different time courses *in vivo* vs. what may be predicted from on/off binding processes *in vitro* alone. It is also particularly challenging to generate *in vitro* disease models with sufficient validity for the purpose (*e.g.*, cognitive behavioural co-treatment involved in studies of antidepressant actions of psychedelics in man). Speculatively, a battery of *in vivo* behavioural (disease-related) models accompanied by robust biomarkers might be partially helpful, for example phenotypic drug screening approaches (*e.g.*, (Waters et al., 2017)). Overall, the mechanisms underlying psychiatric readout responses likely reflect a cascade of events, through multiple circuit and target involvement greatly exceeding the duration of the initial drug-

target interaction process *per se*. A seminal paper discussing some of the challenges in translational pharmacology was published by Green et al. (Green et al., 2011); in the themed issue of BrJPharm on *in vivo* models for CNS diseases).

Human predictions of biomarker responses and PD properties from preclinical *in vivo* are instrumental when designing first-time-in-man studies. The aforementioned examples highlight specifically *in vivo* biomarker applications representing a specific target turnover, data pruning, mechanism-based PD models, and/or how inter-species predictions of PD properties are typically done. In this context, we foresee that inter-species scaling will be particularly important in pediatrics, frail elderly, or in rare diseases (de Aguiar Vallim et al., 2017) where deviating target expression levels and/or turnover rates are likely to occur. Needless to say, while the target behaviour-related modelling refinements represent a clear advancement in these aims, there is still room for further mechanistic enhancements.

Listed below are some general points to consider with respect to inter-species scaling of PD data

- Target knowledge (pathophysiological conditions, rare disease, pediatrics, frail elderly)?
- Drug mechanism(s) of action?
- Is biomarker/disease marker applicable in humans (species-specificity of targets)?
- Does biomarker/disease marker capture target behavior?
- Consider quality of *in vitro* and *in vivo* preclinical data available (*e.g.*, unbound concentrations, and unbound target tissue-to-plasma concentration differences)
- Is quantitative target information available?
- Is allometry applicable to a specific parameter or expression?
- Differences in physiological time (species longevity differences)?
- Information about robust safety marker(s)?
- View model as a knowledge repository and predictions never better than background data used for generating predictions (uncertainty range, sensitivity analysis...)

This section has addressed how target turnover properties will affect *in vivo* potency and efficacy, and thereby predictions of therapeutically meaningful drug dosage. The new expression of *in vivo* potency will be a valuable tool in experimental pharmacology and translational- and regulatory sciences. In the next section incorporation of turnover in drug elimination enzymatic systems, new properties of clearance, time to equilibrium and steady-state solutions of substrate, enzyme and complex will be discussed.

Drug metabolism and the 'open' Michaelis-Menten system

Background to equations and models

In vivo potency guides at which plasma exposure a drug is active, and clearance carries information about how efficiently the body removes the medicine. For linear (first-order) systems, clearance is assumed to be constant independently of a change in the substrate (drug) concentration over time. A robust method to estimate systemic clearance is through intravenous injection of substrate followed by dividing the intravenous dose by the observed total area under the plasma concentration-time profile. At higher substrate (drug) exposure saturation of the eliminating pathways may occur, and clearance is then often expressed by means of the classical 'closed' Michaelis-Menten (MM) model. Since its introduction in 1913, the MM equation has become a central tenet in biomedical sciences in general and as a function of saturable processes in particular (Michaelis and Menten, 1913; Michaelis et al., 2011). The 'closed' MM model has been applied to *in vitro* and *in vivo* systems of acute and chronic data. The limitations of the 'closed' MM system is, however, its lack of enzyme protein synthesis and loss in parallel to its metabolic processes (**Figure 2**; "Metabolic systems", right hand column). This means that the total pool E_{tot} of free E and substrate bound ES enzyme complex is constant and equal to the free baseline pool E_0 at any time. It is often assumed for 'closed' systems that the initial substrate concentration S is much greater, and initially constant, than the total enzyme concentration E_0 . During oral dosing, for example, both the rate and extent of substrate exposure are highly variable, and do not exceed the responsible enzyme concentrations at therapeutic drug concentrations (for review on CYP450:s, see (Zanger and Schwab, 2013). Daily 400 mg oral doses of the anti-inflammatory drug acetaminophen (Mw = 151.16 g/mol) corresponds to a plasma peak concentration of about 10 mg/L (66 μ M; (Raffa et al., 2018). The most abundant hepatic responsible enzyme CYP3A4 for metabolism of acetaminophen, has a total amount of 60-150 nmol/g hepatic tissue (60-150 μ mol/kg liver or 90-225 μ mol/liver; (Zanger and Schwab, 2013), which exceeds drug exposure to acetaminophen at any time.

The underlying assumptions of the 'open' Michaelis-Menten model are that synthesis of free enzyme protein stays constant, but rate of elimination of free enzyme decreases as the free enzyme concentration diminishes when temporarily occupied by substrate molecules (Gabrielsson and Peletier, 2018; Peletier and Gabrielsson, 2022). Total enzyme concentration (free and complex bound) is allowed to vary under chronic drug use, which means that it can exceed the initial enzyme level E_0 . Clearance of free substrate will vary until equilibrium is established. The 'closed' Michaelis-Menten approach assumes that the catalytic reaction rather than substrate-enzyme binding process, is the rate-limiting step. This assumption is not necessary in the 'open' model. The 'open' model does

not exclude that drug-drug metabolic interactions may affect both rate and extent of binding. By including substrate and target turnover (in other words, opening the system) in order to mimic the *in vivo* situation, new kinetic properties of enzyme and substrate enzyme evolve. A consequence of this will be that the 'open' MM equation of clearance (originally denoted as the specificity constant k_{cat}/K_m times the enzyme baseline concentration E_0) and rate of metabolism will take another functional form.

Studying drug metabolism outside the *in vivo* context is most often done *in vitro*. With purified enzymes, neither synthesis nor degradation of enzyme are expected. In cell systems turnover of enzyme may still be an ongoing process. However, the time frame within which this is done is important. Even though the cell system (*in vitro*) may have synthesis and catabolism of enzyme, studies of drug metabolism under chronic *in vitro* conditions are rarely performed. Synthesis and catabolism of enzyme proteins are seldom studied in parallel to drug substrate metabolism. Whereas drug metabolism is typically studied within a time frame of a few hours or maximum a day, enzyme half-lives are most often much longer than that. A closed system approximation may therefore be valid for acute but not chronic situations assuming a stable enzyme level (**Figure 2**) (Magnusson et al., 2008; Ramsden et al., 2015; Rostami-Hodjegan et al., 1999; von Bahr et al., 1998).

In this section we first explore and compare the 'open' model with the traditional 'closed' system MM model derived by Gabrielsson and Peletier (Gabrielsson and Peletier, 2018) and recently further explored (Peletier and Gabrielsson, 2022). We derive steady-state equations of substrate (S , drug), enzyme (E) and complex (ES), and then dissect the new relationship of *in vivo* V_{max} , K_m and clearance Cl . Simulations are done with the 'open' system showing its intrinsic behavior governed by experimental data. From this, conclusions about the drug-drug interaction potential are then drawn.

Let us start with the rate equations of the 'open' system metabolic model of free substrate (S), free enzyme (E) and substrate-enzyme complex (ES), including zero-order input (*Input*) and non-specific clearance ($Cl_{(S)}$) of substrate, and zero-order turnover rate (k_{syn}) and first-order fractional turnover rate (k_{deg}) of enzyme shown in Eqn. 20 (**Figure 2**; Metabolic systems, right hand column). The rate of formation of product (metabolite) via the substrate-enzyme complex activity (k_{cat}) is shown in Eqn. 19 (bottom line).

$$\begin{cases} \frac{dS}{dt} = \frac{Input}{V} - \frac{Cl_{(S)}}{V} \cdot S - k_{on} \cdot S \cdot E + k_{off} \cdot ES \\ \frac{dE}{dt} = k_{syn} - k_{deg} \cdot E - k_{on} \cdot S \cdot E + (k_{off} + k_{cat}) \cdot ES \\ \frac{dES}{dt} = k_{on} \cdot S \cdot E - k_{off} \cdot ES - k_{cat} \cdot ES \\ \frac{dP}{dt} = k_{cat} \cdot ES \end{cases} \quad (Eqn. 20)$$

We assume that free substrate S is only eliminated via enzymatic degradation and therefore set non-specific clearance of $Cl_{(S)}$ to zero.

Equilibrium states and clearance expression of (reversible) metabolic systems

Mechanistic expressions of substrate, free enzyme and substrate-enzyme complex concentrations are derived by incorporating target/enzyme turnover (**Table 8**). In particular, we show that whereas in closed systems there is a built-in saturation beyond which the substrate concentration keeps rising, in open systems involving enzyme turnover this is no longer the case. However, after an initial period of disequilibrium, the expression of intrinsic clearance reduces to a linear expression. Here clearance is assumed to be proportional to the free enzyme concentration $E(t)$ over time, and therefore varies in a similar pattern to $E(t)$. At equilibrium clearance returns to be proportional to the free baseline enzyme concentration E_0 .

A revision of the ‘closed’ MM system to also include enzyme turnover was recently undertaken, to attain a closer resemblance to the *in vivo* situation (Gabrielsson and Peletier, 2018). The revised expressions of intrinsic clearance and rate of elimination at equilibrium are given in Eqn. 21.

$$\begin{cases} Cl = E(t) \cdot k_{cat} \cdot V \cdot \frac{1}{\frac{k_{cat} + k_{off}}{k_{on}}} = \frac{V_{max}(t)}{K_m} \\ Cl_{ss} = E(0) \cdot k_{cat} \cdot V \cdot \frac{1}{\frac{k_{cat} + k_{off}}{k_{on}}} = \frac{V_{max}(0)}{K_m} \\ Rate = \frac{V_{max}(t)}{K_m} \cdot S(t) \\ Rate_{ss} = \frac{V_{max}(0)}{K_m} \cdot S_{ss} \end{cases} \quad (Eq. 21)$$

where $E(t)$ denotes the time course of free enzyme. Since the free enzyme level (E) changes over time and will initially decline during extended drug exposure, both $V_{max}(t)$ and clearance Cl will decrease and appear time-dependent until equilibrium (steady-state, Cl_{ss} and $V_{max}(0)$) is reached (**Figures 12-13**). The equilibrium relationships of target substrate (S_{ss}) free enzyme (E_{ss}) and substrate-enzyme complex (ES_{ss}) are shown in *Eqn. 22*

$$\left\{ \begin{array}{l} S_{ss} = \frac{Input}{Cl_{ss}} \\ E_{ss} = E_0 = \frac{k_{syn}}{k_{deg}} \\ ES_{ss} = \frac{Input}{V \cdot k_{cat}} \end{array} \right. \quad (Eqn. 22)$$

The substrate concentration S_{ss} increases proportionally with *Input rate* at steady-state since clearance is a non-saturable term at equilibrium (steady-state) in the ‘open’ model of drug metabolism, which contrasts the closed system model (**Table 8**).

Table 8 approx here

Surprisingly, the free enzyme level at steady-state E_{ss} returns to the enzyme baseline value E_0 since it is only determined by k_{syn} and k_{deg} (**Table 8; Figure 12**). The equilibrium level of substrate-enzyme complex ES_{ss} is the ratio of substrate *Input* to the catalytic clearance (elimination rate constant k_{cat} times distribution volume) at equilibrium. Substrate clearance Cl is determined by the biological properties of the responsible enzyme, synthesis k'_{syn} and degradation k_{deg} , as well as the binding and catalytic properties k_{off} , k_{on} and k_{cat} . Cl can be simplified to $(k'_{syn}/k_{deg}) \cdot k_{on}$ when k_{cat} is much greater than k_{off} , which means that Cl is a function of free enzyme baseline expression E_0 and the second-order rate constant k_{on} at equilibrium.

Table 8 summarizes the different properties of the ‘open’ and ‘closed’ systems. The time-courses of substrate, enzyme, complex, clearance, and elimination rates display saturable behavior akin to the ‘closed’ system. All of these variables and parameters follow dose-proportional (first-order) kinetics at equilibrium of the ‘open’ model. The duality of the ‘open’ system is that substrate, free enzyme and substrate-enzyme complex also display nonlinear behavior during the time to equilibrium. **Table 8** contrasts Cl derived from the ‘closed’ system, which decreases with increasing substrate exposure S , and Cl of the ‘open’ system, which is independent of the substrate exposure at equilibrium. This

stems from the fact that whilst in the 'closed' system, the total amount of enzyme E_{tot} is fixed to what it is initially E_0 , and the amount of substrate-enzyme complex can never exceed the total amount of enzyme in 'closed' systems. In the 'open' system, free enzyme is continuously synthesized and turned over via irreversible loss and complex formation.

The degree of target-ligand (substrate-enzyme) complex formation is a significant element affecting substrate metabolism rate in the 'open' situation. Thus, as more substrate(drug)-enzyme complex is formed the availability of free enzyme protein declines, and in turn therefore also the rate of elimination of free enzyme – while the rate of synthesis (replenishment) of free enzyme molecules is sustained. That is, the total concentration of enzyme (free + substrate complex-bound) will increase during the period of disequilibrium until a balance between the three entities (free & bound enzyme, and substrate) has been established. Typically, enzyme proteins have relatively long half-lives (Magnusson et al., 2008; Ramsden et al., 2015; Rostami-Hodjegan et al., 1999; von Bahr et al., 1998), often exceeding that of substrate *per se*. It follows that the time to equilibrium between free enzyme, substrate, and substrate-enzyme complex may therefore be much longer than the usual 3-5 substrate half-lives. The classical 'closed' system MM model recognizes the referred disequilibrium as a nonlinear clearance ($Cl = V_{max}/(K_m + C)$) with clearance decreasing as substrate concentrations increase. However, by introducing turnover properties of the enzyme as such, this nonlinear (saturable) clearance term disappears for the equilibrium state, and clearance returns to its equilibrium state V_{max}/K_m , since free enzyme concentration (E) is determined only by the ratio of k_{syn} to k_{deg} at equilibrium (steady-state).

To illustrate the discussion above, *Eqn. 20* was fitted to rapid repeated intravenous dose data in **Figure 12**. Simulations were then done with a constant intravenous infusion over 100 hours to show how the time courses of substrate S , free enzyme E , substrate-enzyme complex ES and clearance of substrate Cl of this 'open' system varied over time (**Figure 13**).

Figures 12 and 13 approx here

Synthesis k_{syn} and clearance of free enzyme stays constant, but rate of elimination of free enzyme decreases as the free enzyme concentration falls when the substrate-enzyme complex is formed. Total enzyme concentrations (free E and complex bound ES) are allowed to vary, which means that they can both exceed and become less than the initial enzyme level E_0 . The time course of clearance may be easier to understand and apply than that of free enzyme and relates to actual observable values. The k_{cat} , k_{deg} , k_{off} , k_{on} and k_{syn} were estimated to 0.151 h^{-1} , 0.986 h^{-1} , 0.109 h^{-1} , $0.0082 \text{ h}^{-1} \cdot (\mu\text{g} \cdot \text{L}^{-1})^{-1}$ and $24.9 \mu\text{g} \cdot \text{L}^{-1} \cdot \text{h}^{-1}$, respectively, with a resulting K_m of $32 \mu\text{g} \cdot \text{L}^{-1}$ and clearance

Cl of about $17 \text{ L} \cdot \text{h}^{-1}$. The reasons behind data of **Figure 12** and **Figure 13** are thus as follows: *i*) An initial decrease in free enzyme concentrations as a consequence of complex formation, resulting in *ii*) a decrease in rate of elimination of free enzyme since free concentrations decrease, *iii*) since free enzyme concentrations decrease the substrate clearance will decrease (change) in parallel ($Cl(S) = E(t) \cdot k_{cat} \cdot V$; **Table 8**), and, *iv*) simultaneously, there is a build-up of substrate-enzyme complex (**Figure 13**). Therefore, total concentration of free and complex bound enzyme increases beyond the baseline concentration E_0 .

A constant substrate clearance model would not have captured the nonlinear concentration-time data in **Figure 12**. For comparison, a time-dependent change in maximum metabolic capacity ('closed' system $V_{max}(t)$, Case study PK22 in (Gabrielsson and Weiner, 2016) captured experimental data in **Figure 12**.

The free enzyme dependent clearance of compound A (substrate) in **Figure 14** (right) demonstrates a transient drop from baseline ① to a trough of 20% ② during the infusion, aiming at a substrate S concentration of about $180 \mu\text{g/L}$. Substrate clearance then returns to its original value (E_0) at about 40-60 hours when equilibrium of the whole system is re-established ③. Substrate clearance has reached its pre-dose value at equilibrium ③. When the infusion is stopped at 100 hours substrate clearance rebounds ④ due to a transient rise in the free enzyme concentration. This is due to the sudden release of free enzyme from the substrate-enzyme complex as product is being formed, and the lack of consumption of free enzyme due to complex formation. Substrate clearance (and free enzyme concentrations) reaches the pre-dose equilibrium terminally ⑤ as all substrate is washed out. The time to equilibrium is substantially prolonged with a rise in substrate infusion rate and *vice versa*. This is also shown schematically in **Figure 13**. The predicted V_{max} , K_m and substrate clearance Cl in Case study PK22 are $544 \mu\text{g/h}$, $32 \mu\text{g/L}$ and 12 L/h , respectively.

Figure 14 approx here

The second example shows simulations of three different intravenous bolus doses of compound X. The substrate concentration-time courses in plasma are shown in **Figure 15** (A) together with the corresponding time-courses of clearance (**Figure 15, B**) and substrate half-life (**Figure 15, C**).

Figure 15 approx here

Note the dose-dependent change of substrate clearance with increasing concentrations after a bolus dose (**Figure 15, B.**), which exhibits the characteristics of a target mediated drug disposition system. The transient dip in clearance over 6-36 hours results in a prolonged half-life ①. The dose-dependent rebound of clearance when concentrations fall below $100 \mu\text{g}\cdot\text{L}^{-1}$ (clearance greater than its baseline value) is due to replenishment of free enzyme from substrate-enzyme complex, and less enzyme is used when substrate concentrations start to fall off. During the lowering of clearance below its baseline value, less free enzyme is available and can be cleared via natural catabolism k_{deg} , (rate of enzyme elimination decreases but rate of synthesis stays constant) which means that the total amount (free + complex) increases. The free enzyme pool is then increased by released free enzyme from the complex pool and there is a rebound in the free enzyme concentration is seen which then causes clearance too to rebound. The temporarily increased clearance results in a decrease in half-life ②, which then increases when clearance returns to its baseline value③ terminally. The manifestation of non-linear plasma concentration-time courses is the archetypal signature of an ‘open’ MM system at *disequilibrium*.

The dynamics of the intertwined differential equations of free substrate, free enzyme and substrate-enzyme complex inherently captures the disequilibrium as a ‘*nonlinearity*’. This is the core difference between the ‘closed system’ (assuming a constant total enzyme pool) and the recently derived ‘open system’ models (**Figures 2 and 14**) (Gabrielsson and Peletier, 2018), which puts clearance into new light. Until simultaneous measurement of the total enzyme concentration implicated is carried out, the possibility cannot be completely discarded that in some cases results previously described as dose- or time-dependent kinetics may actually rather reflect a state of disequilibrium.

Key insights and translational potential

An important advantage of using the ‘open’ system approach is that an apparent temporal nonlinearity, in clearance or rate of elimination does not have to be approximated by means of a saturable expression such as the one shown in **Table 8**. In ‘open’ systems, the nonlinearity observed for higher IV bolus doses in which clearance temporarily decreases and half-life increases is an intrinsic property of the system, which results from the apparent disequilibrium between substrate S , free enzyme E and substrate-enzyme complex ES . Clearance behaves linearly at steady-state (**Table 8**, bottom row, left, V_{max}/K_m).

However, *in vitro* studies in general and metabolic drug-drug interaction studies in particular, operate within a short time frame often less than 24 h and sometimes as short as 15-45 min (Fowler and Zhang, (2008)), hence totally ignoring the impact of enzyme protein turnover. Also, clearance

defined by 'closed' systems is commonly applied even in a physiological context for translation of *in vitro* to *in vivo* metabolic data (Rostami-Hodjegan, 2010). In these cases, the non-equilibrium between substrate (drug), free enzyme and complex is approximated by a nonlinear saturable function. Clearly, a better understanding is required of the biological elements involved, including the origin of the clearance model ('open' or 'closed'). Accurate *in vitro* to *in vivo* predictions are possible only when *in vitro* data are robust, and the biological structure of the clearance model is integrated. Accordingly, we therefore suggest based on the expanded quantitative insights of the MM system presented here, that *in silico* MM-, pharmacological- and transporter models should be built on 'open' systems.

The tools are available to more correctly scale *in vivo* data from pre-clinical species to man, with a reasonable mechanistic structure of the determinants of clearance. Thus, it should be appreciated that V_{max} is expressed as $E(t) \cdot k_{cat}$ (or $k_{syn} \cdot k_{cat}/k_{deg}$ at equilibrium) and K_m equals $(k_{off} + k_{cat})/k_{on}$. The k_{syn} and k_{deg} parameters represent biology and are scalable across different species. The physicochemical parameters k_{on} , k_{off} and k_{cat} may also be species-dependent since the target properties varies across species.

The apparent clearance is determined by the free enzyme expression E and the turnover parameters k_{syn} and k_{deg} rather than its fixed baseline concentration E_0 , which is contrasted by the 'closed' system model where clearance via its V_{max} term is fixed by baseline concentration E_0 . This means that two subjects with the same free enzyme expression (same E_0) will have the same clearance (provided everything else is the same). However, the subject with the higher enzyme synthesis k_{syn} and degradation k_{deg} rates will reach enzymatic equilibrium faster. Therefore, subjects or species will, in spite of similar free enzyme concentrations, display different substrate time courses due to different enzyme protein turnover rates.

Induction or inhibition of enzymatic and catalytic processes

Since clearance of most small drug substances depends upon CYP enzymes, CYP inhibition may lead to overexposure and toxicity, and CYP induction to too low exposure and deficient therapeutic effect. Understanding the cause of inhibition or induction is therefore crucial. A practical example of the time-course of heterologous drug induction is the impact of pentobarbital treatment on the disposition of nortriptyline (NT; (von Bahr et al., 1998). Pentobarbital-induced induction of NT clearance (NT clearance increases due to an increased exposure to enzyme responsible for NT removal) shortened the NT half-life and time to (induced) steady-state. The plasma concentration of NT decreased 50% during pentobarbital treatment. The reverse happens upon cessation of pento-

barbital treatment. The induced NT clearance decreased and half-life increased, resulting in an extended time of post-induction return of NT concentration to its pre-induced state.

Analogously to, *e.g.*, ligand-receptor target interaction discussions above, administration of agents aiming at enzyme proteins may impact the number of target molecules or their activity. An increase in synthesis rate (turnover rate) of enzyme k_{syn} will impact the baseline value of enzyme E_0 and therefore cause an increase in clearance Cl of substrate S at steady-state. An increase in fractional turnover rate of enzyme k_{deg} will decrease the baseline value of enzyme E_0 and, hence, decrease in clearance Cl of substrate S at steady-state (**Table 9**).

Table 9 approx here

This section has demonstrated how enzymatic turnover properties will affect clearance, time to equilibrium and steady-state solutions of substrate, enzyme and complex, and consequently drug dose. The new expression of *in vivo* MM systems will be useful for a quantitative analysis of clearance properties and in translational science contexts.

Discussion

What is the challenge and why is it a problem?

The Introduction section identified two main questions, namely what is the challenge with today's 'closed' system models, and why is it a challenge in pharmacology, metabolism and even for transporter systems. These 'closed' system models, often *in vitro* based, lack robust information about the target protein biology, and, hence, are approximations of the *in vivo* situations. 'Closed' systems models further lack the capability beyond binding to describe drug-drug interactions, time-variant induction, inhibition or displacement (up- or down-regulation of target) of competing drug molecules, or pharmacodynamic drug interactions, as previously described. Moreover, 'closed' systems are limited to binding interactions, hence cannot explain when duration of drug is limited by the turnover of target (see, PPI:s and COX-1 examples above). Finally, 'closed' systems assume a constant clearance in spite of the fact that availability of free enzyme will vary for the drug (substrate), particularly during repeated dosing conditions. Mitigating these limitations are necessary for adequate assessment of *in vivo* potency, efficacy, and clearance.

We have shown that target turnover (k_{syn} , k_{deg}) is an important covariate to *in vivo* potency and efficacy. Thus, the rates (k_{off} , k_{deg} , $k_{e(RL)}$ and k_{on}) or their half-lives determine potency whereas expression level of complex (RL_{max}) and transduction (stimulus force, Rho ρ) determine efficacy (Eqn.

23). *In vivo* potency and efficacy have ligand-target complex loss $k_{e(RL)}$ in common. A change in that property is therefore assumed to impact both potency and efficacy but in opposite directions. When $k_{e(RL)}$ increases potency increases (numerical value decreases) whereas efficacy decreases, and *vice versa*, making the removal rate of ligand-target complex an important player.

$$\begin{cases} EC_{50} = \frac{k_{deg}}{k_{e(RL)}} \cdot \frac{k_{off} + k_{e(RL)}}{k_{on}} \\ E_{max} = \rho \cdot RL_{max} = \rho \cdot \frac{k_{syn}}{k_{e(RL)}} \end{cases} \quad (Eqn. 23)$$

Here, target biology is an important covariate of *in vivo* potency, and may capture between species or inter-individual differences. *Eqn. 23* partly explains why in some cases target concentrations in the micro-molar range only require nanomolar drug exposure and *vice versa*. Still, the ‘open’ model, similarly to the ‘closed’, does not take into account post-target events such as synergy, potentiation, feedback etc. However, incorporating target properties, assessment of activities adjacent to the target will be more apparent.

Blood clearance may be expressed by means of the well-stirred physiological model with blood flow Q_i as

$$Cl = \frac{Q_i \cdot \frac{E(t) \cdot k_{cat} \cdot V}{K_m}}{Q_i + \frac{E(t) \cdot k_{cat} \cdot V}{K_m}} \quad (Eqn. 24)$$

The determinants of free enzyme $E(t)$ concentrations are k_{syn} and k_{deg} . Again, target protein turnover plays an important role and may explain inter-individual differences in the disposition of substrate S . In situations where only plasma data are available of drug, such as in therapeutic drug monitoring TDM, $V_{max}/(K_m + C)$ gives the apparent plasma clearance rather than intrinsic clearance of *Eqn. 23*. V_{max} and K_m are typical parameters in TDM of phenytoin and salicylic acid, and based on the ‘closed’ system expression of clearance (**Table 8**; for a review of the clearance concept, see, (Benet, 2010).

Unifying and separating properties of ‘open’ systems

The ‘open’ models of pharmacological and metabolic systems have several properties in common which unifies these systems. While not explicitly discussed in this article, it appears highly probable that similar reasoning may be applied to ligand interactions with transport proteins as well. The ‘open’ *in vivo* models incorporate all necessary ligand and target protein interactions such as target

binding, target protein turnover and irreversible loss of either complex or the associated drug. By virtue of their more physiological properties, such approaches reach beyond binding and incorporate the actual target (receptor-, enzyme- or transporter protein turnover) properties, thereby encompassing physiological means to explain within- and between-subject differences.

General conclusions and perspectives

This review endeavors to illustrate and exemplify the importance of target protein turnover as a central player in pharmacology and drug metabolism. We hope these thoughts will inspire further development of concepts of *in vivo* pharmacology and drug metabolism to the benefit of basic scientists as well as for drug discovery and development ventures. The introduction of protein turnover unveils the bearing of target dynamics upon pharmacologic as well as metabolic readouts – key components in determining drug responses *in vivo*. Specifically, we describe and provide:

- The presentation of new ('open' model) expressions of *in vivo* potency, efficacy and clearance which notably embody target turnover, binding and complex kinetics, also capturing drug-response descriptors (*i.e.*, full, partial, and inverse agonism, and antagonism)
- Detailed examination and analysis of 'open' models to show what *in vivo* potency, efficacy, and clearance, have in common and how they differ
- A comprehensive literature review showing that target turnover rate varies with several factors: age, species, tissue/subregion, treatment, disease state, hormonal and nutritional state, day-night cycle, and more, and therefore changes *in vivo* potency, efficacy, and clearance

Using this new 'open' model expression which integrates system- (k_{syn} and k_{deg}) and drug- (k_{on} , k_{off} , $k_{e(RL)}$ and k_{cat}) properties, we further show that:

- The fractional turnover rates (k_{deg} and $k_{e(RL)}$), rather than the absolute target expression (R or RL) determines necessary drug exposure via *in vivo* potency EC_{50}
- The absolute ligand-target expression (RL) determines the need of drug, based on *in vivo* efficacy parameter (E_{max}) and the transduction parameter Rho (ρ)

- The free enzyme concentration E determines clearance and the fractional turnover rate (k_{deg}), the time to equilibrium between substrate, free enzyme and substrate-enzyme complex
- Clearance is not a constant term, but is driven by the free enzyme concentration
- The properties of substrate, target, and complex demonstrate non-saturable metabolic behavior at equilibrium within reasonable substrate/ligand concentration ranges
- Nonlinear processes previously referred to as capacity- and time-dependent kinetics may have been disequilibria which the ‘open’ model handles as an intrinsic property
- The ‘open’ model may pinpoint why some subjects differ in their demand of drug, thus defining what makes the outlier an outlier – an issue important to scrutinize from a clinical but also a regulatory point of view

All of the above need to be considered within the framework of projecting potency, efficacy and clearance from *in vitro*, via *in vivo* animal model work, to clinically efficacious exposures in man.

The usefulness of the ‘open’ model approach has attracted increased attention – directly or indirectly – in several recent publications demonstrating its applicability in the assessment of different compounds, targets and systems (Baquero and Levin, 2021; Cardilin et al., 2019; Choi, 2020; Gabrielsson et al., 2019; Gabrielsson et al., 2018a; b; Held et al., 2019; Hong et al., 2008; Jansson-Lofmark et al., 2020; Li et al., 2020; Oakes et al., 2005; Oakes et al., 2001; Saganuwan, 2021; Smith et al., 2018; Song et al., 2021; Tang and Cao, 2021; van Waterschoot et al., 2018; Webster et al., 2020).

To understand and approach the dynamics of target biology in an ‘open’ system, presents new avenues to vastly different areas beyond pharmacology, drug metabolism or cellular (transport) systems. ‘Open’ systems capture *in vivo* disequilibria previously categorized as capacity- and time-dependent kinetics. ‘Open’ systems increase the capability to capture these processes correctly and underpin interpretation of data, translation of functionality across species and explanation of clinical and preclinical variability.

Only by continued integration of the multiple levels of biological and pharmacological insight the precision will be further improved of translational predictions across the drug development process. It is our hope that the current account may be of value to that end, as it emphasizes the importance of ‘*in vivo veritas*’ principles in such endeavors.

Authorship contributions

Participated in research design: Gabrielsson and Hjorth

Conducted experiments: Gabrielsson and Hjorth

Contributed new reagents or analytic tools: Not applicable

Performed data analysis: Gabrielsson

Wrote or contributed to the writing of the manuscript: Gabrielsson and Hjorth

References

- Abelo A, Eriksson UG, Karlsson MO, Larsson H and Gabrielsson J (2000) A turnover model of irreversible inhibition of gastric acid secretion by omeprazole in the dog. *J Pharmacol Exp Ther* **295**:662-669.
- Abou Sawan S, Hodson N, Tinline-Goodfellow C, West DWD, Malowany JM, Kumbhare D and Moore DR (2021) Incorporation of dietary amino acids into myofibrillar and sarcoplasmic proteins in free-living adults is influenced by sex, resistance exercise, and training status. *J Nutr* **151**:3350-3360.
- Adam K and Oswald I (1983) Protein synthesis, bodily renewal and the sleep-wake cycle. *Clin Sci (Lond)* **65**:561-567.
- Adler CH, Meller E and Goldstein M (1985) Recovery of alpha 2-adrenoceptor binding and function after irreversible inactivation by N-ethoxycarbonyl-2-ethoxy-1,2-dihydroquinoline (EEDQ). *Eur J Pharmacol* **116**:175-178.
- Adolph EF (1949) Quantitative relations in the physiological constitutions of mammals. *Science* **109**:579-585.
- Agneter E, Drobný H and Singer EA (1993) Central alpha 2-autoreceptors: agonist dissociation constants and recovery after irreversible inactivation. *Br J Pharmacol* **108**:370-375.
- Albrecht S, Ihmsen H, Hering W, Geisslinger G, Dingemanse J, Schwilden H and Schuttler J (1999) The effect of age on the pharmacokinetics and pharmacodynamics of midazolam. *Clin Pharmacol Ther* **65**:630-639.
- Almquist J, Hovdal D, Ahlstrom C, Fjellstrom O, Gennemark P and Sundqvist M (2018) Overexpressing cell systems are a competitive option to primary adipocytes when predicting in vivo potency of dual GPR81/GPR109A agonists. *Eur J Pharm Sci* **114**:155-165.
- An G (2017) Small-molecule compounds exhibiting Target-Mediated Drug Disposition (TMDD): A minireview. *J Clin Pharmacol* **57**:137-150.
- An G (2020) Concept of pharmacologic Target-Mediated Drug Disposition in large-molecule and small-molecule compounds. *J Clin Pharmacol* **60**:149-163.

- Andersson R, Jirstrand M, Almquist J and Gabrielsson J (2019) Challenging the dose-response-time data approach: Analysis of a complex system. *Eur J Pharm Sci* **128**:250-269.
- Andres TM, McGrane T, McEvoy MD and Allen BFS (2019) Geriatric pharmacology: An update. *Anesthesiol Clin* **37**:475-492.
- Antonini A, Schwarz J, Oertel WH, Pogarell O and Leenders KL (1997) Long-term changes of striatal dopamine D2 receptors in patients with Parkinson's disease: a study with positron emission tomography and [¹¹C]raclopride. *Mov Disord* **12**:33-38.
- Appel SH, Anwyl R, McAdams MW and Elias S (1977) Accelerated degradation of acetylcholine receptor from cultured rat myotubes with myasthenia gravis sera and globulins. *Proc Natl Acad Sci U S A* **74**:2130-2134.
- Arnett CD, Fowler JS, MacGregor RR, Schlyer DJ, Wolf AP, Langstrom B and Halldin C (1987) Turnover of brain monoamine oxidase measured in vivo by positron emission tomography using L-[¹¹C]deprenyl. *J Neurochem* **49**:522-527.
- Baker SP and Pitha J (1982) Irreversible blockade of beta adrenoreceptors and their recovery in the rat heart and lung in vivo. *J Pharmacol Exp Ther* **220**:247-251.
- Baquero F and Levin BR (2021) Proximate and ultimate causes of the bactericidal action of antibiotics. *Nat Rev Microbiol* **19**:123-132.
- Barturen F and Garcia-Sevilla JA (1992) Long term treatment with desipramine increases the turnover of alpha 2-adrenoceptors in the rat brain. *Mol Pharmacol* **42**:846-855.
- Battaglia G, Norman AB and Creese I (1987) Differential serotonin₂ receptor recovery in mature and senescent rat brain after irreversible receptor modification: effect of chronic reserpine treatment. *J Pharmacol Exp Ther* **243**:69-75.
- Battaglia G, Norman AB and Creese I (1988) Age-related differential recovery rates of rat striatal D-1 dopamine receptors following irreversible inactivation. *Eur J Pharmacol* **145**:281-290.
- Battaglia G, Norman AB, Newton PL and Creese I (1986) In vitro and in vivo irreversible blockade of cortical S₂ serotonin receptors by N-ethoxycarbonyl-2-ethoxy-1,2-dihydroquinoline: a technique for investigating S₂ serotonin receptor recovery. *J Neurochem* **46**:589-593.

- Bauer RA (2015) Covalent inhibitors in drug discovery: from accidental discoveries to avoided liabilities and designed therapies. *Drug Discov Today* **20**:1061-1073.
- Beaulieu JM and Gainetdinov RR (2011) The physiology, signaling, and pharmacology of dopamine receptors. *Pharmacol Rev* **63**:182-217.
- Belleau B, Martel R, Lacasse G, Menard M, Weinberg NL and Perron YG (1968) N-carboxylic acid esters of 1,2- and 1,4-dihydroquinolines. A new class of irreversible inactivators of the catecholamine alpha receptors and potent central nervous system depressants. *J Am Chem Soc* **90**:823-824.
- Ben-Menachem E (2011) Mechanism of action of vigabatrin: correcting misperceptions. *Acta Neurol Scand Suppl*:5-15.
- Benet LZ (2010) Clearance (nee Rowland) concepts: a downdate and an update. *J Pharmacokinet Pharmacodyn* **37**:529-539.
- Benet LZ and Hoener BA (2002) Changes in plasma protein binding have little clinical relevance. *Clin Pharmacol Ther* **71**:115-121.
- Benveniste H, Drejer J, Schousboe A and Diemer NH (1984) Elevation of the extracellular concentrations of glutamate and aspartate in rat hippocampus during transient cerebral ischemia monitored by intracerebral microdialysis. *J Neurochem* **43**:1369-1374.
- Berg KA and Clarke WP (2018) Making Sense of Pharmacology: Inverse Agonism and Functional Selectivity. *Int J Neuropsychopharmacol* **21**:962-977.
- Betts AM, Clark TH, Yang J, Treadway JL, Li M, Giovanelli MA, Abdiche Y, Stone DM and Paralkar VM (2010) The application of target information and preclinical pharmacokinetic/pharmacodynamic modeling in predicting clinical doses of a Dickkopf-1 antibody for osteoporosis. *J Pharmacol Exp Ther* **333**:2-13.
- Biolo G, Antonione R, Barazzoni R, Zanetti M and Guarnieri G (2003) Mechanisms of altered protein turnover in chronic diseases: a review of human kinetic studies. *Curr Opin Clin Nutr Metab Care* **6**:55-63.
- Birkenhager TK, van den Broek WW, Mulder PG, Bruijn JA and Moleman P (2004) Efficacy and tolerability of tranylcypromine versus phenelzine: a double-blind study in antidepressant-refractory depressed inpatients. *J Clin Psychiatry* **65**:1505-1510.

- Black JW and Leff P (1983) Operational models of pharmacological agonism. *Proc R Soc Lond B Biol Sci* **220**:141-162.
- Bodenstein J, Venter DP and Brink CB (2005) Phenoxybenzamine and benextramine, but not 4-diphenylacetoxy-N-[2-chloroethyl]piperidine hydrochloride, display irreversible noncompetitive antagonism at G protein-coupled receptors. *J Pharmacol Exp Ther* **314**:891-905.
- Boisvert FM, Ahmad Y, Gierlinski M, Charriere F, Lamont D, Scott M, Barton G and Lamond AI (2012) A quantitative spatial proteomics analysis of proteome turnover in human cells. *Mol Cell Proteomics* **11**:M111 011429.
- Bolanos FJ, Schechter LE, Laporte AM, Hamon M and Gozlan H (1991) Recovery of 5-HT 1A receptors after irreversible blockade by N-ethoxycarbonyl-2-ethoxy-1,2-dihydroquinoline (EEDQ). *Proc West Pharmacol Soc* **34**:387-393.
- Borden LA, Czajkowski C, Chan CY and Farb DH (1984) Benzodiazepine receptor synthesis and degradation by neurons in culture. *Science* **226**:857-860.
- Bosma R, Witt G, Vaas LAI, Josimovic I, Gribbon P, Vischer HF, Gul S and Leurs R (2017) The target residence time of antihistamines determines their antagonism of the G Protein-Coupled histamine H1 receptor. *Front Pharmacol* **8**:667.
- Bowie MW and Slattum PW (2007) Pharmacodynamics in older adults: a review. *Am J Geriatr Pharmacother* **5**:263-303.
- Boxenbaum H (1982) Interspecies scaling, allometry, physiological time, and the ground plan of pharmacokinetics. *J Pharmacokinet Biopharm* **10**:201-227.
- Boxenbaum H and Ronfeld R (1983) Interspecies pharmacokinetic scaling and the Dedrick plots. *Am J Physiol* **245**:R768-775.
- Brynne N, Forslund C, Hallen B, Gustafsson LL and Bertilsson L (1999) Ketoconazole inhibits the metabolism of tolterodine in subjects with deficient CYP2D6 activity. *Br J Clin Pharmacol* **48**:564-572.
- Brynne N, Stahl MM, Hallen B, Edlund PO, Palmer L, Hoglund P and Gabrielsson J (1997) Pharmacokinetics and pharmacodynamics of tolterodine in man: a new drug for the treatment of urinary bladder overactivity. *Int J Clin Pharmacol Ther* **35**:287-295.

- Bullock R, Zauner A, Myseros JS, Marmarou A, Woodward JJ and Young HF (1995a) Evidence for prolonged release of excitatory amino acids in severe human head trauma. Relationship to clinical events. *Ann N Y Acad Sci* **765**:290-297; discussion 298.
- Bullock R, Zauner A, Woodward J and Young HF (1995b) Massive persistent release of excitatory amino acids following human occlusive stroke. *Stroke* **26**:2187-2189.
- Burke TF, Woods JH, Lewis JW and Medzihradsky F (1994) Irreversible opioid antagonist effects of clocinnamox on opioid analgesia and mu receptor binding in mice. *J Pharmacol Exp Ther* **271**:715-721.
- Carbonell L, Cuffi ML and Forn J (2004) Effect of chronic lithium treatment on the turnover of alpha2-adrenoceptors after chemical inactivation in rats. *Eur Neuropsychopharmacol* **14**:497-502.
- Cardilin T, Almquist J, Jirstrand M, Zimmermann A, Lignet F, El Bawab S and Gabrielsson J (2019) Modeling long-term tumor growth and kill after combinations of radiation and radiosensitizing agents. *Cancer Chemother Pharmacol* **83**:1159-1173.
- Chaparro-Riggers J, Liang H, DeVay RM, Bai L, Sutton JE, Chen W, Geng T, Lindquist K, Casas MG, Boustany LM, Brown CL, Chabot J, Gomes B, Garzone P, Rossi A, Strop P, Shelton D, Pons J and Rajpal A (2012) Increasing serum half-life and extending cholesterol lowering in vivo by engineering antibody with pH-sensitive binding to PCSK9. *J Biol Chem* **287**:11090-11097.
- Charlton SJ (2009) Agonist efficacy and receptor desensitization: from partial truths to a fuller picture. *Br J Pharmacol* **158**:165-168.
- Choe S and Lee D (2017) Parameter estimation for sigmoid Emax models in exposure-response relationship. *Transl Clin Pharmacol* **25**:74-84.
- Choi YH (2020) Interpretation of drug interaction using systemic and local tissue exposure changes. *Pharmaceutics* **12**.
- Colovic MB, Krstic DZ, Lazarevic-Pasti TD, Bondzic AM and Vasic VM (2013) Acetylcholinesterase inhibitors: pharmacology and toxicology. *Curr Neuropharmacol* **11**:315-335.
- Commons KG and Linnros SE (2019) Delayed antidepressant efficacy and the desensitization hypothesis. *ACS Chem Neurosci* **10**:3048-3052.

- Cooper GM (2000) Pathways of Intracellular Signal Transduction, in *The Cell: A Molecular Approach*, Sinauer Associates, Sunderland, MA, USA.
- Copeland RA (2016) The drug-target residence time model: a 10-year retrospective. *Nat Rev Drug Discov* **15**:87-95.
- Copeland RA, Pompliano DL and Meek TD (2006) Drug-target residence time and its implications for lead optimization. *Nat Rev Drug Discov* **5**:730-739.
- Corradin O, Cohen AJ, Luppino JM, Bayles IM, Schumacher FR and Scacheri PC (2016) Modeling disease risk through analysis of physical interactions between genetic variants within chromatin regulatory circuitry. *Nat Genet* **48**:1313-1320.
- Corte LD and Tipton KF (1980) The turnover of the A- and B-forms of monoamine oxidase in rat liver. *Biochem Pharmacol* **29**:891-895.
- Corzo J (2006) Time, the forgotten dimension of ligand binding teaching. *Biochem Mol Biol Educ* **34**:413-416.
- Costa T and Herz A (1989) Antagonists with negative intrinsic activity at delta opioid receptors coupled to GTP-binding proteins. *Proc Natl Acad Sci U S A* **86**:7321-7325.
- Cummings J, Isaacson S, Mills R, Williams H, Chi-Burris K, Corbett A, Dhall R and Ballard C (2014) Pimavanserin for patients with Parkinson's disease psychosis: a randomised, placebo-controlled phase 3 trial. *Lancet* **383**:533-540.
- Dahl G and Akerud T (2013) Pharmacokinetics and the drug-target residence time concept. *Drug Discov Today* **18**:697-707.
- Dallmann R, Brown SA and Gachon F (2014) Chronopharmacology: new insights and therapeutic implications. *Annu Rev Pharmacol Toxicol* **54**:339-361.
- Danhof M, de Jongh J, De Lange EC, Della Pasqua O, Ploeger BA and Voskuyl RA (2007) Mechanism-based pharmacokinetic-pharmacodynamic modeling: biophase distribution, receptor theory, and dynamical systems analysis. *Annu Rev Pharmacol Toxicol* **47**:357-400.
- Dayneka NL, Garg V and Jusko WJ (1993) Comparison of four basic models of indirect pharmacodynamic responses. *J Pharmacokinet Biopharm* **21**:457-478.

- de Aguiar Vallim TQ, Lee E, Merriott DJ, Goulbourne CN, Cheng J, Cheng A, Gonen A, Allen RM, Palladino END, Ford DA, Wang T, Baldan A and Tarling EJ (2017) ABCG1 regulates pulmonary surfactant metabolism in mice and men. *J Lipid Res* **58**:941-954.
- De Deurwaerdere P, Bharatiya R, Chagraoui A and Di Giovanni G (2020) Constitutive activity of 5-HT receptors: Factual analysis. *Neuropharmacology* **168**:107967.
- de Witte WEA, Danhof M, van der Graaf PH and de Lange ECM (2018) The implications of target saturation for the use of drug-target residence time. *Nat Rev Drug Discov* **18**:82-84.
- Dewar KM, Paquet M and Reader TA (1997) Alterations in the turnover rate of dopamine D1 but not D2 receptors in the adult rat neostriatum after a neonatal dopamine denervation. *Neurochem Int* **30**:613-621.
- Disse B, Speck GA, Rominger KL, Witek TJ, Jr. and Hammer R (1999) Tiotropium (Spiriva): mechanistical considerations and clinical profile in obstructive lung disease. *Life Sci* **64**:457-464.
- Doody RS, Corey-Bloom J, Zhang R, Li H, Ieni J and Schindler R (2008) Safety and tolerability of donepezil at doses up to 20 mg/day: results from a pilot study in patients with Alzheimer's disease. *Drugs Aging* **25**:163-174.
- Dorrbaum AR, Kochen L, Langer JD and Schuman EM (2018) Local and global influences on protein turnover in neurons and glia. *Elife* **7**.
- Dorszewska J (2013) Cell biology of normal brain aging: synaptic plasticity-cell death. *Aging Clin Exp Res* **25**:25-34.
- Durcan MJ, Morgan PF, Van Etten ML and Linnoila M (1994) Covariation of alpha 2-adrenoceptor density and function following irreversible antagonism with EEDQ. *Br J Pharmacol* **112**:855-860.
- Dutta S and Sengupta P (2016) Men and mice: Relating their ages. *Life Sci* **152**:244-248.
- Earp J, Krzyzanski W, Chakraborty A, Zamacona MK and Jusko WJ (2004) Assessment of drug interactions relevant to pharmacodynamic indirect response models. *J Pharmacokinet Pharmacodyn* **31**:345-380.

- Egashira T and Kamijo K (1979) Synthetic rates of monoamine oxidase in rat liver after clorglyline or deprenyl administration. *Jpn J Pharmacol* **29**:677-680.
- EMA (2018) Guideline on strategies to identify and mitigate risks for first-in-human and early clinical trials with investigational medicinal products, in *EMA/CHMP/SWP/28367/07 Rev 1* ((CHMP)) ECfMPfHU ed), EMA.
- Erwin VG and Deitrich RA (1971) The labeling in vivo of monoamine oxidase by 14 C-pargyline: a tool for studying the synthesis of the enzyme. *Mol Pharmacol* **7**:219-228.
- Esteller M (2008) Epigenetics in cancer. *N Engl J Med* **358**:1148-1159.
- Farrell K, Musaus M, Navabpour S, Martin K, Ray WK, Helm RF and Jarome TJ (2021) Proteomic analysis reveals sex-specific protein degradation targets in the amygdala during fear memory formation. *Front Mol Neurosci* **14**:716284.
- Fearon KC, Hansell DT, Preston T, Plumb JA, Davies J, Shapiro D, Shenkin A, Calman KC and Burns HJ (1988) Influence of whole body protein turnover rate on resting energy expenditure in patients with cancer. *Cancer Res* **48**:2590-2595.
- Felner AE and Waldmeier PC (1979) Cumulative effects of irreversible MAO inhibitors in vivo. *Biochem Pharmacol* **28**:995-1002.
- Fleckenstein AE, Pogun S, Carroll FI and Kuhar MJ (1996) Recovery of dopamine transporter binding and function after intrastriatal administration of the irreversible inhibitor RTI-76 [3 beta-(3p-chlorophenyl) tropan-2 beta-carboxylic acid p-isothiocyanatophenylethyl ester hydrochloride]. *J Pharmacol Exp Ther* **279**:200-206.
- Folmer RHA (2018) Drug target residence time: a misleading concept. *Drug Discov Today* **23**:12-16.
- Fornasiero EF, Mandad S, Wildhagen H, Alevra M, Rammner B, Keihani S, Opazo F, Urban I, Ischebeck T, Sakib MS, Fard MK, Kirli K, Centeno TP, Vidal RO, Rahman RU, Benito E, Fischer A, Dennerlein S, Rehling P, Feussner I, Bonn S, Simons M, Urlaub H and Rizzoli SO (2018) Precisely measured protein lifetimes in the mouse brain reveal differences across tissues and subcellular fractions. *Nat Commun* **9**:4230.
- Fowler JS, Volkow ND, Logan J, Wang GJ, MacGregor RR, Schyler D, Wolf AP, Pappas N, Alexoff D, Shea C and et al. (1994) Slow recovery of human brain MAO B after L-deprenyl (Selegiline) withdrawal. *Synapse* **18**:86-93.

- Freedman NM, Mishani E, Krausz Y, Weininger J, Lester H, Blaugrund E, Ehrlich D and Chisin R (2005) In vivo measurement of brain monoamine oxidase B occupancy by rasagiline, using (11)C-l-deprenyl and PET. *J Nucl Med* **46**:1618-1624.
- Furchgott RF (1966) The use of beta-halo- alkylamines in the differentiation of receptors and in the determination of dissociation constants of receptor-agonist complexes. *Advances in Drug Research* **3**:21-55.
- Furchgott RF and Bursztyn P (1967) Comparison of dissociation constants and of relative efficacies of selected agonists acting on parasympathetic receptors. *Annals of the New York Academy of Sciences* **144**:882-889.
- Fuxe K, Agnati LF, Merlo Pich E, Meller E and Goldstein M (1987) Evidence for a fast receptor turnover of D1 dopamine receptors in various forebrain regions of the rat. *Neurosci Lett* **81**:183-187.
- Gabilondo AM and Garcia-Sevilla JA (1995) Spontaneous withdrawal from long-term treatment with morphine accelerates the turnover of alpha 2-adrenoceptors in the rat brain: up-regulation of receptors associated with increased receptor appearance. *J Neurochem* **64**:2590-2597.
- Gabrielsson J, Andersson R, Jirstrand M and Hjorth S (2019) Dose-response-time data analysis: An underexploited trinity. *Pharmacol Rev* **71**:89-122.
- Gabrielsson J and Peletier LA (2017) Pharmacokinetic steady-states highlight interesting target-mediated disposition properties. *AAPS J* **19**:772-786.
- Gabrielsson J and Peletier LA (2018) Michaelis-Menten from an in vivo perspective: Open versus closed systems. *AAPS J* **20**:102.
- Gabrielsson J, Peletier LA and Hjorth S (2018a) In vivo potency revisited - Keep the target in sight. *Pharmacol Ther* **184**:177-188.
- Gabrielsson J, Peletier LA and Hjorth S (2018b) Lost in translation: What's in an EC50? Innovative PK/PD reasoning in the drug development context. *Eur J Pharmacol* **835**:154-161.
- Gabrielsson J and Weiner D (2000) *Pharmacokinetic and Pharmacodynamic Data Analysis: Concepts and Applications.*, Sw. Pharmaceutical Press, Stockholm, Sweden.

- Gabrielsson J and Weiner D (2016) *Pharmacokinetic and Pharmacodynamic Data Analysis: Concepts and Applications.*, Sw. Pharmaceutical Press, Stockholm, Sweden.
- Gabrielsson JG and Hjorth S (2018) Integration of pharmacokinetic and pharmacodynamic reasoning and its importance in drug discovery., in *Early Drug Development: Bringing a Preclinical Candidate to the Clinic* (Giordanetto F ed) pp 369-400, Wiley-VCH, Weinheim, Germany.
- Garland SL (2013) Are GPCRs still a source of new targets? *J Biomol Screen* **18**:947-966.
- Gedda K, Scott D, Besancon M, Lorentzon P and Sachs G (1995) Turnover of the gastric H⁺,K⁽⁺⁾-adenosine triphosphatase alpha subunit and its effect on inhibition of rat gastric acid secretion. *Gastroenterology* **109**:1134-1141.
- Gierse JK, Koboldt CM, Walker MC, Seibert K and Isakson PC (1999) Kinetic basis for selective inhibition of cyclo-oxygenases. *Biochem J* **339 (Pt 3)**:607-614.
- Giorgi O, Pibiri MG and Biggio G (1991) Differential turnover rates of D1 dopamine receptors in the retina and in distinct areas of the rat brain. *J Neurochem* **57**:754-759.
- Giorgi O, Pibiri MG, Dal Toso R and Ragatzu G (1992) Age-related changes in the turnover rates of D1-dopamine receptors in the retina and in distinct areas of the rat brain. *Brain Res* **569**:323-329.
- Goridis C and Neff NH (1971) Monoamine oxidase: an approximation of turnover rates. *J Neurochem* **18**:1673-1682.
- Gosset JR, Beaumont K, Matsuura T, Winchester W, Attkins N, Glatt S, Lightbown I, Ulrich K, Roberts S, Harris J, Mesic E, van Steeg T, Hijdra D and van der Graaf PH (2017) A cross-species translational pharmacokinetic-pharmacodynamic evaluation of core body temperature reduction by the TRPM8 blocker PF-05105679. *Eur J Pharm Sci* **109S**:S161-S167.
- Gozlan H, Laporte AM, Thibault S, Schechter LE, Bolanos F and Hamon M (1994) Differential effects of N-ethoxycarbonyl-2-ethoxy-1,2-dihydroquinoline (EEDQ) on various 5-HT receptor binding sites in the rat brain. *Neuropharmacology* **33**:423-431.
- Greathouse B, Zahra F and Brady MF (2021) Acetylcholinesterase Inhibitors Toxicity, in *StatPearls*, Treasure Island (FL).

- Green AR, Gabrielsson J and Fone KC (2011) Translational neuropharmacology and the appropriate and effective use of animal models. *Br J Pharmacol* **164**:1041-1043.
- Grimwood S and Hartig PR (2009) Target site occupancy: emerging generalizations from clinical and preclinical studies. *Pharmacol Ther* **122**:281-301.
- Hamblin MW and Creese I (1983) Behavioral and radioligand binding evidence for irreversible dopamine receptor blockade by N-ethoxycarbonyl-2-ethoxy-1,2-dihydroquinoline. *Life Sci* **32**:2247-2255.
- Hamilton CA, Dalrymple HW, Reid JL and Sumner DJ (1984) The recovery of alpha-adrenoceptor function and binding sites after phenoxybenzamine. An index of receptor turnover? *Naunyn Schmiedebergs Arch Pharmacol* **325**:34-41.
- Hamilton CA and Reid JL (1985) The effects of phenoxybenzamine on specific binding and function of central alpha-adrenoceptors in the rabbit. *Brain Res* **344**:89-95.
- Hauser AS, Attwood MM, Rask-Andersen M, Schioth HB and Gloriam DE (2017) Trends in GPCR drug discovery: new agents, targets and indications. *Nat Rev Drug Discov* **16**:829-842.
- Held F, Hoppe E, Cvijovic M, Jirstrand M and Gabrielsson J (2019) Challenge model of TNFalpha turnover at varying LPS and drug provocations. *J Pharmacokinet Pharmacodyn* **46**:223-240.
- Hess CN, Low Wang CC and Hiatt WR (2018) PCSK9 inhibitors: Mechanisms of action, metabolic effects, and clinical outcomes. *Annu Rev Med* **69**:133-145.
- Hinze C, Harland D, Zreika M, Dulery B and Hardenberg J (1990) A double-blind, placebo-controlled study of the tolerability and effects on platelet MAO-B activity of single oral doses of MDL 72.974A in normal volunteers. *J Neural Transm Suppl* **32**:203-209.
- Holford N and Nutt JG (2008) Disease progression, drug action and Parkinson's disease: why time cannot be ignored. *Eur J Clin Pharmacol* **64**:207-216.
- Hong Y, Gengo FM, Rainka MM, Bates VE and Mager DE (2008) Population pharmacodynamic modelling of aspirin- and ibuprofen-induced inhibition of platelet aggregation in healthy subjects. *Clin Pharmacokinet* **47**:129-137.
- Hothersall JD, Brown AJ, Dale I and Rawlins P (2016) Can residence time offer a useful strategy to target agonist drugs for sustained GPCR responses? *Drug Discov Today* **21**:90-96.

- Hoyer D and Boddeke HW (1993) Partial agonists, full agonists, antagonists: dilemmas of definition. *Trends Pharmacol Sci* **14**:270-275.
- Hu Y, Ingelman-Sundberg M and Lindros KO (1995) Induction mechanisms of cytochrome P450 2E1 in liver: interplay between ethanol treatment and starvation. *Biochem Pharmacol* **50**:155-161.
- Igawa T, Ishii S, Tachibana T, Maeda A, Higuchi Y, Shimaoka S, Moriyama C, Watanabe T, Takubo R, Doi Y, Wakabayashi T, Hayasaka A, Kadono S, Miyazaki T, Haraya K, Sekimori Y, Kojima T, Nabuchi Y, Aso Y, Kawabe Y and Hattori K (2010) Antibody recycling by engineered pH-dependent antigen binding improves the duration of antigen neutralization. *Nat Biotechnol* **28**:1203-1207.
- Ito K, Asakura A, Yamada Y, Nakamura K, Sawada Y and Iga T (1997) Prediction of the therapeutic dose for benzodiazepine anxiolytics based on receptor occupancy theory. *Biopharm Drug Dispos* **18**:293-303.
- Jacobs JR, Reves JG, Marty J, White WD, Bai SA and Smith LR (1995) Aging increases pharmacodynamic sensitivity to the hypnotic effects of midazolam. *Anesth Analg* **80**:143-148.
- Jann MW (2000) Rivastigmine, a new-generation cholinesterase inhibitor for the treatment of Alzheimer's disease. *Pharmacotherapy* **20**:1-12.
- Jansson-Lofmark R, Hjorth S and Gabrielsson J (2020) Does in vitro potency predict clinically efficacious concentrations? *Clin Pharmacol Ther* **108**:298-305.
- Jordan S, Regardie K, Johnson JL, Chen R, Kambayashi J, McQuade R, Kitagawa H, Tadori Y and Kikuchi T (2007) In vitro functional characteristics of dopamine D2 receptor partial agonists in second and third messenger-based assays of cloned human dopamine D2Long receptor signalling. *J Psychopharmacol* **21**:620-627.
- Joyce AR, Easterling K, Holtzman SG and Kuhar MJ (2006) Modeling the onset of drug dependence: a consideration of the requirement for protein synthesis. *J Theor Biol* **240**:531-537.
- Kalvass JC, Olson ER, Cassidy MP, Selley DE and Pollack GM (2007) Pharmacokinetics and pharmacodynamics of seven opioids in P-glycoprotein-competent mice: assessment of unbound brain EC50,u and correlation of in vitro, preclinical, and clinical data. *J Pharmacol Exp Ther* **323**:346-355.

- Kang YJ, Mbonye UR, DeLong CJ, Wada M and Smith WL (2007) Regulation of intracellular cyclooxygenase levels by gene transcription and protein degradation. *Prog Lipid Res* **46**:108-125.
- Keck BJ and Lakoski JM (1996b) Region-specific serotonin_{1A} receptor turnover following irreversible blockade with EEDQ. *Neuroreport* **7**:2717-2721.
- Keck BJ and Lakoski JM (2000) Regional heterogeneity of serotonin_{1A} receptor inactivation and turnover in the aging female rat brain following EEDQ. *Neuropharmacology* **39**:1237-1246.
- Keck J and Lakoski JM (1996a) Age-related assessment of central 5-HT_{1A} receptors following irreversible inactivation by N-ethoxycarbonyl-2-ethoxy-1,2-dihydroquinoline (EEDQ). *Brain Res* **728**:130-134.
- Kenakin T (2013) New concepts in pharmacological efficacy at 7TM receptors: IUPHAR review 2. *Br J Pharmacol* **168**:554-575.
- Kenakin T (2016) The mass action equation in pharmacology. *Br J Clin Pharmacol* **81**:41-51.
- Kenakin T (2018) *A Pharmacology Primer - Techniques for More Effective and Strategic Drug Discovery*, Academic Press.
- Kenakin TP (2017) *Pharmacology in Drug Discovery and Development*, Academic Press.
- Khan DD (2016) Pharmacokinetic-Pharmacodynamic modeling and prediction of antibiotic effects, in *Department of Pharmaceutical Biosciences* p 56, Uppsala University, Uppsala.
- Kimmel HL, Carroll FI and Kuhar MJ (2000) Dopamine transporter synthesis and degradation rate in rat striatum and nucleus accumbens using RTI-76. *Neuropharmacology* **39**:578-585.
- Kimmel HL, Carroll FI and Kuhar MJ (2003) Withdrawal from repeated cocaine alters dopamine transporter protein turnover in the rat striatum. *J Pharmacol Exp Ther* **304**:15-21.
- Kleiber M (1947) Body size and metabolic rate. *Physiol Rev* **27**:511-541.
- Kroon T, Baccega T, Olsen A, Gabrielsson J and Oakes ND (2017) Nicotinic acid timed to feeding reverses tissue lipid accumulation and improves glucose control in obese Zucker rats[S]. *J Lipid Res* **58**:31-41.

Kuhar MJ (2009) On the use of protein turnover and half-lives. *Neuropsychopharmacology* **34**:1172-1173.

Kuhar MJ and Joyce AR (2001) Slow onset of CNS drugs: can changes in protein concentration account for the delay? *Trends Pharmacol Sci* **22**:450-456.

Kuhar MJ and Joyce AR (2003) Is the onset of psychoactive drug effects compatible with a protein-synthesis mechanism? *Neuropsychopharmacology* **28 Suppl 1**:S94-97.

Kula NS, George T and Baldessarini RJ (1992) Rate of recovery of D1 and D2 dopaminergic receptors in young vs. adult rat striatal tissue following alkylation with ethoxycarbonyl-ethoxy-dihydroquinoline (EEDQ). *Brain Res Dev Brain Res* **66**:286-289.

Kwon D, Chae JB, Park CW, Kim YS, Lee SM, Kim EJ, Huh IH, Kim DY and Cho KD (2001) Effects of IY-81149, a newly developed proton pump inhibitor, on gastric acid secretion in vitro and in vivo. *Arzneimittelforschung* **51**:204-213.

Lappe-Siefke C, Loebrich S, Hevers W, Waidmann OB, Schweizer M, Fehr S, Fritschy JM, Dikic I, Eilers J, Wilson SM and Kneussel M (2009) The ataxia (axJ) mutation causes abnormal GABAA receptor turnover in mice. *PLoS Genet* **5**:e1000631.

Larsson J, Hoppe E, Gautrois M, Cvijovic M and Jirstrand M (2021) Second-generation TNFalpha turnover model for improved analysis of test compound interventions in LPS challenge studies. *Eur J Pharm Sci* **165**:105937.

Lee JH, Jeong SK, Kim BC, Park KW and Dash A (2015) Donepezil across the spectrum of Alzheimer's disease: dose optimization and clinical relevance. *Acta Neurol Scand* **131**:259-267.

Leff SE, Gariano R and Creese I (1984) Dopamine receptor turnover rates in rat striatum are age-dependent. *Proc Natl Acad Sci U S A* **81**:3910-3914.

Levesque D and Di Paolo T (1991) Dopamine receptor reappearance after irreversible receptor blockade: effect of chronic estradiol treatment of ovariectomized rats. *Mol Pharmacol* **39**:659-665.

Levy G (1998) Predicting effective drug concentrations for individual patients. Determinants of pharmacodynamic variability. *Clin Pharmacokinet* **34**:323-333.

- Li X, Jusko WJ and Cao Y (2018) Role of interstitial fluid turnover on target suppression by therapeutic biologics using a minimal physiologically based pharmacokinetic model. *J Pharmacol Exp Ther* **367**:1-8.
- Li Z, Radin A, Li M, Hamilton JD, Kajiwarra M, Davis JD, Takahashi Y, Hasegawa S, Ming JE, DiCioccio AT, Li Y, Kovalenko P, Lu Q, Ortemann-Renon C, Ardeleanu M and Swanson BN (2020) Pharmacokinetics, pharmacodynamics, safety, and tolerability of dupilumab in healthy adult subjects. *Clin Pharmacol Drug Dev* **9**:742-755.
- Liang J, Zbieg JR, Blake RA, Chang JH, Daly S, DiPasquale AG, Friedman LS, Gelzleichter T, Gill M, Giltneane JM, Goodacre S, Guan J, Hartman SJ, Ingalla ER, Kategaya L, Kiefer JR, Kleinheinz T, Labadie SS, Lai T, Li J, Liao J, Liu Z, Mody V, McLean N, Metcalfe C, Nannini MA, Oeh J, O'Rourke MG, Ortwine DF, Ran Y, Ray NC, Roussel F, Sambrone A, Sampath D, Schutt LK, Vinogradova M, Wai J, Wang T, Wertz IE, White JR, Yeap SK, Young A, Zhang B, Zheng X, Zhou W, Zhong Y and Wang X (2021) GDC-9545 (Giredestrant): A Potent and Orally Bioavailable Selective Estrogen Receptor Antagonist and Degradable with an Exceptional Preclinical Profile for ER+ Breast Cancer. *J Med Chem*.
- Lin JH (1991) Pharmacokinetic and pharmacodynamic properties of histamine H₂-receptor antagonists. Relationship between intrinsic potency and effective plasma concentrations. *Clin Pharmacokinet* **20**:218-236.
- Lu H and Tonge PJ (2010) Drug-target residence time: critical information for lead optimization. *Curr Opin Chem Biol* **14**:467-474.
- Lynch CJ, Deth RC and Steer ML (1983) Simultaneous loss and reappearance of alpha 1-adrenergic responses and [3H]prazosin binding sites in rat liver after irreversible blockade by phenoxybenzamine. *Biochim Biophys Acta* **757**:156-163.
- Lyons HR, Gibbs TT and Farb DH (2000) Turnover and down-regulation of GABA(A) receptor alpha1, beta2S, and gamma1 subunit mRNAs by neurons in culture. *J Neurochem* **74**:1041-1048.
- Mager DE, Woo S and Jusko WJ (2009) Scaling pharmacodynamics from in vitro and preclinical animal studies to humans. *Drug Metab Pharmacokinet* **24**:16-24.
- Magnusson MO, Dahl ML, Cederberg J, Karlsson MO and Sandstrom R (2008) Pharmacodynamics of carbamazepine-mediated induction of CYP3A4, CYP1A2, and P-gp as assessed by probe substrates midazolam, caffeine, and digoxin. *Clin Pharmacol Ther* **84**:52-62.

- Marshall JW, Cummings RM, Bowes LJ, Ridley RM and Green AR (2003) Functional and histological evidence for the protective effect of NXY-059 in a primate model of stroke when given 4 hours after occlusion. *Stroke* **34**:2228-2233.
- Mateos-Aparicio P and Rodriguez-Moreno A (2019) The Impact of Studying Brain Plasticity. *Front Cell Neurosci* **13**:66.
- Mbonye UR, Wada M, Rieke CJ, Tang HY, Dewitt DL and Smith WL (2006) The 19-amino acid cassette of cyclooxygenase-2 mediates entry of the protein into the endoplasmic reticulum-associated degradation system. *J Biol Chem* **281**:35770-35778.
- McKernan RM and Campbell IC (1982) Measurement of alpha-adrenoceptor 'turnover' using phenoxybenzamine. *Eur J Pharmacol* **80**:279-280.
- Mestas J and Hughes CC (2004) Of mice and not men: differences between mouse and human immunology. *J Immunol* **172**:2731-2738.
- Michaelis L and Menten ML (1913) Die Kinetik der Invertinwirkung. *Biochem Z* **49**:333-369.
- Michaelis L, Menten ML, Johnson KA and Goody RS (2011) The original Michaelis constant: translation of the 1913 Michaelis-Menten paper. *Biochemistry* **50**:8264-8269.
- Miida H, Arakawa S, Shibaya Y, Honda K, Kiyosawa N, Watanabe K, Manabe S, Takasaki W and Ueno K (2008) Toxicokinetic and toxicodynamic analysis of clofibrate based on free drug concentrations in nagase analbuminemia rats (NAR). *J Toxicol Sci* **33**:349-361.
- Miller LG, Lumpkin M, Galpern WR, Greenblatt DJ and Shader RI (1991a) Modification of gamma-aminobutyric acidA receptor binding and function by N-ethoxycarbonyl-2-ethoxy-1,2-dihydroquinoline in vitro and in vivo: effects of aging. *J Neurochem* **56**:1241-1247.
- Miller LG, Lumpkin M, Greenblatt DJ and Shader RI (1991b) Accelerated benzodiazepine receptor recovery after lorazepam discontinuation. *FASEB J* **5**:93-97.
- Morey TM, Esmaili MA, Duennwald ML and Rylett RJ (2021) SPAAC Pulse-Chase: A novel click chemistry-based method to determine the half-life of cellular proteins. *Front Cell Dev Biol* **9**:722560.

- Morissette M, Levesque D and Di Paolo T (1992) Effect of chronic estradiol treatment on brain dopamine receptor reappearance after irreversible blockade: an autoradiographic study. *Mol Pharmacol* **42**:480-488.
- Moss DE, Perez RG and Kobayashi H (2017) Cholinesterase inhibitor therapy in Alzheimer's Disease: The limits and tolerability of irreversible CNS-selective acetylcholinesterase inhibition in primates. *J Alzheimers Dis* **55**:1285-1294.
- Mouton JW, Muller AE, Canton R, Giske CG, Kahlmeter G and Turnidge J (2018) MIC-based dose adjustment: facts and fables. *J Antimicrob Chemother* **73**:564-568.
- Mullard A (2021) Targeted protein degraders crowd into the clinic. *Nat Rev Drug Discov* **20**:247-250.
- Nagashima R, O'Reilly RA and Levy G (1969) Kinetics of pharmacologic effects in man: the anticoagulant action of warfarin. *Clin Pharmacol Ther* **10**:22-35.
- Nelson CA, Muther TF, Pitha J and Baker SP (1986) Differential recovery of beta adrenoreceptor antagonist and agonist high affinity binding sites in the guinea-pig lung after irreversible blockade. *J Pharmacol Exp Ther* **237**:830-836.
- Neubig RR, Spedding M, Kenakin T, Christopoulos A, International Union of Pharmacology Committee on Receptor N and Drug C (2003) International Union of Pharmacology Committee on Receptor Nomenclature and Drug Classification. XXXVIII. Update on terms and symbols in quantitative pharmacology. *Pharmacol Rev* **55**:597-606.
- Neve KA, Loesch S and Marshall JF (1985) Denervation accelerates the reappearance of neostriatal D-2 receptors after irreversible receptor blockade. *Brain Res* **329**:225-231.
- Nickerson M and Goodman LS (1947) Pharmacological properties of a new adrenergic blocking agent: N,N-dibenzyl-beta-chloroethylamine (dibenamine). *J Pharmacol Exp Ther* **89**:167-185.
- Nilsson P, Hillered L, Ponten U and Ungerstedt U (1990) Changes in cortical extracellular levels of energy-related metabolites and amino acids following concussive brain injury in rats. *J Cereb Blood Flow Metab* **10**:631-637.
- Nilvebrant L, Hallen B and Larsson G (1997) Tolterodine--a new bladder selective muscarinic receptor antagonist: preclinical pharmacological and clinical data. *Life Sci* **60**:1129-1136.

- Norman AB, Battaglia G and Creese I (1987) Differential recovery rates of rat D2 dopamine receptors as a function of aging and chronic reserpine treatment following irreversible modification: a key to receptor regulatory mechanisms. *J Neurosci* **7**:1484-1491.
- Nowak G and Zak J (1989) Repeated electroconvulsive shock (ECS) enhances striatal D-1 dopamine receptor turnover in rats. *Eur J Pharmacol* **167**:307-308.
- Nowak G and Zak J (1991a) Effect of repeated treatment with antidepressant drugs and electroconvulsive shock (ECS) on the D2 dopaminergic receptor turnover in the rat brain. *Pharmacol Toxicol* **69**:87-89.
- Nowak G and Zak J (1991b) The turnover of rat cortical alpha 1-adrenoceptors is not modified by repeated electroconvulsive treatment. *J Neurochem* **56**:2004-2006.
- Oakes ND, Thalen P, Hultstrand T, Jacinto S, Camejo G, Wallin B and Ljung B (2005) Tesaglitazar, a dual PPAR{alpha}/{gamma} agonist, ameliorates glucose and lipid intolerance in obese Zucker rats. *Am J Physiol Regul Integr Comp Physiol* **289**:R938-946.
- Oakes ND, Thalen PG, Jacinto SM and Ljung B (2001) Thiazolidinediones increase plasma-adipose tissue FFA exchange capacity and enhance insulin-mediated control of systemic FFA availability. *Diabetes* **50**:1158-1165.
- Obach RS (2013) Pharmacologically active drug metabolites: impact on drug discovery and pharmacotherapy. *Pharmacol Rev* **65**:578-640.
- Oreland L, Jossan SS, Hartvig P, Aquilonius SM and Langstrom B (1990) Turnover of monoamine oxidase B (MAO-B) in pig brain by positron emission tomography using 11C-L-deprenyl. *J Neural Transm Suppl* **32**:55-59.
- Peletier LA and Gabrielsson J (2012) Dynamics of target-mediated drug disposition: characteristic profiles and parameter identification. *J Pharmacokinet Pharmacodyn* **39**:429-451.
- Peletier LA and Gabrielsson J (2018) New equilibrium models of drug-receptor interactions derived from Target-Mediated Drug Disposition. *AAPS J* **20**:69.
- Peletier LA and Gabrielsson J (2022) Impact of enzyme turnover on the dynamics of the Michaelis-Menten model. *Math Biosci* **346**:108795.

- Peletier LA, Jansson-Lofmark R and Gabrielsson J (2021) Comparisons of basic target-mediated drug disposition (TMDD) and ligand facilitated target removal (LFTR). *Eur J Pharm Sci* **162**:105835.
- Pereira ER, Liao N, Neale GA and Hendershot LM (2010) Transcriptional and post-transcriptional regulation of proangiogenic factors by the unfolded protein response. *PLoS One* **5**.
- Pich EM, Benfenati F, Farabegoli C, Fuxe K, Meller E, Aronsson M, Goldstein M and Agnati LF (1987) Chronic haloperidol affects striatal D2-dopamine receptor reappearance after irreversible receptor blockade. *Brain Res* **435**:147-152.
- Pineda J, Ruiz-Ortega JA and Ugedo L (1997) Receptor reserve and turnover of alpha-2 adrenoceptors that mediate the clonidine-induced inhibition of rat locus coeruleus neurons in vivo. *J Pharmacol Exp Ther* **281**:690-698.
- Pinto W and Battaglia G (1994) Comparative recovery kinetics of 5-hydroxytryptamine 1A, 1B, and 2A receptor subtypes in rat cortex after receptor inactivation: evidence for differences in receptor production and degradation. *Mol Pharmacol* **46**:1111-1119.
- Pitha J, Hughes BA, Kusiak JW, Dax EM and Baker SP (1982) Regeneration of beta-adrenergic receptors in senescent rats: a study using an irreversible binding antagonist. *Proc Natl Acad Sci U S A* **79**:4424-4427.
- Planz G, Quiring K and Palm D (1972a) Rates of recovery of irreversibly inhibited monoamine oxidases: a measure of enzyme protein turnover. *Naunyn Schmiedeberg's Arch Pharmacol* **273**:27-42.
- Planz G, Quiring K and Palm D (1972b) Turnover rates of monoamine oxidases: recovery of the irreversibly inhibited enzyme activity and the influence of isoproterenol. *Life Sci* **11**:147-160.
- Powell-Tuck J, Garlick PJ, Lennard-Jones JE and Waterlow JC (1984) Rates of whole body protein synthesis and breakdown increase with the severity of inflammatory bowel disease. *Gut* **25**:460-464.
- Prager EM, Aroniadou-Anderjaska V, Almeida-Suhett CP, Figueiredo TH, Aplan JP, Rossetti F, Olsen CH and Braga MF (2014) The recovery of acetylcholinesterase activity and the progression of neuropathological and pathophysiological alterations in the rat basolateral amygdala after soman-induced status epilepticus: relation to anxiety-like behavior. *Neuropharmacology* **81**:64-74.

- Price JC, Guan S, Burlingame A, Prusiner SB and Ghaemmaghami S (2010) Analysis of proteome dynamics in the mouse brain. *Proc Natl Acad Sci U S A* **107**:14508-14513.
- Raffa RB, Pawasauskas J, Pergolizzi JV, Jr., Lu L, Chen Y, Wu S, Jarrett B, Fain R, Hill L and Devarakonda K (2018) Pharmacokinetics of oral and intravenous paracetamol (acetaminophen) when co-administered with intravenous morphine in healthy adult subjects. *Clin Drug Investig* **38**:259-268.
- Raghupathi RK, Artymyshyn R and McGonigle P (1996b) Regional variability in changes in 5-HT_{2A} receptor mRNA levels in rat brain following irreversible inactivation with EEDQ. *Brain Res Mol Brain Res* **39**:198-206.
- Raghupathi RK, Brousseau DA and McGonigle P (1996a) Time-course of recovery of 5-HT_{1A} receptors and changes in 5-HT_{1A} receptor mRNA after irreversible inactivation with EEDQ. *Brain Res Mol Brain Res* **38**:233-242.
- Ramsay RR and Tipton KF (2017) Assessment of enzyme inhibition: A review with examples from the development of monoamine oxidase and cholinesterase inhibitory drugs. *Molecules* **22**.
- Ramsden D, Zhou J and Tweedie DJ (2015) Determination of a degradation constant for CYP3A4 by direct suppression of mRNA in a novel human hepatocyte model, HepatoPac. *Drug Metab Dispos* **43**:1307-1315.
- Rask-Andersen M, Almen MS and Schioth HB (2011) Trends in the exploitation of novel drug targets. *Nat Rev Drug Discov* **10**:579-590.
- Rego JC, Syringas M, Leblond B, Costentin J and Bonnet JJ (1999) Recovery of dopamine neuronal transporter but lack of change of its mRNA in substantia nigra after inactivation by a new irreversible inhibitor characterized in vitro and ex vivo in the rat. *Br J Pharmacol* **128**:51-60.
- Ribas C, Miralles A, Busquets X and Garcia-Sevilla JA (2001) Brain alpha(2)-adrenoceptors in monoamine-depleted rats: increased receptor density, G coupling proteins, receptor turnover and receptor mRNA. *Br J Pharmacol* **132**:1467-1476.
- Ribas C, Miralles A, Escriba PV and Garcia-Sevilla JA (1998) Effects of the alkylating agent EEDQ on regulatory G proteins and recovery of agonist and antagonist alpha2-adrenoceptor binding sites in rat brain. *Eur J Pharmacol* **351**:145-154.

- Ribas C, Miralles A and Garcia-Sevilla JA (1993) Acceleration by chronic treatment with clorgyline of the turnover of brain alpha 2-adrenoceptors in normotensive but not in spontaneously hypertensive rats. *Br J Pharmacol* **110**:99-106.
- Richardson K and Rose SP (1971) A diurnal rhythmicity in incorporation of lysine into rat brain regions. *Nat New Biol* **233**:182-184.
- Rolan PE (1994) Plasma protein binding displacement interactions--why are they still regarded as clinically important? *Br J Clin Pharmacol* **37**:125-128.
- Rostami-Hodjegan A (2010) Translation of in vitro metabolic data to predict in vivo drug-drug interactions: IVIVE and Modeling and Simulation, in *Enzyme- and Transporter-Based Drug-Drug Interactions: Progress and Future Challenges* (Pang PS, Rodrigues AD and Peter RM eds) pp 317-341, Springer, New York, USA.
- Rostami-Hodjegan A, Wolff K, Hay AW, Raistrick D, Calvert R and Tucker GT (1999) Population pharmacokinetics of methadone in opiate users: characterization of time-dependent changes. *Br J Clin Pharmacol* **48**:43-52.
- Rowland M and Tozer TN (2011) *Clinical Pharmacokinetics and Pharmacodynamics: Concepts and Applications*, Wolters Kluwer | Lippincott Williams & Wilkins.
- Ryazanov AG and Nefsky BS (2002) Protein turnover plays a key role in aging. *Mech Ageing Dev* **123**:207-213.
- Saber H, Simpson N, Ricks TK and Leighton JK (2019) An FDA oncology analysis of toxicities associated with PBD-containing antibody-drug conjugates. *Regul Toxicol Pharmacol* **107**:104429.
- Saganuwan SA (2021) Application of modified Michaelis - Menten equations for determination of enzyme inducing and inhibiting drugs. *BMC Pharmacol Toxicol* **22**:57.
- Sarkar CA, Lowenhaupt K, Horan T, Boone TC, Tidor B and Lauffenburger DA (2002) Rational cytokine design for increased lifetime and enhanced potency using pH-activated "histidine switching". *Nat Biotechnol* **20**:908-913.
- Savage VM, Allen AP, Brown JH, Gillooly JF, Herman AB, Woodruff WH and West GB (2007) Scaling of number, size, and metabolic rate of cells with body size in mammals. *Proc Natl Acad Sci U S A* **104**:4718-4723.

- Schmidt-Nielsen K (1984) *Scaling: Why is animal size so important?*, Cambridge University Press, Cambridge, UK.
- Sher E and Clementi F (1984) Effect of specific antibodies on acetylcholine receptor turnover: increased degradation controls low density of cell surface receptor. *Neurology* **34**:208-211.
- Simon GM, Niphakis MJ and Cravatt BF (2013) Determining target engagement in living systems. *Nat Chem Biol* **9**:200-205.
- Singh K, Hotchkiss KM, Mohan AA, Reedy JL, Sampson JH and Khasraw M (2021) For whom the T cells troll? Bispecific T-cell engagers in glioblastoma. *J Immunother Cancer* **9**.
- Sladeczek F and Bockaert J (1983) Turnover in vivo of alpha 1-adrenergic receptors in rat submaxillary glands. *Mol Pharmacol* **23**:282-288.
- Smith DA, Di L and Kerns EH (2010) The effect of plasma protein binding on in vivo efficacy: misconceptions in drug discovery. *Nat Rev Drug Discov* **9**:929-939.
- Smith DA, van Waterschoot RAB, Parrott NJ, Olivares-Morales A, Lave T and Rowland M (2018) Importance of target-mediated drug disposition for small molecules. *Drug Discov Today* **23**:2023-2030.
- Song Y, Jeong H, Kim SR, Ryu Y, Baek J, Kwon J, Cho H, Kim KN and Lee JJ (2021) Dissecting the impact of target-binding kinetics of protein binders on tumor localization. *iScience* **24**:102104.
- Sosa-Hernandez JE, Villalba-Rodriguez AM, Romero-Castillo KD, Aguilar-Aguila-Isaias MA, Garcia-Reyes IE, Hernandez-Antonio A, Ahmed I, Sharma A, Parra-Saldivar R and Iqbal HMN (2018) Organs-on-a-chip module: A review from the development and applications perspective. *Micromachines (Basel)* **9**.
- Spector IM (1974) Animal longevity and protein turnover rate. *Nature* **249**:66.
- Sriram K and Insel PA (2018) G Protein-Coupled Receptors as targets for approved drugs: How many targets and how many drugs? *Mol Pharmacol* **93**:251-258.
- Stahl SM (2017) Neuronal traffic signals in tardive dyskinesia: not enough "stop" in the motor striatum. *CNS Spectr* **22**:427-434.

- Steindl D, Boehmerle W, Korner R, Praeger D, Haug M, Nee J, Schreiber A, Scheibe F, Demin K, Jacoby P, Tauber R, Hartwig S, Endres M and Eckardt KU (2021) Novichok nerve agent poisoning. *Lancet* **397**:249-252.
- Stephenson RP (1956) A modification of receptor theory. *Br J Pharmacol Chemother* **11**:379-393.
- Swovick K, Welle KA, Hryhorenko JR, Seluanov A, Gorbunova V and Ghaemmaghami S (2018) Cross-species comparison of proteome turnover kinetics. *Mol Cell Proteomics* **17**:580-591.
- Sykes DA and Charlton SJ (2012) Slow receptor dissociation is not a key factor in the duration of action of inhaled long-acting beta2-adrenoceptor agonists. *Br J Pharmacol* **165**:2672-2683.
- Sykes DA, Dowling MR, Leighton-Davies J, Kent TC, Fawcett L, Renard E, Trifilieff A and Charlton SJ (2012) The Influence of receptor kinetics on the onset and duration of action and the therapeutic index of NVA237 and tiotropium. *J Pharmacol Exp Ther* **343**:520-528.
- Tang Y and Cao Y (2021) Modeling pharmacokinetics and pharmacodynamics of therapeutic antibodies: Progress, challenges, and future directions. *Pharmaceutics* **13**.
- Taouis M, Berlan M and Lafontan M (1987) Alpha 2-adrenergic receptor turnover in adipose tissue and kidney: irreversible blockade of alpha 2-adrenergic receptors by benextramine. *Mol Pharmacol* **31**:89-96.
- Thompson IA, de Vries EFJ and Sommer IEC (2020) Dopamine D2 up-regulation in psychosis patients after antipsychotic drug treatment. *Curr Opin Psychiatry* **33**:200-205.
- Thurmann PA (2020) Pharmacodynamics and pharmacokinetics in older adults. *Curr Opin Anaesthesiol* **33**:109-113.
- Trifiro G and Spina E (2011) Age-related changes in pharmacodynamics: focus on drugs acting on central nervous and cardiovascular systems. *Curr Drug Metab* **12**:611-620.
- Tumer N, Scarpace PJ and Lowenthal DT (1992) Geriatric pharmacology: basic and clinical considerations. *Annu Rev Pharmacol Toxicol* **32**:271-302.
- Turnheim K (2003) When drug therapy gets old: pharmacokinetics and pharmacodynamics in the elderly. *Exp Gerontol* **38**:843-853.

- van Waterschoot RAB, Parrott NJ, Olivares-Morales A, Lave T, Rowland M and Smith DA (2018) Impact of target interactions on small-molecule drug disposition: an overlooked area. *Nat Rev Drug Discov* **17**:299.
- Vane JR and Botting RM (2003) The mechanism of action of aspirin. *Thromb Res* **110**:255-258.
- Vauquelin G (2010) Rebinding: or why drugs may act longer in vivo than expected from their in vitro target residence time. *Expert Opin Drug Discov* **5**:927-941.
- Vauquelin G and Charlton SJ (2010) Long-lasting target binding and rebinding as mechanisms to prolong in vivo drug action. *Br J Pharmacol* **161**:488-508.
- Vicentic A, Battaglia G, Carroll FI and Kuhar MJ (1999) Serotonin transporter production and degradation rates: studies with RTI-76. *Brain Res* **841**:1-10.
- Vinod KY, Subhash MN and Srinivas BN (2001) Differential protection and recovery of 5-HT1A receptors from N-ethoxycarbonyl-2-ethoxy-1,2-dihydroquinoline (EEDQ) inactivation in regions of rat brain. *Neurochem Res* **26**:113-120.
- Visser SA, Huntjens DR, van der Graaf PH, Peletier LA and Danhof M (2003) Mechanism-based modeling of the pharmacodynamic interaction of alphaxalone and midazolam in rats. *J Pharmacol Exp Ther* **307**:765-775.
- von Bahr C, Steiner E, Koike Y and Gabrielsson J (1998) Time course of enzyme induction in humans: effect of pentobarbital on nortriptyline metabolism. *Clin Pharmacol Ther* **64**:18-26.
- Wallmark B, Lorentzon P and Larsson H (1985) The mechanism of action of omeprazole--a survey of its inhibitory actions in vitro. *Scand J Gastroenterol Suppl* **108**:37-51.
- Wang H, Shao F, Liu X, Xu W, Ou N, Qin X, Liu F, Hou X, Hu H and Jiang J (2019) Efficacy, safety and pharmacokinetics of ilaprazole infusion in healthy subjects and patients with esomeprazole as positive control. *Br J Clin Pharmacol* **85**:2547-2558.
- Wanwimolruk S and Levy G (1987) Effect of age on the pharmacodynamics of phenobarbital and ethanol in rats. *J Pharm Sci* **76**:503-507.
- Waterlow JC (1984) Protein turnover with special reference to man. *Q J Exp Physiol* **69**:409-438.

- Waters S, Svensson P, Kullingsjo J, Ponten H, Andreasson T, Sunesson Y, Ljung E, Sonesson C and Waters N (2017) In Vivo Systems Response Profiling and Multivariate Classification of CNS Active Compounds: A Structured Tool for CNS Drug Discovery. *ACS Chem Neurosci* **8**:785-797.
- Webster L, Gudin J, Raffa RB, Kuchera J, Rauck R, Fudin J, Adler J and Mallick-Searle T (2020) Understanding buprenorphine for use in chronic pain: Expert opinion. *Pain Med* **21**:714-723.
- Wentholt RJ, Mahler HR and Moore WJ (1974) The half-life of acetylcholinesterase in mature rat brain. *J Neurochem* **22**:941-943.
- Wu QJ, Sun X, Teves L, Mayor D and Tymianski M (2021) Mice and rats exhibit striking inter-species differences in gene response to acute stroke. *Cell Mol Neurobiol*.
- Yocum RR, Rasmussen JR and Strominger JL (1980) The mechanism of action of penicillin. Penicillin acylates the active site of *Bacillus stearothermophilus* D-alanine carboxypeptidase. *J Biol Chem* **255**:3977-3986.
- Youdim MB and Tipton KF (2002) Rat striatal monoamine oxidase-B inhibition by l-deprenyl and rasagiline: its relationship to 2-phenylethylamine-induced stereotypy and Parkinson's disease. *Parkinsonism Relat Disord* **8**:247-253.
- Zanger UM and Schwab M (2013) Cytochrome P450 enzymes in drug metabolism: regulation of gene expression, enzyme activities, and impact of genetic variation. *Pharmacol Ther* **138**:103-141.
- Zernig G, Burke T, Lewis JW and Woods JH (1996) Mechanism of clocinnamox blockade of opioid receptors: evidence from in vitro and ex vivo binding and behavioral assays. *J Pharmacol Exp Ther* **279**:23-31.
- Zernig G, Butelman ER, Lewis JW, Walker EA and Woods JH (1994) In vivo determination of mu opioid receptor turnover in rhesus monkeys after irreversible blockade with clocinnamox. *J Pharmacol Exp Ther* **269**:57-65.
- Zhang D, Hop C, Patilea-Vrana G, Gampa G, Seneviratne HK, Unadkat JD, Kenny JR, Nagapudi K, Di L, Zhou L, Zak M, Wright MR, Bumpus NN, Zang R, Liu X, Lai Y and Khojasteh SC (2019) Drug concentration asymmetry in tissues and plasma for small molecule-related therapeutic modalities. *Drug Metab Dispos* **47**:1122-1135.
- Zhou LW, Weiss B, Freilich JS and Greenberg LH (1984) Impaired recovery of alpha 1- and alpha 2-adrenergic receptors in brain tissue of aged rats. *J Gerontol* **39**:538-546.

Zou LL, Cai ST and Jin GZ (1996) Chronic treatment with (-)-stepholidine alters density and turnover of D1 and D2 receptors in striatum. *Zhongguo Yao Li Xue Bao* **17**:485-489.

Conflict of interest statement: None of the authors has an actual or perceived conflict of interest with the contents of this article.

Funding statement and List of Footnotes:

No external funding was received for this paper.

¹ *Clinical efficacy is the maximum desired target-elicited effect, in the presence of a composite of integrated buffering, amplifying, and compensatory processes. Importantly, clinical efficacy is also limited to what is possible to attain regarding a specific functional response without jeopardizing patient health (safety, tox).*
(on p. 12)

² *The target recovery half-lives presented in Tables 1, 2, and 4 are used as an in vivo proxy that may also encompass processes other than de novo target synthesis and degradation.* (on p. 15)

³ *In an “open” system context “occupancy” is defined as in **Table 3**.* (on p. 21)

⁴ *The in vivo efficacy parameter E_{max} is observed in response-time data, maximum ligand-target complex concentration in vivo RL_{max} may be measurable in certain instances, which allows prediction of the transduction parameter Rho , ρ , from E_{max}/RL_{max} .* (on p. 22)

Tables

Table 1. Target half-life vs. age and in the rat or mouse†

Target	Inactivating treatment	Organ/tissue	Subregion	Age, months	Recovery half-life	Reference
Dopamine D1 receptor	EEDQ	Brain	Striatum	4	3.5 d (84 h)	(Battaglia et al., 1988)
	EEDQ	Brain	Striatum	4	3.1-3.3 d (74-80 h)	(Giorgi et al., 1991)
	EEDQ	Brain	Striatum	23	6.1 d (146 h)	(Giorgi et al., 1992)
	EEDQ	Brain	Striatum	28	5.8 d (138 h)	(Battaglia et al., 1988)
	EEDQ	Brain	N. accumbens	4	2.7 d (64 h)	(Giorgi et al., 1991; Giorgi et al., 1992)
	EEDQ	Brain	N. accumbens	23	4.5 d (108 h)	(Giorgi et al., 1992)
	EEDQ	Brain	Subst. nigra	4	7.6-8.3 d (182-200 h)	(Giorgi et al., 1991)
	EEDQ	Brain	Subst. nigra	23	9.6 d (230 h)	(Giorgi et al., 1992)
	EEDQ	Eye	Retina	4	2.2-2.3 d (53-56 h)	(Giorgi et al., 1991)
	EEDQ	Eye	Retina	23	2.9 d (70 h)	(Giorgi et al., 1992)

Dopamine D2 receptor	EEDQ	Brain	Striatum	1	1.9 d (45 h)	(Leff et al., 1984)
	EEDQ	Brain	Striatum	4	3.3 d (79 h)	(Norman et al., 1987)
	EEDQ	Brain	Striatum	9	5.0 d (120 h)	(Norman et al., 1987)
	EEDQ	Brain	Striatum	9-12	5.0 d (119 h)	(Leff et al., 1984)
	EEDQ	Brain	Striatum	28	5.7 d (136 h)	(Norman et al., 1987)
Alpha1-adrenoceptor	PBZ	Brain	Cortex	3	7 d (168 h)	(Zhou et al., 1984)
	PBZ	Brain	Cortex	24	14 d (336 h)	(Zhou et al., 1984)
	PBZ	Brain	Hypothalamus	3	8 d (192 h)	(Zhou et al., 1984)
	PBZ	Brain	Hypothalamus	24	15 d (360 h)	(Zhou et al., 1984)
Alpha2-adrenoceptor	PBZ	Brain	Cortex	3	5 d (120 h)	(Zhou et al., 1984)
	PBZ	Brain	Cortex	24	20 d (480 h)	(Zhou et al., 1984)
Beta1-adrenoceptor	BAAM	Heart	-	1-2	~3.8 d (~90 h)*	(Baker and Pitha, 1982; Pitha et al., 1982)
	BAAM	Heart	-	28	~13.3 d (~320 h)*	(Baker and Pitha, 1982; Pitha et al., 1982)
Beta2-adrenoceptor	BAAM	Lung	-	1-2	~10 d (~250 h)*	(Baker and Pitha, 1982; Pitha et al., 1982)
	BAAM	Lung	-	28	~16.7 d (~400 h)*	(Baker and Pitha, 1982; Pitha et al., 1982)
5-HT1A receptor	EEDQ	Brain	Hippocampus	3	6.3 d (151 h)	(Keck and Lakoski, 2000)
	EEDQ	Brain	Hippocampus	~6-12	1.8 d (43 h)	(Keck and Lakoski, 1996a)
	EEDQ	Brain	Hippocampus	22	2.2 d (53 h)	(Keck and Lakoski, 2000)

	EEDQ	Brain	Cortex	~6-12	7.7 d (185 h)	(Keck and Lakoski, 1996a)
5-HT2 receptor	EEDQ	Brain	Cortex	4	1.9 d (45 h)	(Battaglia et al., 1987)
	EEDQ	Brain	Cortex	28	4.1 d (98 h)	(Battaglia et al., 1987)
GABAA receptor/Bz site†	EEDQ	Brain	Cortex	2	1.1 d (25 h)	(Miller et al., 1991a)
	EEDQ	Brain	Cortex	20	3.1 d (75 h)	(Miller et al., 1991a)

*Estimated from data in (Baker and Pitha, 1982; Pitha et al., 1982).

Table 2. Target half-life vs. species and organ/tissue

Target	Inactivating agent	Comment	Parameter	Species	Organ/ tissue	Subregion	Recovery Half-life	Reference
Dopamine D1 receptor	EEDQ	Young (1.5 mths)		Rat	Brain	Striatum	1.4 d (34 h)	(Fuxe et al., 1987)
	EEDQ	Young (1.5 mths)		Rat	Brain	Clastrum	1.8 d (43 h)	(Fuxe et al., 1987)
	EEDQ	Young (1.5 mths)		Rat	Brain	Olfactory tubercle	1.0 d (25 h)	(Fuxe et al., 1987)
	EEDQ	Young (1.5 mths)		Rat	Brain	N. accumbens	0.9 d (22 h)	(Fuxe et al., 1987)
Alpha1-adrenoceptor PBZ				Rat	Brain	Cortex	5 d (120 h)	(McKernan and Campbell, 1982)
	PBZ			Rat	Brain	Brain stem	6 d (144 h)	(McKernan and Campbell, 1982)
	PBZ			Rabbit	Brain	Forebrain	10.8 d (259 h)	(Hamilton and Reid, 1985)

	PBZ	Rabbit	Brain	Hindbrain	13.3 d (319 h)	(Hamilton and Reid, 1985)
	PBZ	Rabbit	Spleen	-	3.6 d (86 h)	(Hamilton et al., 1984)
	PBZ	Rat	Submaxillary gland	-	1.4 d (33 h)	(Sladeczek and Bockaert, 1983)
	PBZ	Rat	Liver	-	1.8 d (42 h)	(Lynch et al., 1983)
Alpha2-adrenoceptor	Benextramine	Golden hamster	Kidney	-	1.3 d (31 h)	(Taouis et al., 1987)
	Benextramine	Golden hamster	Adipose tissue	-	1.9 d (46 h)	(Taouis et al., 1987)
	PBZ	Rabbit	Brain	Forebrain	6.1 d (146 h)	(Hamilton and Reid, 1985)
	PBZ	Rabbit	Brain	Hindbrain	4.6 d (110 h)	(Hamilton and Reid, 1985)
	PBZ	Rabbit	Spleen	-	1.6 d	(Hamilton and Reid, 1985)

						(38 h)	
EEDQ			Rat	Brain	Cortex	4.1 d (98 h)	(Adler et al., 1985)
EEDQ	<i>Ex vivo</i> slices	Agonist inhibition of NA release	Rat	Brain	Cortex	2.4 d (58 h)	(Adler et al., 1985)
EEDQ	<i>Ex vivo</i> slices	Agonist inhibition of 5-HT release	Rat	Brain	Cortex	4.6 d (110 h)	(Adler et al., 1985)
EEDQ	Antagonist- labelled		Rat	Brain	Cortex	4.9 d (118 h)	(Ribas et al., 1998)
EEDQ	Agonist- labelled		Rat	Brain	Cortex	7.4 d (178 h)	(Ribas et al., 1998)
EEDQ			Rat	Brain	Cortex	3.9 d (94 h)	(Barturen and Garcia-Sevilla, 1992)
EEDQ			Rat	Brain	Locus coeruleus	1.5 d (37 h)	(Pineda et al., 1997)
EEDQ		NA neuronal cell firing <i>in vivo</i>	Rat	Brain	Locus coeruleus	0.6 d (14 h)	(Pineda et al., 1997)

5-HT1A receptor	EEDQ		Rat	Brain	Brain stem	2.6 d (62 h)	(Barturen and Garcia-Sevilla, 1992)
	EEDQ		Rat	Brain	Hippocampus	4.3 d (103 h)	(Barturen and Garcia-Sevilla, 1992)
	EEDQ		Rat	Brain	Hypothalamus	2.1 d (50 h)	(Barturen and Garcia-Sevilla, 1992)
	EEDQ		Rat	Brain	Striatum	2.1 d (50 h)	(Barturen and Garcia-Sevilla, 1992)
	EEDQ	<i>Ex vivo</i> slices	Rat	Brain	Cortex	18.5 d (445 h)	(Agneter et al., 1993)
	EEDQ	<i>Ex vivo</i> slices	Rat	Brain	Cortex	0.8-2.7 d (20-64 h)	(Agneter et al., 1993)
	EEDQ	Young (~2 mths)	Mouse	Brain	-	5.3 d (126 h)	(Durcan et al., 1994)
Beta2-adrenoceptor	BAAM		Guinea-pig	Lung	-	3.8-5 d (90-120 h)*	(Nelson et al., 1986)
5-HT1A receptor	EEDQ	Mature-Aged	Rat	Brain	Cortex	7.7 d	(Keck and Lakoski, 1996a)

(~6-12 mths)				(185 h)		
EEDQ		Rat	Brain	Cortex	5.2 d (124 h)	(Pinto and Battaglia, 1994)
EEDQ		Rat	Brain	Cortex	2.8 d (67 h)	(Vinod et al., 2001)
EEDQ		Rat	Brain	Cortex layers	3.9-4.3 d (94-103 h)	(Raghupathi et al., 1996a)
EEDQ	Mature-Aged (~6-12 mths)	Rat	Brain	Hippocampus	1.8 d (43 h)	(Keck and Lakoski, 1996b)
EEDQ		Rat	Brain	Hippocampus	4.7 d (113 h)	(Gozlan et al., 1994)
EEDQ		Rat	Brain	Hippocampus	5.3 d (127 h)	(Vinod et al., 2001)
EEDQ		Rat	Brain	Hippocampus	2.7 d (65 h)	(Bolanos et al., 1991)
EEDQ		Rat	Brain	Lateral septum	4.0 d (96 h)	(Gozlan et al., 1994)

	EEDQ	Rat	Brain	Dentate gyrus	4.2 d (101 h)	(Gozlan et al., 1994)
	EEDQ	Rat	Brain	Parietal cortex	3.9 d (94 h)	(Gozlan et al., 1994)
	EEDQ	Rat	Brain	Hippocampal subareas	2.3-3.6 d (55-86 h)	(Raghupathi et al., 1996a)
	EEDQ	Rat	Brain	Dorsal raphe	3.2 d (77 h)	(Gozlan et al., 1994)
	EEDQ	Rat	Brain	Dorsal raphe	2.7 d (69 h)	(Bolanos et al., 1991)
	EEDQ	Rat	Brain	Dorsal raphe	2.8 d (67 h)	(Raghupathi et al., 1996a)
5-HT1B receptor	EEDQ	Rat	Brain	Cortex	8.9 d (213 h)	(Pinto and Battaglia, 1994)
5-HT2 receptor	EEDQ	Rat	Brain	Cortex	~4.5 d (~108 h)	(Battaglia et al., 1986)
5-HT2A receptor	EEDQ	Rat	Brain	Cortex	2.9 d	(Gozlan et al., 1994)

	EEDQ		Rat	Brain	Cortex	2.5 d (58.9 h)	(Pinto and Battaglia, 1994)
	EEDQ		Rat	Brain	Cortex	2.6-3.3 d (62-79 h)	(Raghupathi et al., 1996b)
	EEDQ		Rat	Brain	Caudate-Putamen	9.0 d (216 h)	(Raghupathi et al., 1996b)
MOP	Clocinnamox		Mouse	Brain	-	2.7-4.2 d (65-101 h)	(Burke et al., 1994; Zernig et al., 1996)
	Clocinnamox	Thermal heat pain <i>in vivo</i>	Rhesus monkey	N/A	N/A	6.3-6.6 d (151-158 h)	(Zernig et al., 1994)
DAT	RTI-76		Rat	Brain	Striatum	2.1-2.9 d (50-70 h)	(Kimmel et al., 2000)
	RTI-76		Rat	Brain	Nucleus accumbens	1.9-2.0 d (46-48 h)	(Kimmel et al., 2000)
	RTI-76	Intrastriatal RTI-76	Rat	Brain	Striatum	6.3 d (151 h)	(Fleckenstein et al., 1996)

	DEEP-NCS	Intrastriatal DEEP-NCS	V_{max} & K_m change	Rat	Brain	Striatum	6.1 d (146 h)	(Rego et al., 1999)
	DEEP-NCS	Intrastriatal DEEP-NCS	<i>Ex vivo</i> DA reuptake	Rat	Brain	Striatum	5.3 d (127 h)	(Rego et al., 1999)
	DEEP-NCS	Intrastriatal DEEP-NCS	Receptor number	Rat	Brain	Striatum	5.8 d (138 h)	(Rego et al., 1999)
SERT	RTI-76			Rat	Brain	Hippocampus	3.4 d (82 h)	(Vicentic et al., 1999)
	RTI-76			Rat	Brain	Striatum	3.8 d (91 h)	(Vicentic et al., 1999)
MAO A	Clorgyline			Rat	Liver	-	2.6-3.1 d (62-74 h)	(Corte and Tipton, 1980)
	Clorgyline			Rat	Liver	-	3.5 d (84 h)	(Egashira and Kamijo, 1979)
MAO B	Deprenyl			Rat	Brain	-	7.9 d (190 h)	(Felner and Waldmeier, 1979)
	Deprenyl			Pig	Brain	-	6.5 d	(Oreland et al., 1990)

				(156 h)	
Deprenyl	Baboon	Brain	-	~30 d (~720 h)	(Arnett et al., 1987)
Deprenyl	Human	Brain	Several regions, healthy & PD	~40 d (~960 h)	(Fowler et al., 1994)
Deprenyl	Rat	Brain	Caudate	9.2 d (221 h)	(Youdim and Tipton, 2002)
Rasagiline	Rat	Brain	Caudate	9.6 d (230 h)	(Youdim and Tipton, 2002)
Pargyline	Rat	Brain	Caudate	13 d (312 h)	(Goridis and Neff, 1971)
Pargyline	Rat	Brain	Hypothalamus	10 d (240 h)	(Goridis and Neff, 1971)
Pargyline	Rat	Brain	Cerebellum	9.1 d (218 h)	(Goridis and Neff, 1971)
Pargyline	Rat	Brain	-	9.1 d (218 h)	(Planz et al., 1972a)

Benmoxine	Rat	Brain	-	10.3 d (247 h)	(Planz et al., 1972a)
3A2O	Rat	Brain	-	10.9 d (262 h)	(Planz et al., 1972a)
3A2O	Rat	Brain homogenate	-	10.9 d (262 h)	(Planz et al., 1972b)
3A2O	Rat	Brain mitochondria	-	10.9 d (262 h)	(Planz et al., 1972b)
Pargyline	Rat	Brain	-	9.1 d (218 h)	(Planz et al., 1972b)
	Rat	Brain	-	9.6 d (230 h)	(Planz et al., 1972b)
Nialamide	Rat	Heart	-	10.4 d (250 h)	(Planz et al., 1972b)
Nialamide	Rat	Heart	-	12.9 d (310 h)	(Planz et al., 1972b)
3A2O	Rat	Liver	-	4.1 d	(Planz et al., 1972b)

			homogenate	(98 h)	
3A20		Rat	Liver	4.0 d	(Planz et al., 1972b)
			mitochondria	(96 h)	
Benmoxine		Rat	Liver	3.9 d	(Planz et al., 1972b)
				(94 h)	
Pargyline		Rat	Liver	4.3 d	(Planz et al., 1972b)
				(103 h)	
	Leucine incorporation	Rat	Liver	3.7 d	(Planz et al., 1972b)
			mitochondria	(89 h)	
Deprenyl		Rat	Liver	2.6 d	(Egashira and Kamijo, 1979)
				(62 h)	
Pargyline		Rat	Liver	3.5 d	(Erwin and Deitrich, 1971)
				(84 h)	
Pargyline		Rat	Liver	4.0 d	(Planz et al., 1972a)
				(96 h)	
Benmoxine		Rat	Liver	3.9 d	(Planz et al., 1972a)
				(94 h)	

3A2O	Rat	Liver	-	4.1 d (98 h)	(Planz et al., 1972a)
MDL72974A	Human	Platelets	-	~7 d (~168 h)	(Hinze et al., 1990)
Pargyline	Rat	Submaxillary gland	-	3.8 d (91 h)	(Goridis and Neff, 1971)
Nialamide	Rat	Submandibular gland	-	6.0 d (144 h)	(Planz et al., 1972b)
Benmoxine	Rat	Submandibular gland	-	4.1 d (98 h)	(Planz et al., 1972b)
	Rat	Submandibular gland	-	4.2 d (101 h)	(Planz et al., 1972b)
Pargyline	Rat	Superior cervical ganglion	-	4.6 d (110 h)	(Goridis and Neff, 1971)
3A2O	Rat	Small intestine	Mucus layer	4.0 d (96 h)	(Planz et al., 1972a)
3A2O	Rat	Small intestine	Muscularis	0.5 d	(Planz et al., 1972a)

					layer	(12 h)	
	Deprenyl		Rat	Liver	-	2.3 d (55 h)	(Youdim and Tipton, 2002)
	Rasagiline		Rat	Liver	-	2.2 d (53 h)	(Youdim and Tipton, 2002)
	-	Turnover in dermal fibroblasts	Mouse	N/A	-	3.3 d (79 h)	(Swovick et al., 2018)
AChE	-	Leucine incorporation	Rat	Brain	Cortex	2.8 d (67 h)	(Wenthhold et al., 1974)
	Soman	Young (~1.5 mths)	Rat	Brain	BLA	5.9 d (141 h)*	(Prager et al., 2014)
	Soman	Young (~1.5 mths)	Rat	Brain	Prelimbic cortex	7.7 d (185 h)*	(Prager et al., 2014)
	Soman	Young (~1.5 mths)	Rat	Brain	Piriform cortex	8.0 d (193 h)*	(Prager et al., 2014)
	Soman	Young (~1.5 mths)	Rat	Brain	Hippocampus	6.6 d (159 h)*	(Prager et al., 2014)

* Graphically estimated

MOP = μ opioid receptor; DAT = dopamine reuptake transporter; SERT = serotonin reuptake transporter; TryH = tryptophan hydroxylase; PD = Parkinson's Disease; MAO = monoamine oxidase; AChE = acetylcholine esterase; 3A2O = 3-amino-2-oxazolidinone; BLA = basolateral amygdala

Table 3. Generic expressions of ‘Open’- and ‘closed’ pharmacological systems and their properties

Properties	‘Open’ system	‘Closed’ system
Receptor R_{ss}	$R_{ss} = R_0 \cdot \left(1 - \frac{L_{ss}}{L_{ss} + EC_{50}}\right)$ $R_{ss} = \frac{k_{syn}}{k_{deg}} \cdot \left(1 - \frac{L_{ss}}{L_{ss} + EC_{50}}\right)$ $R_{ss} = \frac{k_{syn}}{k_{deg}} \cdot 0.5 \text{ where } L = EC_{50}$	$R_{ss} = R_0 \cdot \left(1 - \frac{L_{ss}}{L_{ss} + K_d}\right)$
Complex RL_{ss}	$RL_{ss} = R_0 \cdot \frac{k_{deg}}{k_{e(RL)}} \cdot \frac{L_{ss}}{L_{ss} + EC_{50}}$ $RL_{ss} = \frac{k_{syn}}{k_{e(RL)}} \cdot \frac{L_{ss}}{L_{ss} + EC_{50}}$ $RL_{ss} = \frac{k_{syn}}{k_{e(RL)}} \cdot 0.5 \text{ where } L = EC_{50}$	$RL_{ss} = R_0 \cdot \frac{L_{ss}}{L_{ss} + K_d}$
K_d	$K_d = \frac{k_{off}}{k_{on}}$	$K_d = \frac{k_{off}}{k_{on}}$
K_m	$K_m = \frac{k_{off} + k_{e(RL)}}{k_{on}}$	-
Occupancy	$\frac{L_{ss}}{L_{ss} + \frac{k_{deg}}{k_{e(RL)}} \cdot \frac{k_{off} + k_{e(RL)}}{k_{on}}}$	$\frac{L_{ss}}{L_{ss} + K_d}$
Reversible system EC_{50}	$EC_{50} = \frac{k_{deg}}{k_{e(RL)}} \cdot \frac{k_{off} + k_{e(RL)}}{k_{on}}$	-
Irreversible system EC_{50}	$EC_{50} \propto \frac{k_{deg}}{k_{on}}$ $EC_{50} \propto \frac{k_{deg}}{k_{irr}}$	-
Efficacy parameter E_{max}	$E_{max} = \rho \cdot [RL_{max}] = \rho \cdot \frac{k_{syn}}{k_{e(RL)}}$	$E_{max} = B_{max}$
Efficacy parameter I_{max}	$I_{max} = -\rho \cdot [RL_{max}] = -\rho \cdot \frac{k_{syn}}{k_{e(RL)}}$	
Baseline E_0	$E_0 \propto \frac{k_{syn}}{k_{deg}} \text{ or constitutive activity}$	

R_{max} and RL_{max} are the maximum observed response *in vivo*, and maximum level of the ligand-target complex, respectively. E_0 is defined as above of an empirical function of time to capture baseline variability e.g., oscillations.

Table 4. Treatment vs. target half-life in the rat or mouse† brain.

Target	Treatment	Inactivating agent	Species	Subregion	Recovery	Reference
					Half-life	
Dopamine D1 receptor	Control (ECS)	EEDQ	Rat	Striatum	3.3 d (80 h)	(Nowak and Zak, 1989)
	Repeat ECS	EEDQ	Rat	Striatum	2.3 d (55 h)	(Nowak and Zak, 1989)
	Vehicle	EEDQ	Rat	Striatum	2.2 d (53 h)	(Dewar et al., 1997)
	6-OHDA	EEDQ	Rat	Striatum	4.3 d (103 h)	(Dewar et al., 1997)
	Chronic vehicle	EEDQ	Rat	Striatum	6.0 d (144 h)	(Zou et al., 1996)
	Chronic (-)stepholidine	EEDQ	Rat	Striatum	4.9 d (118 h)	(Zou et al., 1996)
	Chronic vehicle (OVX)	EEDQ	Rat	Striatum	2.3 d (55 h)	(Levesque and Di Paolo, 1991)
	Chronic estradiol (OVX)	EEDQ	Rat	Striatum	4.4 d (107 h)	(Levesque and Di Paolo, 1991)
	Chronic vehicle (OVX)	EEDQ	Rat	nigra	1.7 d (42 h)	(Morissette et al., 1992)
	Chronic estradiol	EEDQ	Rat	Substantia	1.4 d (34 h)	(Morissette et al., 1992)

	(OVX)			nigra		
	Chronic vehicle					
	(OVX)	EEDQ	Rat	Striatum (posterior)	1.7 d (41 h)	(Morissette et al., 1992)
	Chronic estradiol			Striatum		
	(OVX)	EEDQ	Rat	(posterior)	3.8 d (91 h)	(Morissette et al., 1992)
Dopamine D2 receptor	Chronic vehicle	EEDQ	Rat	Striatum	3.9 d (94 h)	(Pich et al., 1987)
	Chronic haloperidol	EEDQ	Rat	Striatum	5.7 d (137 h)	(Pich et al., 1987)
	Chronic vehicle	EEDQ	Rat	Striatum	5.9 d (141 h)	(Zou et al., 1996)
	Chronic (-)-stepholidine	EEDQ	Rat	Striatum	3.5 d (85 h)	(Zou et al., 1996)
	Control (ECS)	EEDQ	Rat	Striatum	1.2 d (29 h)	(Nowak and Zak, 1991a)
	Repeat ECS	EEDQ	Rat	Striatum	2.4 d (58 h)	(Nowak and Zak, 1991a)
	Chronic vehicle	EEDQ	Rat	Striatum	3.0 d (73 h) [†]	(Leff et al., 1984)
	Chronic reserpine	EEDQ	Rat	Striatum	5.4 d (130 h) [†]	(Leff et al., 1984)
	Vehicle	EEDQ	Rat	Striatum	4.8 d (116 h)	(Neve et al., 1985)
	6-OHDA	EEDQ	Rat	Striatum	5.3 d (128 h)	(Neve et al., 1985)
	Vehicle	EEDQ	Rat	Striatum	3.8 d (90 h)	(Dewar et al., 1997)
	6-OHDA	EEDQ	Rat	Striatum	4 d (96 h)	(Dewar et al., 1997)

	Chronic vehicle			Striatum		
	(OVX)	EEDQ	Rat	(posterior)	2.4 d (58 h)	(Morissette et al., 1992)
	Chronic estradiol			Striatum		
	(OVX)	EEDQ	Rat	(posterior)	4 d (95 h)	(Morissette et al., 1992)
	Chronic vehicle					
	(OVX)	EEDQ	Rat	Pituitary	0.75 d (18 h)	(Levesque and Di Paolo, 1991)
	Chronic estradiol					
	(OVX)	EEDQ	Rat	Pituitary	2.1 d (51 h)	(Levesque and Di Paolo, 1991)
Alpha1-adrenoceptor	Control (ECS)	EEDQ	Rat	Cortex	1.6 d (39 h)	(Nowak and Zak, 1991b)
	Repeat ECS	EEDQ	Rat	Cortex	1.5 d (36 h)	(Nowak and Zak, 1991b)
Alpha2-adrenoceptor	Chronic vehicle	EEDQ	Rat	Cortex	3.9 d (94 h)	(Barturen and Garcia-Sevilla, 1992)
	Chronic desipramine	EEDQ	Rat	Cortex	1.5-1.7 d (36-41 h)	(Barturen and Garcia-Sevilla, 1992)
	Chronic vehicle	EEDQ	Rat*	Cortex	4.9 d (118 h)	(Ribas et al., 1993)
	Chronic clorgyline	EEDQ	Rat*	Cortex	3.6 d (86 h)	(Ribas et al., 1993)
	Chronic vehicle	EEDQ	Rat#	Cortex	8.1 d (194 h)	(Ribas et al., 1993)
	Chronic clorgyline	EEDQ	Rat#	Cortex	2.1 d (51 h)	(Ribas et al., 1993)

	Chronic vehicle	EEDQ	Rat	Cortex	6.4 d (154 h)	(Ribas et al., 2001)
	Chronic reserpine	EEDQ	Rat	Cortex	6.1 d (146 h)	(Ribas et al., 2001)
	Chronic vehicle	EEDQ	Rat	Cortex	8.2 d (197 h)	(Carbonell et al., 2004)
	Chronic lithium	EEDQ	Rat	Cortex	4.1 d (98 h)	(Carbonell et al., 2004)
	Chronic vehicle	EEDQ	Rat	Cortex	4.4 d (106 h)	(Gabilondo and Garcia-Sevilla, 1995)
	Chronic morphine	EEDQ	Rat	Cortex	5.0 d (120 h)	(Gabilondo and Garcia-Sevilla, 1995)
	Morphine withdrawal	EEDQ	Rat	Cortex	2.7 d (65 h)	(Gabilondo and Garcia-Sevilla, 1995)
GABAA receptor	Chronic vehicle	EEDQ	Mouse	Cortex	1.3 d (31 h)	(Miller et al., 1991b)
/Bz site†	Chronic lorazepam	EEDQ	Mouse	Cortex	0.8 d (19 h)	(Miller et al., 1991b)
	Chronic vehicle	EEDQ	Mouse	Cerebellum	1.8 d (42 h)	(Miller et al., 1991b)
	Chronic lorazepam	EEDQ	Mouse	Cerebellum	1.5 d (35 h)	(Miller et al., 1991b)
Dopamine transporter	Chronic vehicle	RTI-76	Rat	Striatum	2.1 d (50 h)	(Kimmel et al., 2003)
(DAT)	Chronic cocaine	RTI-76	Rat	Striatum	0.94 d (23 h)	(Kimmel et al., 2003)
	Chronic vehicle	RTI-76	Rat	Nucleus accumbens	2.2 d (53 h)	(Kimmel et al., 2003)
	Chronic cocaine	RTI-76	Rat	Nucleus accumbens	2.2 d (53 h)	(Kimmel et al., 2003)

† Extrapolated from data in (Leff et al., 1984)

* SHR rats, # Wistar-Kyoto rats

Table 5. Impact of up- and down-regulation on relevant pharmacological parameters for agonists

Target change	Cause	Baseline R_0	Complex RL_{ss}	Potency EC_{50} (numerical value=nv)	Efficacy parameter E_{max}	Comment
Upregulation (increased concentration of target R or complex RL)	$k_{syn} \uparrow$	\uparrow	\uparrow	\leftrightarrow	\uparrow	Baseline and complex and efficacy increase since target synthesis rate impacts all (Eqn. 3). Potency remains unchanged (Eqn. 2).
	$k_{deg} \downarrow$	\uparrow	\leftrightarrow	\uparrow (nv= \downarrow)	\leftrightarrow	Baseline and potency increase (lower numerical value, Eqn. 2) whereas complex and efficacy remain unchanged.
	$k_{e(RL)} \downarrow$	\leftrightarrow	\uparrow	\downarrow (nv= \uparrow)	\uparrow	Baseline unchanged, complex and efficacy increase, but potency drops (increased numerical value (Eqns. 2 and 3)
Downregulation (decreased concentration of target R or complex RL)	$k_{syn} \downarrow$	\downarrow	\downarrow	\leftrightarrow	\downarrow	Baseline, complex, and efficacy decrease since target synthesis rate impacts all (Eqn. 3). Potency remains unchanged (Eqn. 2).
	$k_{deg} \uparrow$	\downarrow	\leftrightarrow	\downarrow (nv= \uparrow)	\leftrightarrow	Baseline and potency decrease (higher numerical value, Eqn. 2) whereas complex and efficacy remain unchanged.
	$k_{e(RL)} \uparrow$	\leftrightarrow	\downarrow	\uparrow (nv= \downarrow)	\downarrow	Baseline unchanged, complex and efficacy decrease, but increased potency (decreased numerical value (Eqns. 2 and 3)

Table 6. Response duration dependence on drug and target half-lives in irreversible and reversible conditions

Half-life	Irreversible H ⁺ /K ⁺ -ATPase inhibitor (omeprazole)	Irreversible COX-1 inhibitor (ASA; platelet aggregation)	Reversible COX- 1 inhibitor (ibuprofen; platelet aggregation)	Reversible COX- 1 inhibitor (naproxen; platelet aggregation)	Irreversible MAO-B inhibitor (rasagiline)	Reversible ACh esterase inhibitor (donepezil)	Reversible GSECR inhibitor (experimental cmpd)
Drug half-life	45 min	10-15 min	2 hr	12-17 hr	1.5-3.5 hr	60-70 hr	2 hr
Target half-life	15-20 hr ^①	33 hr ^②	33 hr ^②	33 hr ^②	30-45 days ^③	10-11 days ^④	20 min ^⑤
Rate-limiting step	Target, k_{deg}	Target(/tissue), k_{deg}	Complex dissociation	$k_{deg} \gg k_{off}$	Target, k_{deg}	Exposure	Exposure
Response duration	$T_{1/2, target}$	$T_{1/2, target}$	$T_{1/2, k_{off}}$	$T_{1/2, plasma}$	$T_{1/2, target}$	Presence of unbound exposure C_u	Presence of unbound exposure C_u

① Estimated target half-life (Wallmark et al., 1985)

② Estimated target half-life (Hong et al., 2008).

③ Estimated target half-life (Fowler et al., 1994).

④ Estimated target half-life (Moss et al., 2017).

⑤ Estimated target half-life (Gabrielsson and Weiner, 2016).

Table 7. Comparisons of *in vitro* K_d with *in vivo* potency EC_{50} properties (Betts et al., 2010).

Parameter	Rat	Monkey	Man
k_{off} (d ⁻¹)	1.72	16.2	0.1728
k_{on} (nM ⁻¹ d ⁻¹)	49.4	316	112
K_d (nM)	0.0348	0.0513	0.00154
EC_{50} (nM)	2.22	3.39	0.29
EC_{50} to K_d ratio	64	66	188

The EC_{50} values are calculated by means of Eqn. 2 based on the original model parameters given in (Betts et al., 2010).

Table 8. Generic expressions of the ‘open’ and ‘closed’ system properties of enzymes

Metabolic system	‘Open’ system	‘Closed’ system
$V_{max}(t)$	$E(t) \cdot k_{cat} \cdot V$	$E_0 \cdot k_{cat} \cdot V$
$V_{max}(0)$	$E(0) \cdot k_{cat} \cdot V$	$E_0 \cdot k_{cat} \cdot V$
K_m	$\frac{k_{cat} + k_{off}}{k_{on}}$	$\frac{k_{cat} + k_{off}}{k_{on}}$
Substrate S_{ss}	$S_{ss} = \frac{Input}{V \cdot \frac{V_{max}(0)}{K_m}}$	$S_{ss} = \frac{Input}{V \cdot \frac{V_{max}}{K_m + S_{ss}}}$
Free enzyme E_{ss}	$E_{ss} = E_0 = \frac{k_{syn}}{k_{deg}}$	$E_{ss} = K_m \cdot \frac{ES_{ss}}{S_{ss}}$
Complex ES_{ss}	$ES_{ss} = \frac{Input}{V \cdot k_{cat}} = \frac{S_{ss}}{\frac{E_0}{K_m}}$	$ES_{ss} = \frac{E_0 \cdot S_{ss}}{K_m + S_{ss}}$
Clearance at disequilibrium $Cl(t)$	$E(t) \cdot k_{cat} \cdot V \frac{1}{\frac{k_{cat} + k_{off}}{k_{on}}} = \frac{V \cdot V_{max}(t)}{K_m}$	$E_0 \cdot k_{cat} \cdot V \frac{1}{\frac{k_{cat} + k_{off}}{k_{on}} + S(t)} = \frac{V \cdot V_{max}}{K_m + S(t)}$
Clearance at equilibrium Cl_{ss}	$E(0) \cdot k_{cat} \cdot V \frac{1}{\frac{k_{cat} + k_{off}}{k_{on}}} = \frac{V \cdot V_{max}(0)}{K_m}$	$E_0 \cdot k_{cat} \cdot V \frac{1}{\frac{k_{cat} + k_{off}}{k_{on}} + S} = \frac{V \cdot V_{max}}{K_m + S_{ss}}$
Elimination rate at disequilibrium $v(t)$	$\frac{V \cdot V_{max}(t)}{K_m} \cdot S(t)$	$\frac{V_{max} \cdot V}{K_m + S(t)} \cdot S(t)$
Elimination rate at equilibrium v_{ss}	$\frac{V \cdot V_{max}(0)}{K_m} \cdot S_{ss}$	$\frac{V_{max} \cdot V}{K_m + S} \cdot S$

E_0 of the ‘closed’ system is fixed over time unless changes occur due to changes in synthesis (induction/inhibition) or catabolism. The ‘closed’ system demonstrates saturation of free enzyme, complex, clearance and rate of elimination at equilibrium in contrast to the ‘open’ system which behaves nonlinearly until equilibrium is reached.

Table 9. Induction, inhibition or catalytic change in enzyme activity.

Observation	Cause	V_{max}	K_m	$Cl(S)$	Commentary
Induction	$k_{syn} \uparrow$	\uparrow	\leftrightarrow	\uparrow	If k_{syn} increases free enzyme E concentration increases. K_m is unaffected. Substrate clearance increases (von Bahr et al., 1998)
	$k_{deg} \downarrow$	\uparrow	\leftrightarrow	\uparrow	If k_{deg} decreases free enzyme E concentration increases. K_m is unaffected. Substrate clearance increases (Ethanol induction of CYP2E1 in (Hu et al., 1995)
Inhibition	$k_{syn} \downarrow$	\downarrow	\leftrightarrow	\downarrow	If k_{syn} decreases free enzyme E concentration decreases. K_m is unaffected (Ramsay and Tipton, 2017)
	$k_{deg} \uparrow$	\downarrow	\leftrightarrow	\downarrow	If k_{deg} increases free enzyme E concentration decreases. K_m is unaffected (Ramsay and Tipton, 2017)
Catalytic change	$k_{cat} \uparrow$	\uparrow	\uparrow	$\leftrightarrow (\uparrow)$	If k_{cat} increases V_{max} increases. K_m increases if $k_{cat} \approx k_{off}$. Substrate clearance is unaffected if V_{max} and K_m changes the same.
	$k_{cat} \downarrow$	\downarrow	\downarrow	$\leftrightarrow (\downarrow)$	If k_{cat} decreases V_{max} decreases. K_m decreases if $k_{cat} > k_{off}$. Substrate clearance is unaffected if V_{max} and K_m changes the same.

Induction is related to the metabolic activity (increase in free enzyme E or catalytic activity k_{cat}) which means an increase in synthesis k_{syn} or decrease in loss k_{deg} , or increase in k_{cat} . *Inhibition* involves the opposite.

Figure Legends

Figure 1. Schematic outline of various topics related to turnover concepts in this review. The strategy is to cover turnover from both a pharmacological- and a metabolic (clearance) point of view. The review covers also how turnover is controlled and what potential covariates (age, sex, species, disease) related to the topic. The review covers how turnover may differ across different tissues and proposes means for inter-species scaling. Finally, a set of points to consider related to experimental design, interpretation of data and translational issues are listed.

Figure 2. Row 1: ‘Closed’ pharmacodynamic (left) and metabolic (right) systems. The ‘closed’ system presented in most pharmacology text books assumes a constant pool of total target (left plot, free target R (blue box representing e.g., concentration of free binding sites) and ligand-target complex bound RL) or a constant pool of total enzyme (right plot, free enzyme E and substrate-enzyme complex bound ES). Free enzyme is regenerated after the catalytic formation of product P from ES . R , k_{on} , k_{off} and RL represent free target, second-order complex formation rate constant, first-order complex disintegration rate constant and complex concentration, respectively. The k_{cat} parameter denote the first-order rate constant of the catalytic process. **Row 2:** The ‘open’ system has an ongoing zero-order production k_{syn} and first-order loss k_{deg} of target protein (blue box representing e.g., concentration of free binding sites at receptor in left and free enzyme concentration in right). In , L and $Cl(s)$ denote the input-rate of ligand, ligand concentration and ligand clearance, respectively. The k_{syn} , k_{deg} and $k_{e(RL)}$ parameters are target synthesis- and target degradation-rate and ligand-target complex elimination constants. **Row 3:** The ‘open’ systems used for capturing irreversible mechanisms. **Row 4:** The ‘open’ system for Ligand Facilitated Target Removal, LFTR, where target is degraded and ligand is returned to its free pool. **Right hand column:** (Metabolic systems) Schematic comparisons of the ‘closed’ (Row 1) and ‘open’ (Rows 2-4) enzymatic systems. In and S denote the input-rate of substrate and substrate concentration, respectively. k_{syn} , E and k_{deg} are enzyme protein synthesis rate, free enzyme concentration and enzyme degradation rate constant. k_{on} , k_{off} , ES and k_{cat} represent second-order substrate-enzyme complex formation rate constant, first-order complex disintegration rate constant, substrate-enzyme complex and the catabolic rate constant, respectively.

Figure 3. Impact of changes in the parameters of in vivo potency in Equation 2. **Graph A:** In vivo potency versus target degradation rate- k_{deg} and complex dissociation rate- k_{off} constants. The complex elimination rate constant $k_{e(RL)}$ is set to 0.1 time^{-1} . In vivo EC_{50} moves towards infinity when $k_{e(RL)}$ approaches zero. The system approaches an irreversible behavior when $k_{e(RL)}$ is (much) greater than k_{off} . **Graph B:** In vivo potency versus target degradation rate- k_{deg} and complex elimination rate- $k_{e(RL)}$ constants. The complex dissociation rate constant k_{off} is set to 0.1 time^{-1} . In vivo EC_{50} moves towards infinity when $k_{e(RL)}$ approaches zero. The system approaches an irreversible behavior when $k_{e(RL)}$ is (much) greater than k_{off} . EC_{50} is plotted on a linear scale in graphs **A** and **B** and on a

logarithmic scale in **C** and **D**. The multiplicative effect of changes in k_{deg} and $k_{e(RL)}$ are shown in **B** and **D** and therefore requires a larger range of scale.

Figure 4. Age vs. dopamine D1 (filled triangles) and D2 (filled circles) receptor turnover in rat striatum expressed in log-lin plot of data from Table 1; joint (D1/D2) line correlation and corresponding coefficient (R^2 ; inset) also shown.

Figure 5. Brain MAO B turnover for 5 mammalian species (see, **Table 1**) vs. lifespan (left) and adult body mass (right), expressed in log-log diagrams (line correlations and corresponding coefficients (R^2) shown as insets). MAO B data taken from refs. in **Table 2**; max lifespan potential data taken from Boxenbaum (Boxenbaum, 1982) and AnAge (The Animal Aging & Longevity database: <https://genomics.senescence.info/species/>).

Figure 6. In vitro lipolysis (pEC_{50}) versus in vivo potency (pEC_{50}) data redrawn from Almqvist et al (2018). Grey dashed line (lower diagonal) represents line of unity and red (upper diagonal) line regression of all data. For all prediction models, both in vitro and in vivo potency are expressed on a logarithmic scale normalized to 1 molar (1M), according to $pEC_{50} = -\log_{10}(EC_{50}/1M)$. Note the pEC_{50} scale, meaning that compounds become more potent towards the upper right corner. The endogenous ligand nicotinic acid NiAc is specifically identified in the graph.

Figure 7. A. Efficacy parameter E_{max} versus different maximum complex concentrations RL_{max} (Eqn. 4).

Upper row left: Agonism: the steepness of the slope (Rho denoted ρ in text) is a correlate of the efficacy of the agonist ligand-target complex to generate a cellular response, i.e., ① > ② > ③. Assuming that ① represents a full agonist, ② and ③ depict partial agonists with gradually lower efficacy. **Upper row middle:** Antagonism: the ligand-target complex has no intrinsic power to generate a cell response. Once bound to the target the antagonist can, however, compete with and displace an endogenous agonist ligand from the target site (in turn leading to a lower response, bottom middle plot). **Upper row right:** Inverse agonism: when even in the absence of a drug-target complex there may be a constitutive activity/cell signal. This activity diminishes upon increased amounts of inverse agonist ligand forming a complex with the available target. Similarly, to the 'classic' agonist case described (upper row left), the steepness of the slope correlates with the relative efficacy of the inverse agonist ligand-target complex to alter the cellular response (① > ② > ③). However, in contrast to the antagonist case above, the inverse agonist ligand-target complex will weaken the baseline constitutive cell activity. NB!: Even though a neutral antagonist will not change a baseline target constitutive activity, it is able to counter the actions of 'classic' as well as inverse agonist ligands, bringing both back to their corresponding baseline level.

B. Log (ligand concentration L) versus Response.

Bottom row left: Agonism: Log (ligand concentration L) versus Response is a saturable function ('Model C', in (Gabrielsson and Peletier, 2018; Gabrielsson et al., 2018a)). With a transduction parameter ρ (Rho) > 0 , the response will increase from the baseline with increasing ligand concentrations; ① represents a full agonist, ② and ③ depict partial agonists with gradually lower efficacy. **Bottom row middle: Antagonism:** the endogenous agonist ligand is displaced by increasing concentrations of an antagonist drug ligand, thereby gradually reducing the baseline response ('endogenous tone'). The antagonist displacement of endogenous agonist ligand binding to target not only decreases the pharmacological response but also the concentration of free receptors available. **Bottom row right: Inverse agonism:** the constitutive activity of the target drops with more and more drug ligand bound to the target, forming an RL complex. L versus RL is a nonlinear/saturable function which gives a declining, sigmoidal, ligand (L)-versus-response curve. Here, the transduction parameter ρ (Rho) < 0 , and results in a progressively decremental response from the baseline as the concentration of ligand increases; ① represents a full inverse agonist, ② and ③ depict partial inverse agonists with gradually lower efficacy.

Figure 8. Schematic illustration of ligand concentration C-response relationships following changes in target turnover rate (k_{syn}), fractional target turnover rate (k_{deg}) or ligand-target complex ($k_{\text{e(RL)}}$). Note that only $k_{\text{e(RL)}}$ impacts both in vivo potency and efficacy. Changes in k_{syn} shifts intensity of response and k_{deg} changes in vivo potency. If E_{max} is changed without any concomitant changes in baseline it is most probably due to changes in either $k_{\text{e(RL)}}$ or ρ . Baseline response E_0 is governed by target exposure $k_{\text{syn}}/k_{\text{deg}}$ and target constitutive activity, whereas maximum ligand induced response E_{max} by $\rho \cdot k_{\text{syn}}/k_{\text{e(RL)}}$. "Altered" implies the new concentration-response relationship after parameter change.

Figure 9. Schematic depiction of response (arbitrary units; a.u.) vs. test compound concentration (a.u.) for situations along an irreversible/reversible ligand-target interaction scale. Shown are simulations of changes in ligand-target complex elimination $k_{\text{e(RL)}}$ and corresponding impact on in vivo potency EC_{50} . ① **Blue curve, right:** A reversible system where $k_{\text{e(RL)}}$ is much less than k_{off} . Potency $\text{EC}_{50} \sim k_{\text{deg}}/k_{\text{e(RL)}} \cdot K_d$; off-rate k_{off} from ligand-target complex binding will be an important covariate. ② **Red curve, middle:** $k_{\text{e(RL)}} = k_{\text{off}}$; EC_{50} corresponds to Equation 2. ③ **Black curve, left:** Irreversible in the sense that there is only an infinitesimal contribution of ligand regenerated from the ligand-target complex pool since $k_{\text{e(RL)}}$ is much greater than k_{off} . Potency $\text{EC}_{50} \sim k_{\text{deg}}/k_{\text{on}}$; target turnover will again be an important covariate as in Eqn. 2.

Figure 10. Left: Schematic illustration of reversible loss of ligand-target complex where $k_{\text{e(RL)}} \ll k_{\text{off}}$. In vivo potency (Eqn. 2) may then be approximated according to the bottom row expression where ligand-target binding components as well as target turnover and ligand-target complex removal will impact in vivo potency. **Right:** Schematic illustration of irreversible loss of ligand-target complex where $k_{\text{e(RL)}} \gg k_{\text{off}}$. In vivo potency (Eqn. 2) may then be approximated according to the bottom row expression where target turnover k_{deg} and ligand-target association rate k_{on} will impact in

vivo potency. The $k_{e(RL)}$ parameter is the first-order loss of ligand-target complex (Gabrielsson and Peletier, 2017) corresponding to " $L_T/V_T \times (1 - \sigma_v)$ " in the work by (Li et al., 2018) (L_T , V_T and σ_v represent lymph flow through target tissue, interstitial flow of target tissue and vascular reflection coefficient of target tissue, respectively).

Figure 11. Schematic illustration of unbound plasma concentration C_u and unbound tissue (target) concentration C_{uT} at steady-state. **Case A:** Only concentration different diffusion of drug molecules is responsible for drug distribution between plasma and target tissue. Hence, unbound concentrations in plasma and are equal at steady-state. In vivo potency based on plasma or target tissue will be the same. **Case B:** Efflux transporters, clearance, irreversible binding, ionization (pH differences between plasma and tissue) or bulk flow are responsible for decreasing unbound concentration in target tissue. Unbound concentrations in plasma are higher than unbound concentrations in tissue at steady-state. In vivo potency based on plasma is lower (numerically higher) than estimated from target tissue. **Case C:** Uptake transporters or ionization favour increased unbound concentrations at target tissue. Unbound concentrations in plasma are lower than unbound concentrations in tissue at steady-state. In vivo potency based on plasma is higher (numerically lower) than estimated from target tissue.

Figure 12. Observed (solid symbols) and regressed (Eqn. 9, solid line) concentration-time data of compound X after ten repeated intravenous injections. The first 120 mg intravenous injection was followed by nine 40 mg intravenous injections given every 8th hour. Concentration-time data and doses are taken from Case study PK22 in (Gabrielsson and Weiner, 2016). This dataset was included to demonstrate the flexibility of the 'open' MM model.

Figure 13. Left: Model simulations of concentration-time courses of substrate S, free enzyme E and substrate-enzyme complex ES after a 100 hour constant-rate infusion aiming at about 200 $\mu\text{g}\cdot\text{L}^{-1}$ of test compound analyzed in **Figure 12**. Therapeutic concentrations fall in the range of 100-500 $\mu\text{g}\cdot\text{L}^{-1}$. **Right:** Model simulations of concentration-time courses of free enzyme (blue line) and clearance (red line). The free enzyme level decreases transiently from its baseline value ① to a trough ② during the initial rise in plasma concentration of substrate since substrate will bind to free enzyme. An apparent steady-state is reached between 40 to 60 hours ③ and lasts until the end of infusion. Only synthesis k_{syn} and loss k_{deg} of free enzyme govern the steady-state free enzyme concentration. There is a rapid rise in free enzyme concentrations upon stop of infusion due to stop of complex formation (no further consumption of free enzyme for complex formation), and release of free enzyme from the substrate-enzyme complex pool ④ as rate of substrate input stops. The free enzyme concentration returns to the equilibrium concentration terminally ⑤. ①-⑤ correspond to the different stages schematically shown in **Figure 14**.

Figure 14. Schematic presentation of free enzyme and substrate levels pre-, during and post-dosing. The free enzyme level (dashed blue line) decreases from its baseline value (Pre-dose ①) to a trough value (after the start of infusion ②) during the initial rise in plasma substrate concentration (dotted red line), since substrate will allocate portions of free enzyme during a constant rate infusion. Steady-state is reached (yellow shaded area ③) and lasts until the stop of infusion. Only synthesis k_{syn} and loss k_{deg} of free enzyme govern the steady-state free enzyme concentration. There is a rapid rise in free enzyme concentrations upon stop of substrate infusion (Washout ④); this is due to discharge of free enzyme from the disintegrating substrate-enzyme complex pool and no further free drug infusion to form a substrate-enzyme complex. The free enzyme concentration returns to the equilibrium concentration terminally (Post-dose ⑤).

Figure 15. A: Semi-logarithmic plot of simulated concentration-time courses of compound X after three different bolus doses. The starting concentrations are 300, 1000 and 3000 $\mu\text{g}\cdot\text{L}^{-1}$. Therapeutic concentrations fall in the range of 100-500 $\mu\text{g}\cdot\text{L}^{-1}$. **B:** Simulated time-courses of clearance after three bolus time courses. **C:** Simulated time-courses of half-life after three bolus time courses. Numbers 1-5 correspond to the different stages schematically shown in **Figure 14**. The numbers correspond to stages in **Figure 13**. Note that stage number 3 of **Figure 15** is not applicable to the bolus situation since there is no steady-state during dosing, and is therefore omitted.

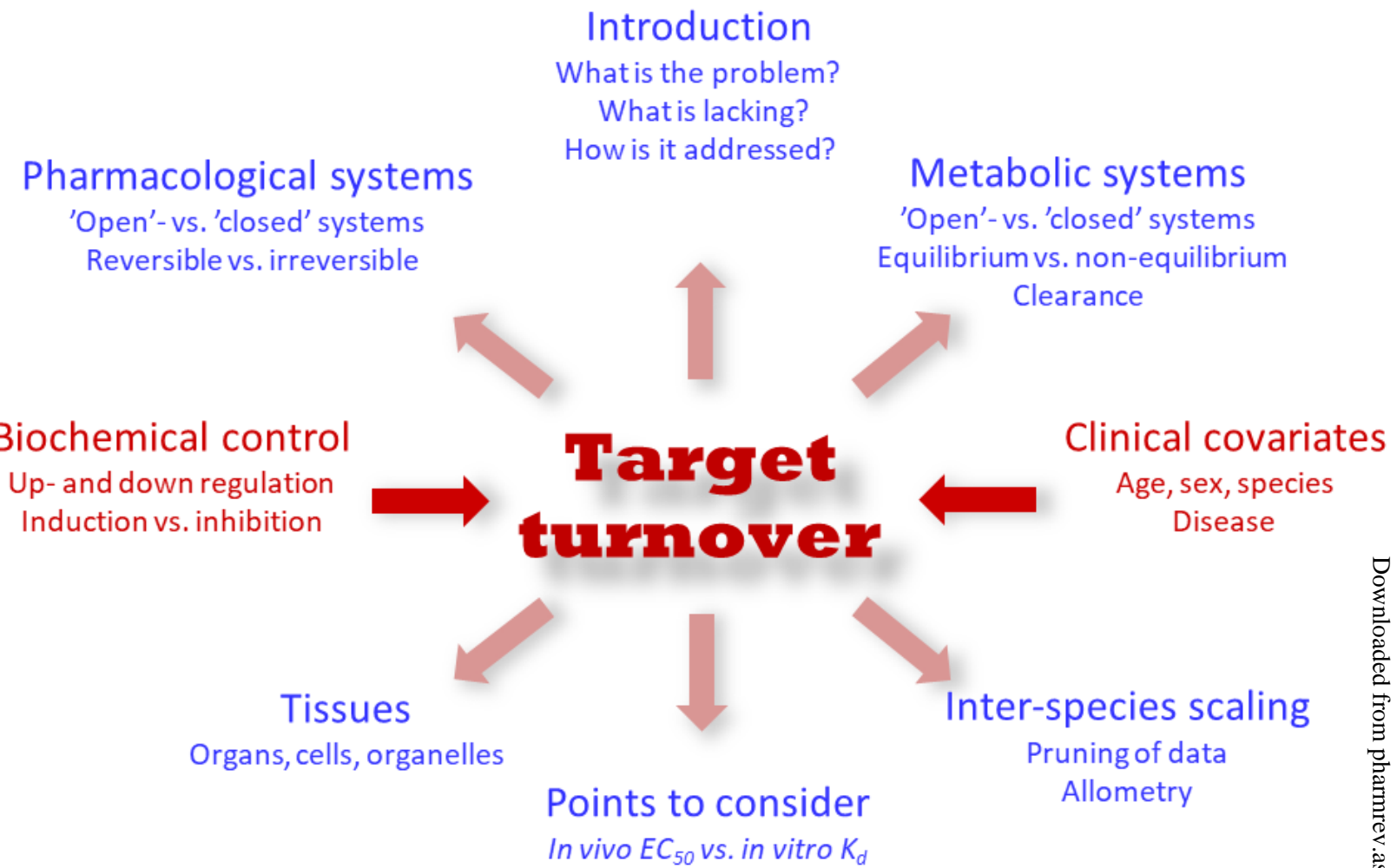


Fig. 1

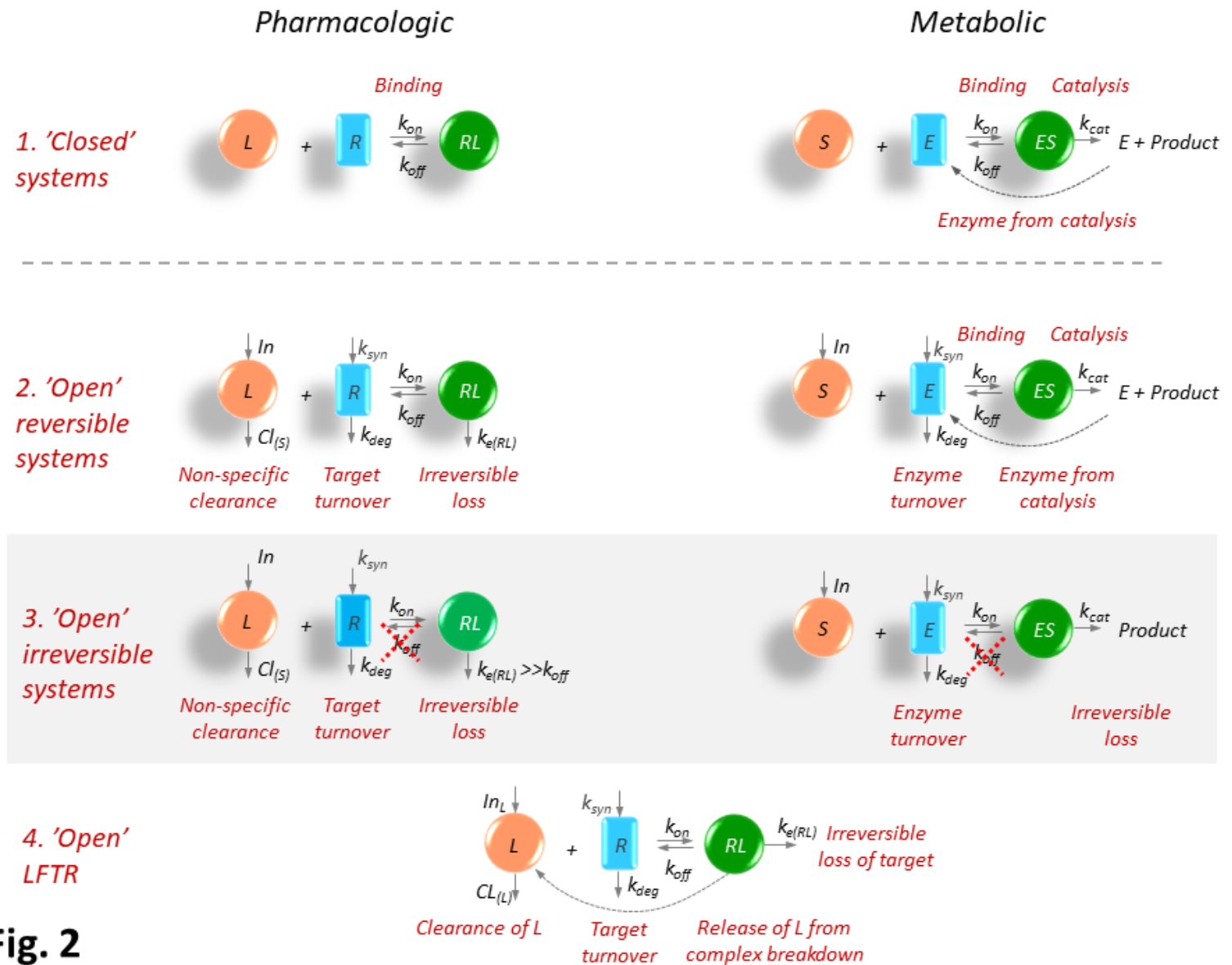


Fig. 2

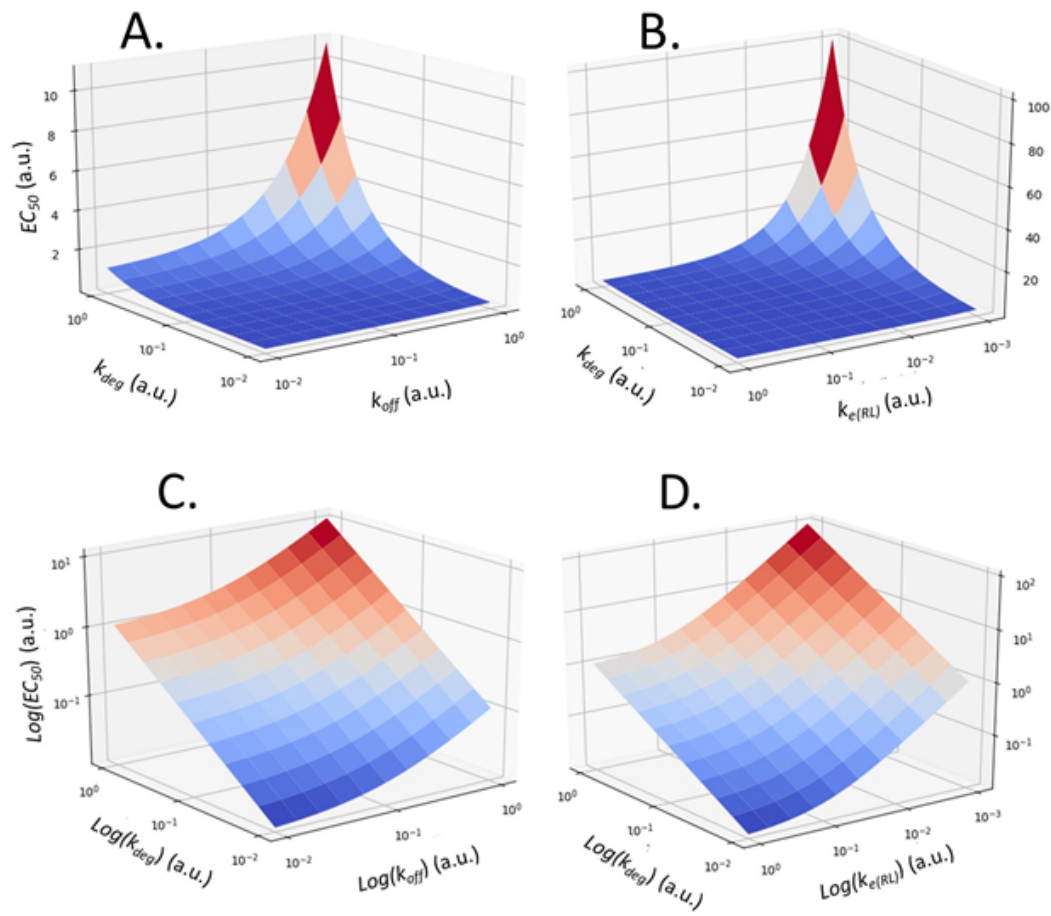


Fig. 3

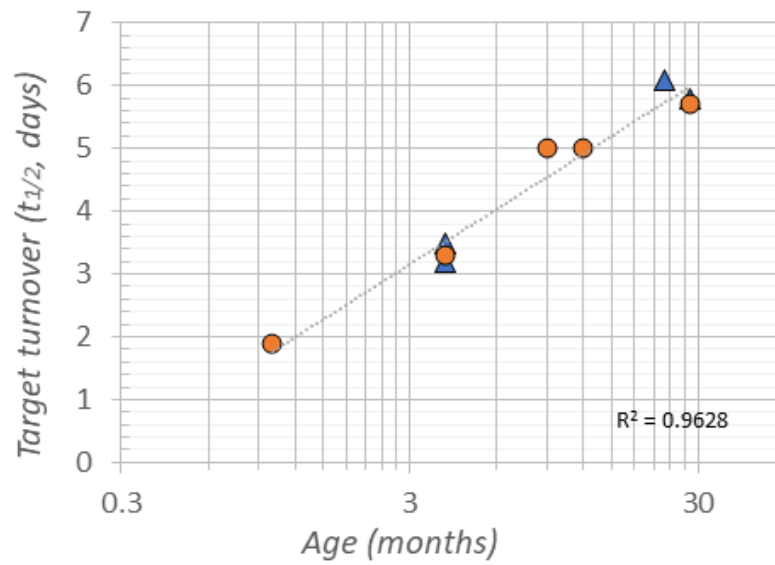


Fig. 4

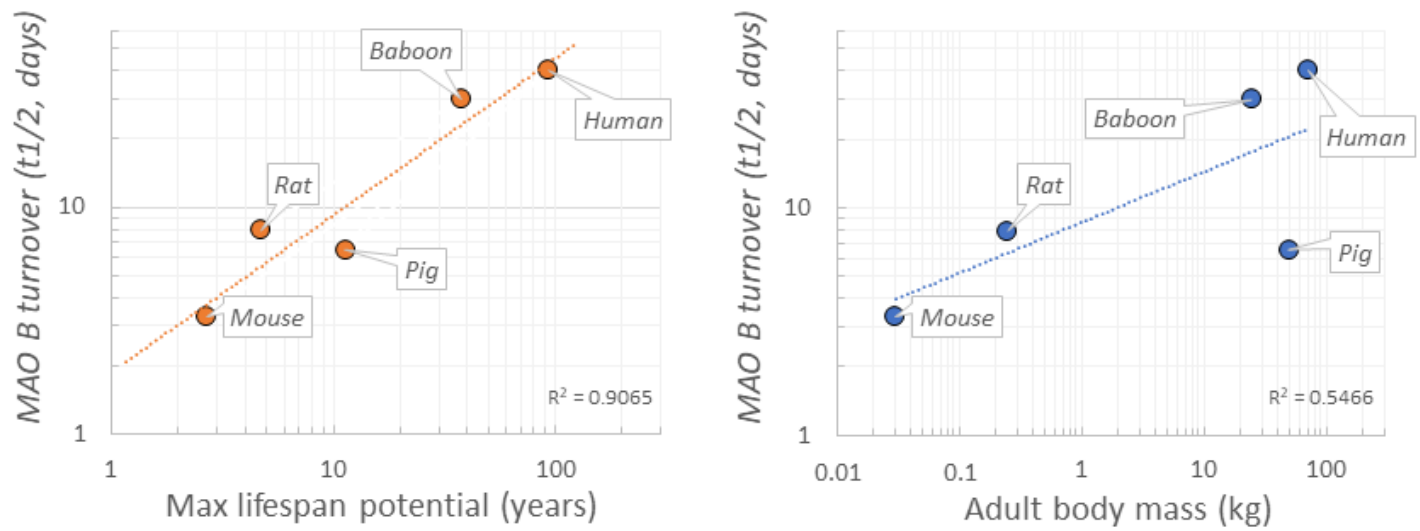


Fig. 5

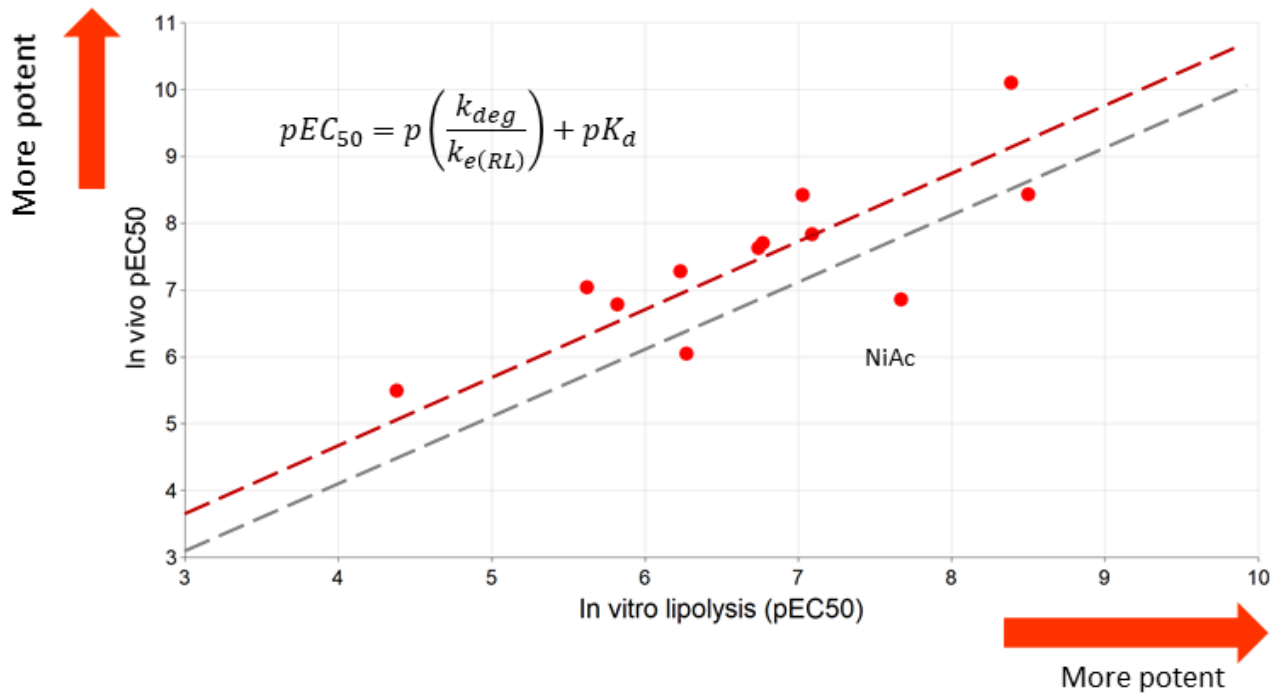


Fig. 6

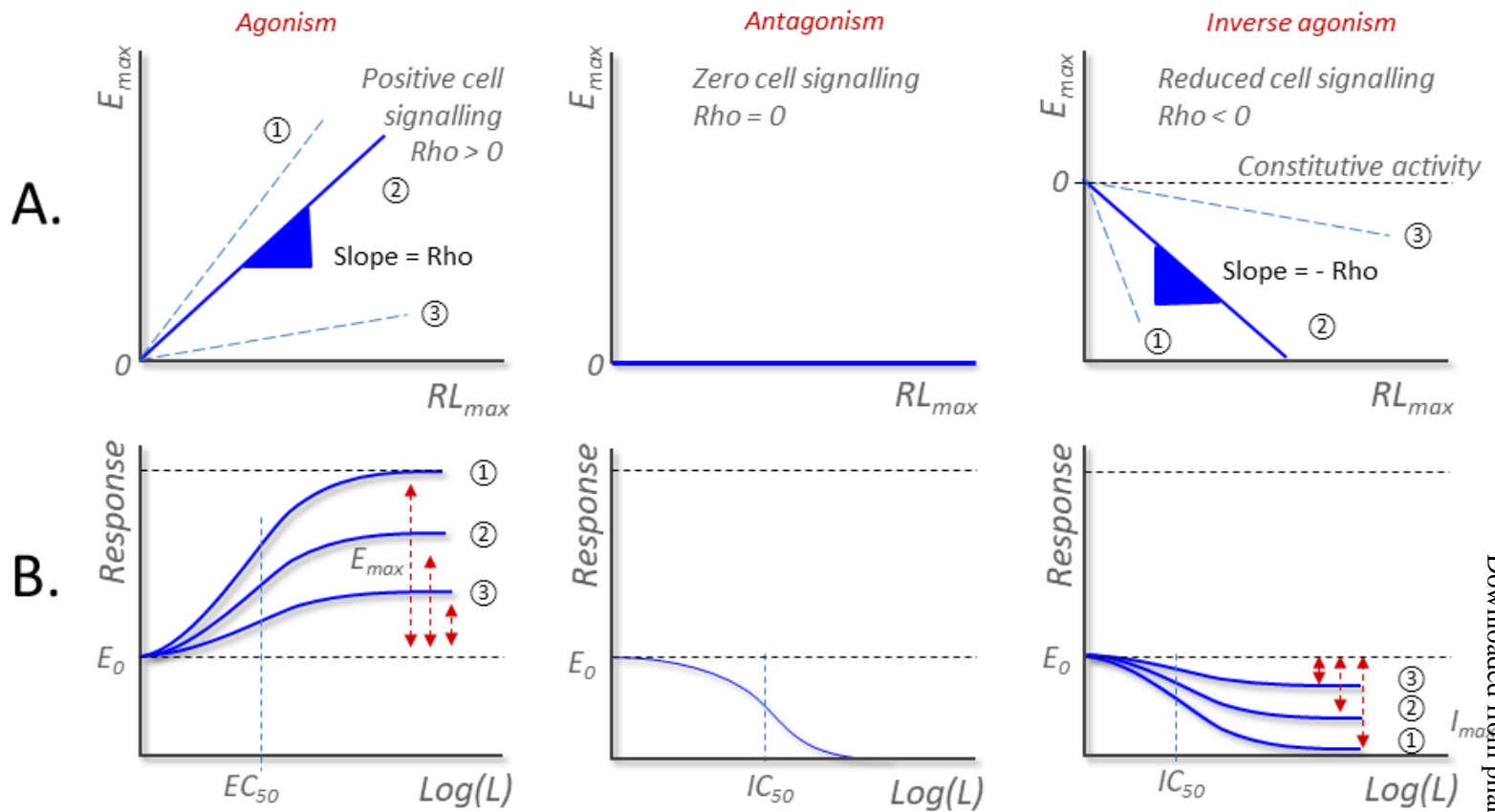


Fig. 7

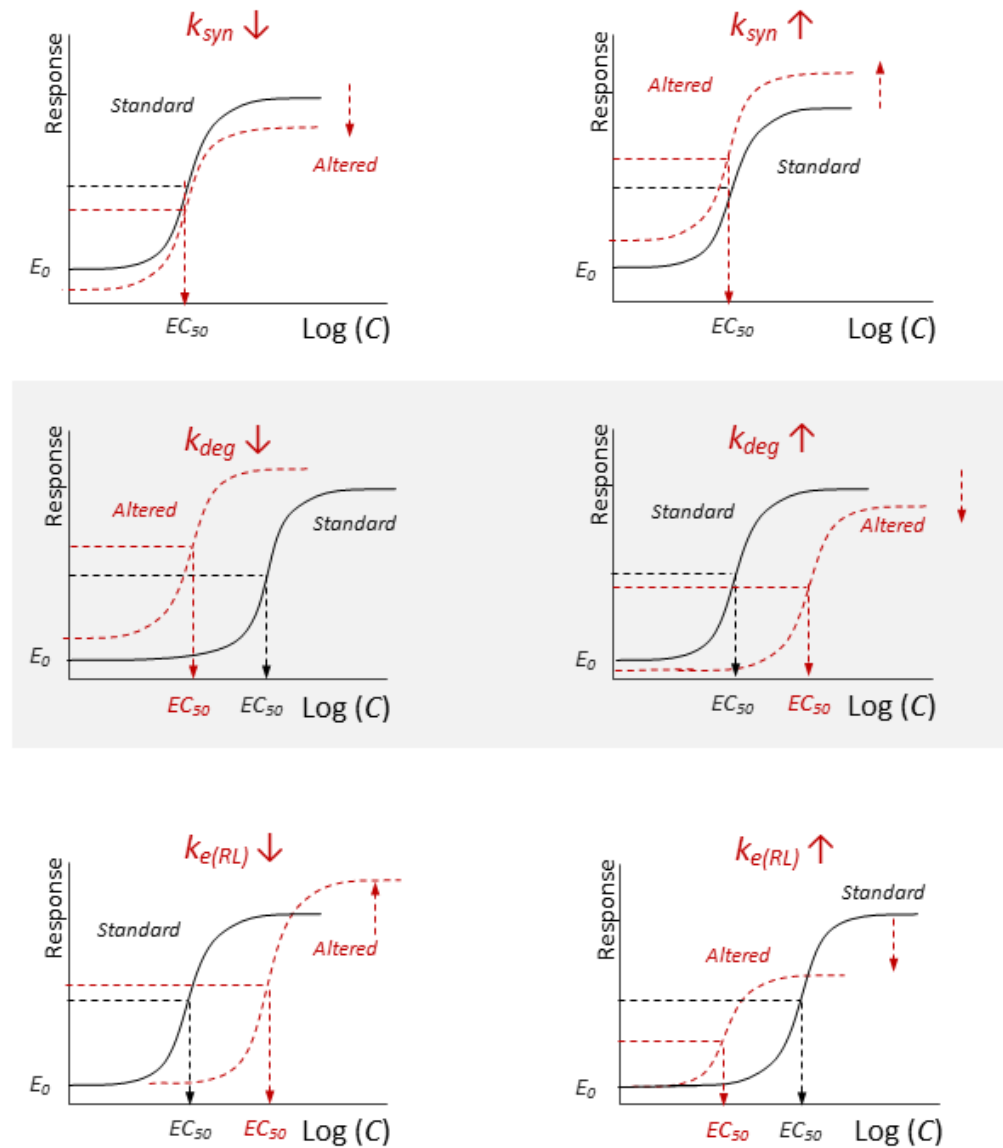


Fig. 8

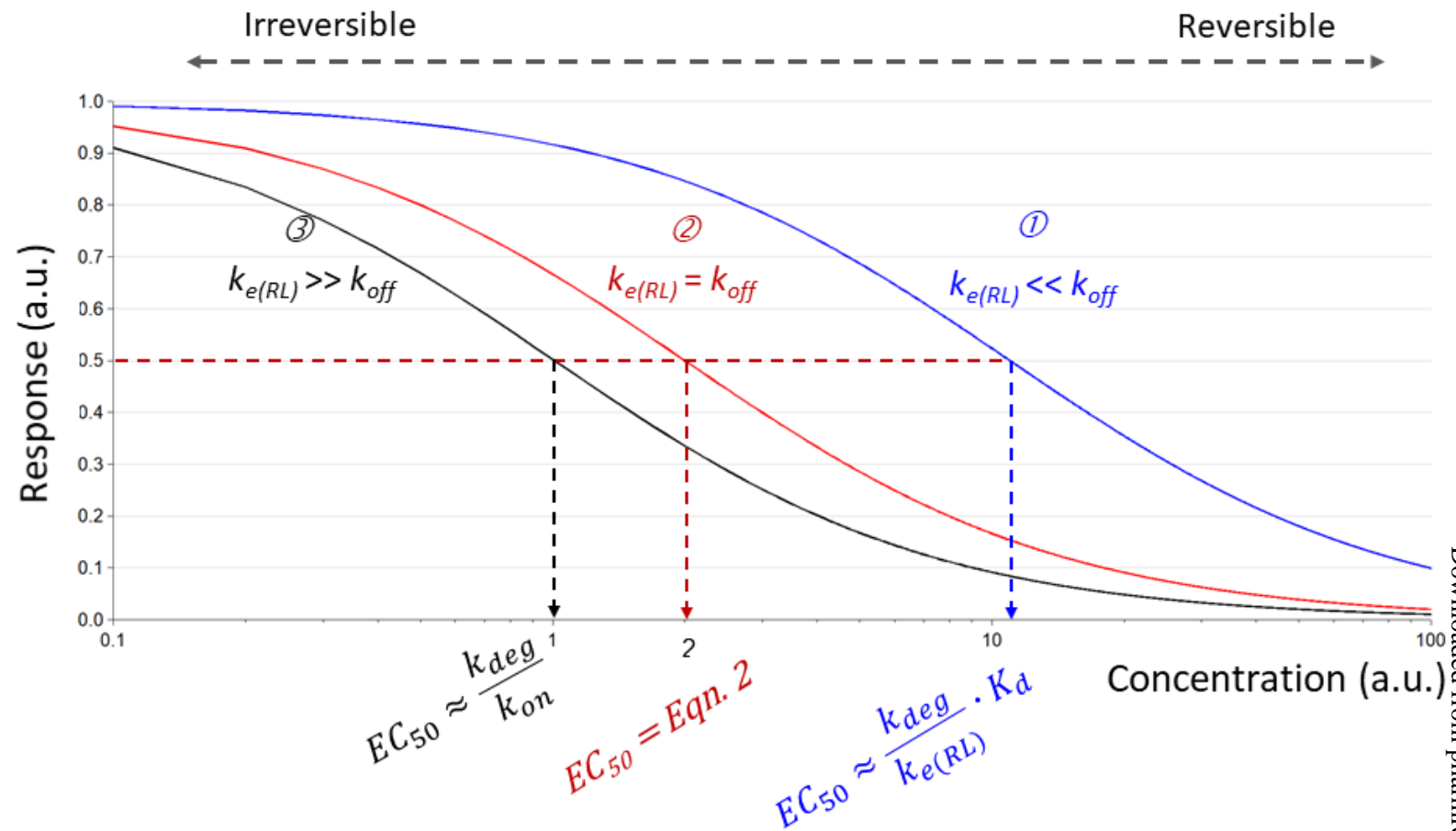


Fig. 9

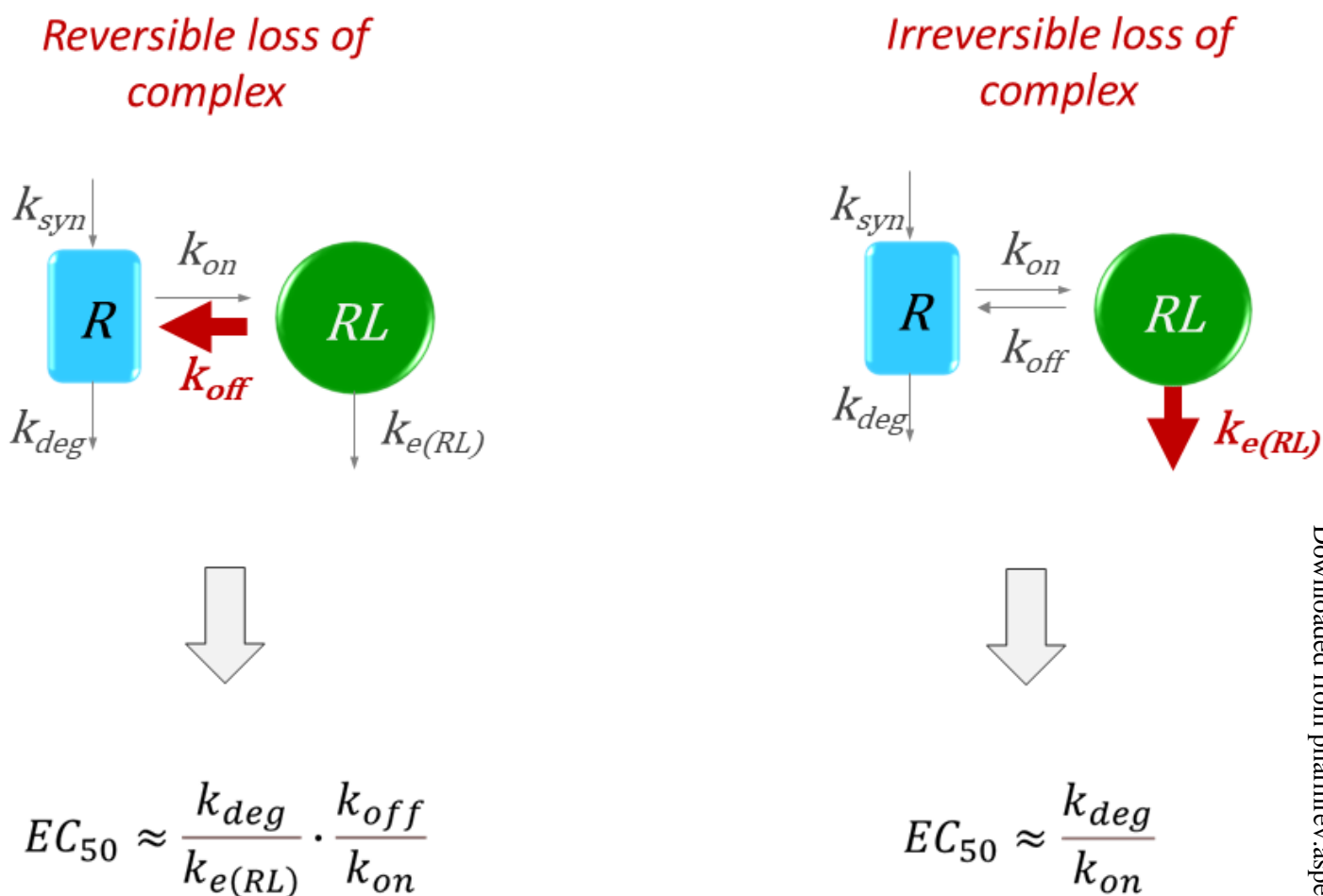


Fig. 10

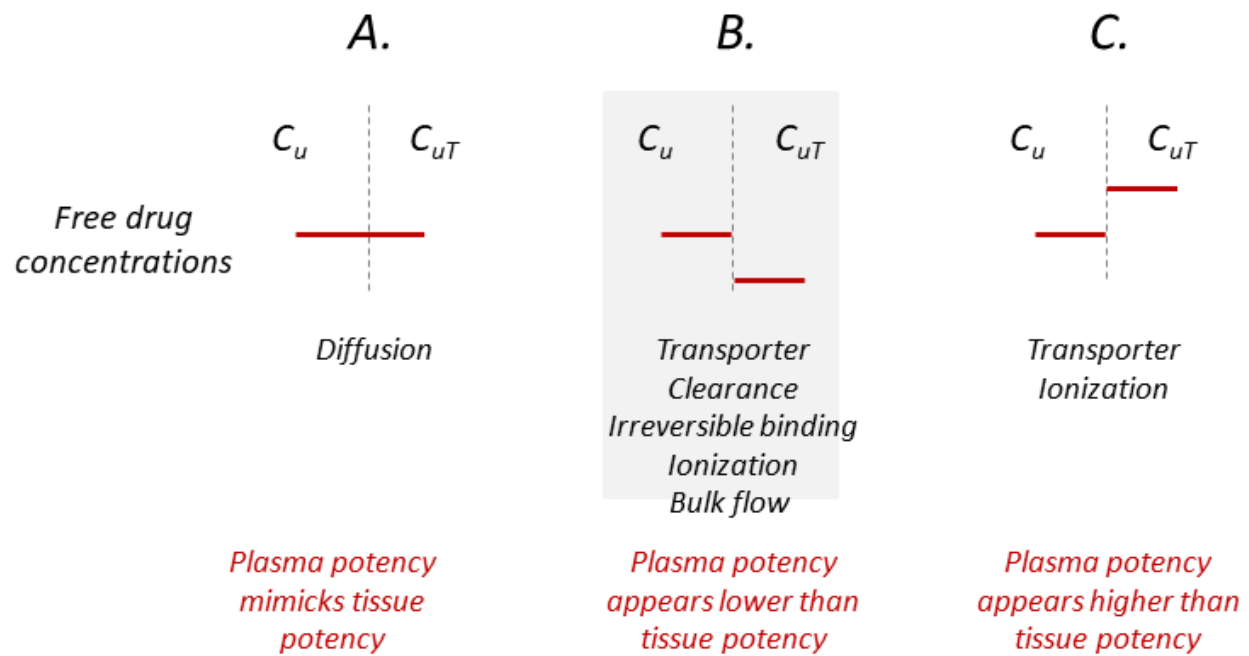


Fig. 11

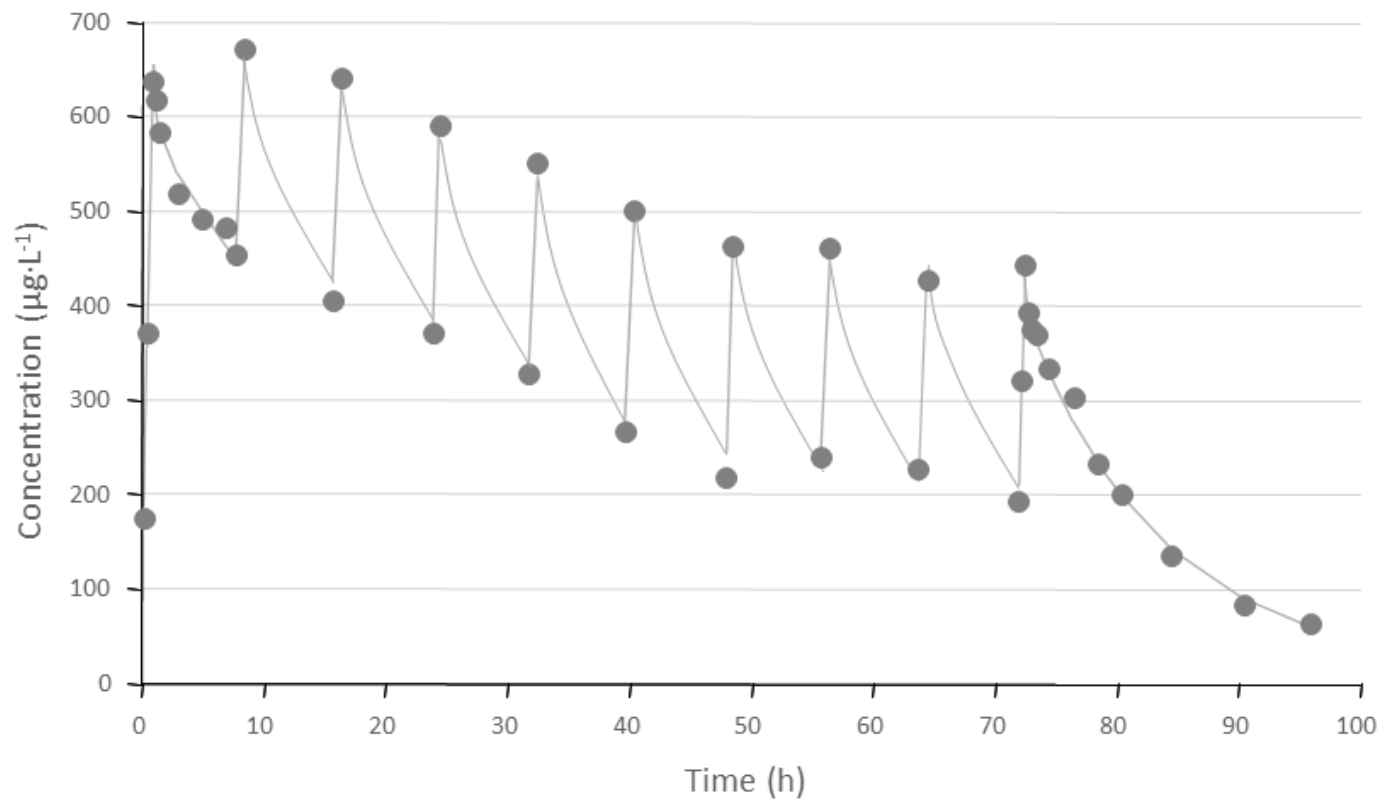


Fig. 12

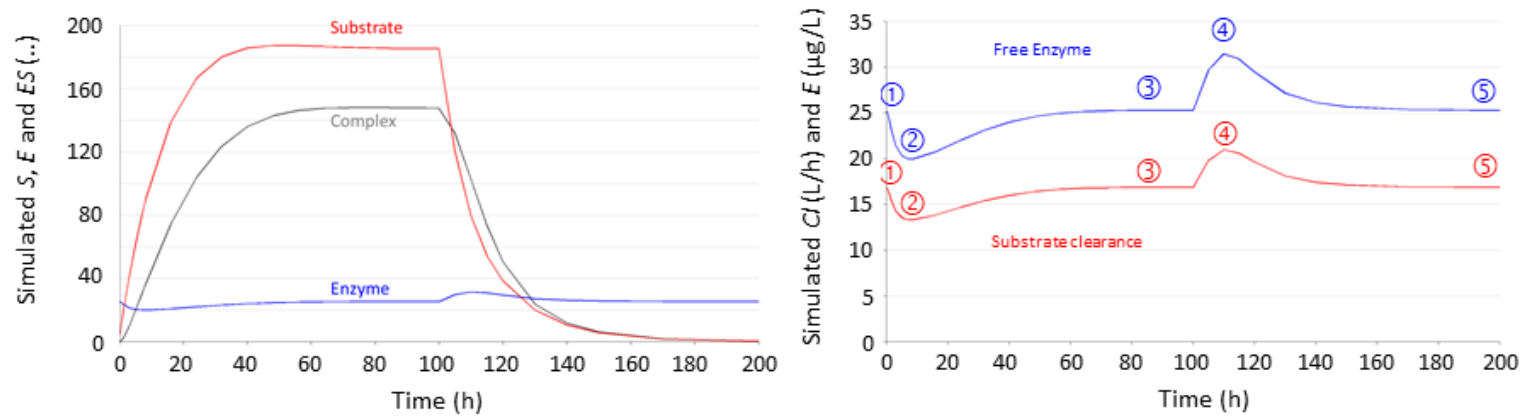


Fig. 13

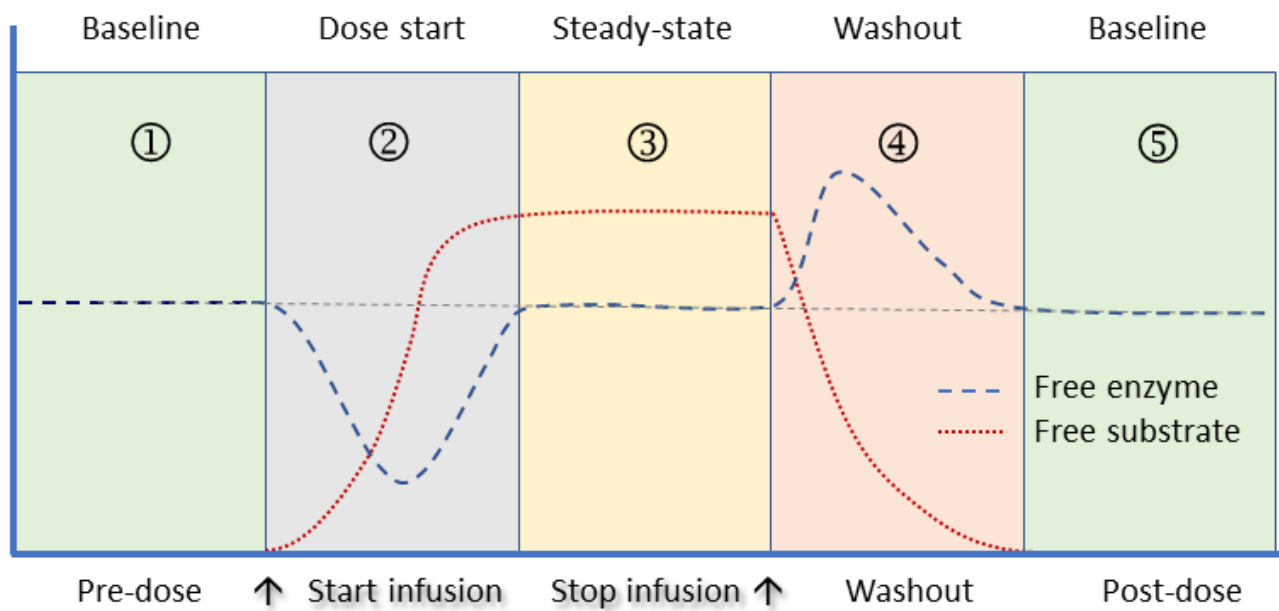


Fig. 14

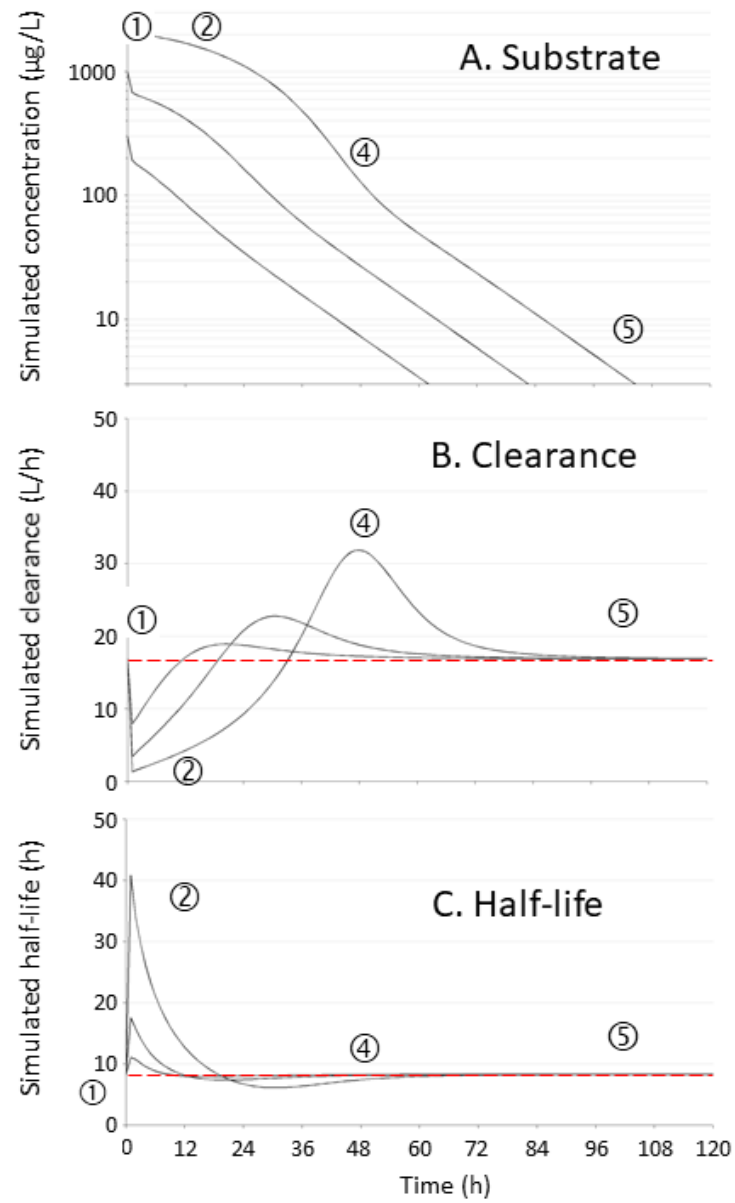


Fig. 15